CAPITAL UNIVERSITY OF SCIENCE AND TECHNOLOGY, ISLAMABAD

Development and Characterization of Ciprofloxacin - Loaded Nanostructured Lipid Carriers: A Promising Approach to Enhance Antibacterial Activity

by

Maira Anwar

A thesis submitted in partial fulfillment for the degree of Master of Philosophy

in the

Faculty of Pharmacy
Department of Pharmaceutics

2026

CERTIFICATE OF APPROVAL

Development and Characterization of Ciprofloxacin-Loaded Nanostructured Lipid Carriers: A Promising Approach to Enhance Antibacterial Activity

by

Maira Anwar

(MPH241004)

THESIS EXAMINING COMMITTEE

S. No.	Examiner	Name	Organization
(a)	External Examiner	Dr. M. Iqbal Nasri	HU, Islamabad
(b)	Internal Examiner	Dr. Mahira Zeeshan	CUST, Islamabad

Dr. Nadia Shamshad Malik
Thesis Supervisor
February, 2026

Dr. Nadia Shamshad Malik
Head
Department. of Pharmaceutics
February, 2026

Dr. Muzaffar Abbas
Dean
Faculty of Pharmacy
February, 2026

Author's Declaration

I, **Maira Anwar** hereby state that my MPhil thesis titled "**Development and Characterization of Ciprofloxacin - Loaded Nanostructured Lipid Carriers: A Promising Approach to Enhance Antibacterial Activity**" is my own work and has not been submitted previously by me for taking any degree from Capital University of Science and Technology, Islamabad or anywhere else in the country/abroad.

At any time if my statement is found to be incorrect even after my graduation, the University has the right to withdraw my MPhil Degree.

(Maira Anwar)

Registration No: MPH241004

Plagiarism Undertaking

I solemnly declare that research work presented in this thesis titled "**Development and Characterization of Ciprofloxacin - Loaded Nanostructured Lipid Carriers: A Promising Approach to Enhance Antibacterial Activity**" is solely my research work with no significant contribution from any other person. Small contribution/help wherever taken has been duly acknowledged and that complete thesis has been written by me.

I understand the zero tolerance policy of the HEC and Capital University of Science and Technology towards plagiarism. Therefore, I as an author of the above titled thesis declare that no portion of my thesis has been plagiarized and any material used as reference is properly referred/cited.

I undertake that if I am found guilty of any formal plagiarism in the above titled thesis even after award of MPhil Degree, the University reserves the right to withdraw/revoke my MPhil degree and that HEC and the University have the right to publish my name on the HEC/University website on which names of students are placed who submitted plagiarized work.

(Maira Anwar)
Registration No: MPH241004

Acknowledgement

First and foremost, I am profoundly grateful to Allah, the Most Gracious and the Most Merciful, for granting me the strength, perseverance, and wisdom to complete this academic endeavor. His divine guidance has been a constant source of support throughout this journey.

I would like to express my sincere appreciation to Dr. Nadia Shamshad Malik, my research supervisor, for her invaluable guidance, continuous encouragement, and constructive feedback throughout the course of this study. Her expertise, insightful suggestions, and unwavering support were critical to the successful completion of this thesis. Her dedication to academic excellence and mentorship influenced the quality and direction of my research.

I extend my heartfelt thanks to my family, whose unwavering support, encouragement, and belief in my potential have been a constant source of motivation. Their patience and understanding provided me with the emotional strength needed to navigate this journey. My sincere gratitude also goes to my research group colleagues and peers, whose collaboration, thoughtful discussions, and shared commitment to academic growth created a stimulating and supportive research environment.

I am also thankful to my friends, whose encouragement, positivity, and timely support brought balance and joy throughout this academic pursuit.

Lastly, I gratefully acknowledge my institute for providing the academic platform, resources, and conducive research environment that made this work possible. The infrastructure and administrative support played a significant role in facilitating various aspects of my research.

(Maira Anwar)

Abstract

Ciprofloxacin, a Biopharmaceutics Classification System (BCS) class IV drug characterized by low solubility and low permeability, was incorporated into nanostructured lipid carriers (NLCs) using Compritol® 888 ATO and oleic acid as the solid and liquid lipids, respectively. Formulation optimization was performed employing a three-factor three-level Box–Behnken design (BBD), with solid lipid concentration, Tween-80 concentration, and homogenization time (min) as independent variables. The optimized formulation consisted of 70% w/w solid lipid, 2% w/w surfactant, and 10 min of homogenization time. The optimized NLC formulation exhibited a mean particle size of 137.7 nm, a polydispersity index of 0.2630, a zeta potential of -27.90 mV, and an entrapment efficiency of 87.85%. FTIR, DSC, and XRD analyses confirmed successful encapsulation of ciprofloxacin in an amorphous state within the lipid matrix, while SEM and TEM revealed uniformly dispersed spherical nanoparticles. In vitro drug release studies demonstrated a sustained biphasic release profile, best described by the Korsmeyer–Peppas model (n = 0.5663), indicating anomalous transport behavior. Incorporation of the optimized NLCs into a Carbopol gel resulted in significantly higher ex vivo permeation (1151.6 μg/cm^2) and steady-state flux (75.5 μg/cm^2/h) compared with plain ciprofloxacin gel. Dermal irritation studies confirmed excellent skin compatibility, with a primary irritation index of 0.00. Furthermore, the NLC-based gel exhibited superior antibacterial activity against methicillin-resistant Staphylococcus aureus (MRSA) compared with blank NLCs and plain gel. Overall, the developed NLC gel represents a stable and biocompatible lipid-based system for transdermal delivery of ciprofloxacin.

Keywords: Ciprofloxacin; Nanostructured lipid carriers; Transdermal drug delivery; Antimicrobial resistance; MRSA; Quality by Design

Contents

List of Figures

List of Tables

Abbreviations

API	Active Pharmaceutical Ingredient
AMR	Antimicrobial resistance
BBD	Box–Behnken Design
BCS	Biopharmaceutics Classification System
Carbopol	Carbomer Polymer
CIP	Ciprofloxacin
DSC	Differential Scanning Calorimetry
DMSO	Dimethyl sulfoxide
EE	Entrapment Efficiency
FTIR	Fourier Transform Infrared Spectroscopy
HA-MRSA	Hospital acquired Methicillin-Resistant *Staphylococcus aureus*
CA-MRSA	Community acquired Methicillin-Resistant *Staphylococcus aureus*
LMICs	Low- and middle-income countries
MRSA	Methicillin-Resistant *Staphylococcus aureus*
NLC	Nanostructured Lipid Carrier
PBS	Phosphate Buffered Saline
PDI	Polydispersity Index
PII	Primary Irritation Index
QbD	Quality by Design
SEM	Scanning Electron Microscopy
SLN	Solid Lipid Nanoparticle
TEM	Transmission Electron Microscopy
TEA	Triethnolamine
Tween-80	Polyoxyethylene (20) Sorbitan Monooleate

XRD	X-Ray Diffraction
ZOI	Zone of inhibition

Chapter 1

Introduction

1.1 Overview of Antimicrobial Resistance : A Global Health Threat

The rapid rise of antimicrobial resistance (AMR) has become an increasingly serious global concern to public health, endangering decades of progress in fighting infectious diseases. The World Health Organization defines antimicrobial resistance (AMR) as the capacity of microorganisms to remain viable in the presence of antimicrobial substances. Extensive and inappropriate application of antibiotics in medical treatment, veterinary practice, and agricultural production has contributed to the increased prevalence of resistant organisms. As a consequence, infections that were previously responsive to standard antimicrobial therapy now present greater therapeutic difficulty and are associated with elevated morbidity and mortality [1].

Global estimates indicate that antimicrobial resistance has been associated with approximately 1.27 million deaths directly and nearly 4.95 million additional deaths worldwide, while future projections suggest that annual fatalities could rise to around 10 million by 2050, accompanied by global economic losses exceeding 100 trillion US dollars [2].

The burden of antimicrobial-resistant infections is rising globally, affecting both high-income and low-to-middle-income countries (LMICs), albeit with varying patterns of prevalence and impact. In high-income countries, robust antimicrobial stewardship programs and surveillance systems have been established and enforced, whereas LMICs often face challenges in implementing such measures, contributing to the continued spread of resistance. Poor healthcare infrastructures and non-regulated sales of antimicrobials remain the main problems in LMICs. For example, 70% of antibiotic sales in Pakistan are without prescriptions, encouraging misuse and resistance [3].

In Pakistan, concerning AMR levels are shown in key pathogens, with 60-70% resistance to certain antibiotics even in the hospitals. AMR not only raises healthcare costs because of extended hospitalization and more costly treatment but also jeopardizes economic stability. The World Bank estimates that uncontrolled AMR could plunge millions of people into extreme poverty. Furthermore, growing resistance puts at risk the outcome of major medical interventions that rely on effective antibiotics. The WHO views AMR as one of the highest global health priorities, calling for global efforts toward enhanced surveillance, better stewardship, and new treatments [4].

1.2 Methicillin - Resistant *Staphylococcus aureus* as a Key Resistant Pathogen

Staphylococcus aureus is an important human pathogen capable of causing a wide range of clinical conditions, from localized skin involvement to life-threatening invasive disorders. Since the emergence of methicillin-resistant *S. aureus* (MRSA) in 1961, this organism has become an increasing concern for global public health. MRSA is widespread both in hospitals (HA-MRSA) and in the community (CA-MRSA), with rates differing by region. For North America and Europe, the prevalence among *S. aureus* isolates is between 20-50%, while in Asia and parts of Africa, it is often above 50% [5].

MRSA prevalence is particularly high in Pakistan, with reported rates in studies ranging from 36% to 61% in urban hospitals. CA-MRSA has shown a marked increase in prevalence and is now a common cause of infections involving the skin and underlying soft tissues. The absence of an integrated national surveillance system complicates the efforts to understand the full epidemiological picture [6].

Infections due to MRSA can vary from superficial problems such as abscesses to severe diseases like pneumonia and bacteremia. These infections tend to cause more serious health complications and are linked with a higher incidence of mortality than those caused by methicillin-sensitive *Staphylococcus aureus* (MSSA). The acquisition of resistance determinants, notably the mecA gene, confers *Staphylococcus aureus* with resistance to β-lactam antibiotics and frequently to multiple other antibiotic classes. Resistance has been heightened by the inappropriate use of antibiotics in countries like Pakistan [7].

Economically, MRSA raises health care costs because of extended hospital stays and complicated treatment. The presence of MRSA in biofilms enhances persistence and reinforces resistance, making effective responses to infection quite challenging.

1.3 Mechanisms of Resistance in MRSA

MRSA expresses multidrug resistance mediated by complex genetic, molecular, and phenotypic mechanisms. β-lactam resistance in *Staphylococcus aureus* is primarily due to the mecA gene, which encodes PBP2a, a modified penicillin-binding protein that sustains cell wall synthesis despite β-lactam exposure. The variant mecC also exists in some isolates. In most regions, including Pakistan, studies have shown high prevalence rates of mecA greater than 90% and mecC co-occurrence at rates ranging from 5 to 15% [8].

Resistance of MRSA to fluoroquinolones, including ciprofloxacin, is largely linked to changes in the DNA gyrase enzymes, specifically the genes responsible for subunits A and B. Efflux pumps, such as those of the Nor family, actively expel

antibiotics from bacterial cells, thereby enhancing resistance. Studies indicate that over 90 of MRSA isolates in Bangladesh harbor multiple efflux pump genes. In addition, biofilm formation provides further protection, allowing MRSA to survive in hostile conditions and tolerate antibiotic exposure. Regulatory elements contribute significantly to controlling the expression of resistance and enable the transfer of resistance genes between bacterial cells [9].

These factors collectively highlight the resilience of MRSA and the need for new treatments to address this persistent health challenge.

1.4 Ciprofloxacin: Role, Limitations and Resistance Issues

Ciprofloxacin, a second-generation fluoroquinolone, is a widely employed broad-spectrum antibiotic. It demonstrates strong antimicrobial activity against a variety of Gram-negative bacteria and some Gram-positive species. Its bactericidal action results from interference with DNA gyrase and topoisomerase IV, enzymes critical for DNA replication, recombination, and repair, thereby impairing bacterial growth and survival [10].

Although widely used for its effectiveness against a range of bacterial pathogens, ciprofloxacin exhibits several limitations related to its pharmacokinetic behavior and physicochemical properties. It is classified as Class IV in the Biopharmaceutics Classification System (BCS), indicating that it has low solubility and poor permeability. As a result, ciprofloxacin typically exhibits low bioavailability after oral administration, often requiring high and frequent doses. Additionally, its relatively short half-life of about 3 to 5 hours and the potential for systemic side effects, such as liver toxicity and gastrointestinal irritation, further constrain its clinical use [11].

Furthermore, resistance to ciprofloxacin is rising rapidly, particularly among bacteria with resistance to multiple antibiotics, including MRSA. Mutations affecting

the quinolone-sensitive domains of gyrA and grlA, together with the contribution of efflux systems, play a central role in limiting the activity of quinolone antibiotics [12].

Regions such as South Asia have documented a ciprofloxacin resistance rate exceeding 80% among MRSA isolates. Similarly, several studies conducted in Pakistan have reported resistance levels ranging from 70% to 90%. The global scenario has also indicated an increase in the trend of ciprofloxacin resistance among MRSA isolates in both hospital and community settings. The antibiotic has also been found to cause adverse reactions like gastrointestinal disturbances and tendinopathy. Its oral formulation usually exhibits variable bioavailability, thereby compromising treatment response for serious infections [13].

Given these challenges, there is an urgent need for innovative strategies to enhance the clinical utility of ciprofloxacin, including the use of novel drug delivery systems that may modulate both the solubility and penetration of drugs while evading resistance mechanisms.

1.5 Problem Statement

AMR represents an increasingly severe global health challenge, compromising the efficacy of conventional antibiotics, causing an estimated 1.27 million deaths each year, and jeopardizing critical medical procedures [14]. Among multidrug-resistant infections, MRSA presents a considerable clinical challenge because of its augmented pathogenicity, biofilm production, and extensive resistance to β-lactams and other frequently utilized antibiotics [15]. Ciprofloxacin, a broad-spectrum fluoroquinolone, retains activity against MRSA but is limited by poor biopharmaceutical properties. Ciprofloxacin has been classified as a BCS Class IV drug (low solubility and low permeability). It possesses an aqueous solubility of merely 0.1-0.3 mg/mL under physiological conditions, exhibits pH-dependent solubility, has low and variable oral bioavailability (50-70%), and has a short elimination half-life of 3-5 hours [11].

These limitations necessitate frequent high dosing, which increases the emergence of adverse effects such as tendinopathy, peripheral neuropathy, and QT interval prolongation, compromising patient adherence and therapeutic outcomes [16].

Despite advances in lipid-based nanocarriers, strategies to achieve systemic delivery of ciprofloxacin via transdermal administration remain underexplored.

Consequently, there is an immediate requirement for alternate delivery methods that might enhance systemic drug exposure, sustain therapeutic plasma concentrations, and mitigate dose-dependent toxicity.

1.6 Nanotechnology in Drug Delivery

Nanotechnology is transforming pharmaceutical sciences by overcoming limitations in traditional drug therapies. Nanotechnology involves the precise engineering of materials at the nanoscale (approximately 1-1000 nm), imparting unique physicochemical properties such as enhanced bioavailability and improved interactions with biological membranes. Nanoparticles act as carriers that can enhance the solubility of drugs with limited water solubility and enable more precise, targeted delivery. Several classes of nanocarriers such as liposomes, polymeric nanoparticles, dendrimers, and metallic nanoparticles have been widely investigated for their potential to improve the delivery and therapeutic efficacy of poorly soluble compounds [17].

Nanocarriers are pivotal in enhancing the transport of therapeutic agents to sites of infection, facilitating penetration of biological barriers, and providing sustained drug release, thereby helping to mitigate the emergence of antimicrobial resistance. For example, nanoparticles can disrupt biofilms, allowing for better accumulation of drugs within cells and facilitating higher concentrations of antibiotics at the target site compared to traditional methods. Additionally, modifying the surfaces of nanocarriers may enable targeted delivery, enhance efficacy while minimizing effects on unintended sites [18].

Evidence from multiple studies supports the utility of nanocarriers in drug delivery. Liposomal formulations of antibiotics, such as vancomycin, demonstrate improved results against MRSA biofilms. Furthermore, polymeric nanoparticles enable targeted intracellular delivery of fluoroquinolones, thereby increasing drug penetration into host-cell-resident bacteria and enhancing therapeutic efficacy. Lipid-based nanocarriers, especially nanostructured lipid carriers, hold considerable promise for the development of novel formulations against resistant pathogens due to their favorable biocompatibility and efficient drug-loading capacity [19].

1.7 Nanostructured Lipid Carriers as Proposed Solution

Nanostructured lipid carriers (NLCs) represent an advanced lipid-based nanocarrier platform designed to address the limitations of solid lipid nanoparticles (SLNs) and traditional drug delivery systems. By incorporating both solid and liquid lipids, NLCs form a partially disordered crystalline structure, which provides several benefits, including enhanced drug-loading efficiency, greater physical stability, and the capability for sustained or controlled drug release. These characteristics make NLCs especially suitable for delivering poorly soluble drugs like ciprofloxacin [20].

NLCs exhibit enhanced storage stability relative to liposomes, which are frequently susceptible to physical degradation, vesicle aggregation, and early drug release over time. In addition, NLCs can be prepared using relatively simple and scalable techniques, such as hot homogenization, making them more cost-effective and industrially feasible for pharmaceutical manufacturing. Unlike polymeric nanoparticles, which may require the use of toxic organic solvents during formulation, NLCs are typically composed of Generally Recognized as Safe (GRAS) lipids. This lipid-based composition ensures high biocompatibility, reduced toxicity, and improved patient safety, further supporting the suitability of NLCs for clinical and commercial drug delivery applications [21].

NLCs possess a distinct advantage in terms of enhanced drug entrapment and formulation stability, which arises from their imperfect crystalline structure formed by the combination of solid and liquid lipids. This disordered lipid matrix accommodates higher drug payloads and minimizes drug expulsion compared to SLNs. Such structural characteristics are particularly beneficial for antibiotics like ciprofloxacin, which require a stable lipid environment to maintain therapeutic efficacy. Moreover, NLCs enable controlled and tunable drug release profiles, allowing formulation customization to meet the pharmacokinetic demands of different infectious conditions [22].

Additionally, NLCs can improve transdermal drug delivery by disrupting the lipid organization within the stratum corneum, which promotes enhanced penetration into deeper skin layers and supports prolonged drug release. This feature is particularly useful for managing skin and soft tissue infections caused by resistant bacteria such as MRSA. By delivering higher localized and systemic concentrations of antibiotics, NLCs can improve antibacterial efficacy against resistant strains. Overall, the favorable biocompatibility, high drug-loading capacity, excellent physical stability, sustained release behavior, and enhanced skin permeation render NLCs superior to other nanocarrier systems for transdermal antibiotic delivery in combating antimicrobial resistance [23].

1.8 Rationale of the Study

The limitations of conventional ciprofloxacin administration underscore the need for alternative drug delivery strategies. Transdermal delivery offers potential strategies to address these issues by overcoming gastrointestinal degradation and first-pass metabolism, enabling sustained systemic drug exposure and improved patient compliance. NLCs represent a sophisticated lipid-based nanocarrier system aimed at enhancing drug solubility, attaining superior encapsulation efficiency, and facilitating sustained or controlled drug release. Their nanoscale size (typically 50-300 nm) and lipidic composition allow intimate interaction with the stratum corneum, facilitating both intercellular and trans-appendageal permeation

pathways. Incorporation of poorly soluble drugs like ciprofloxacin into NLCs can improve solubility, enhance systemic absorption, and maintain therapeutic plasma levels over prolonged period, addressing the pharmacokinetic and biopharmaceutical limitations of conventional formulations. Moreover, the use of a systematic formulation strategy, such as Quality by Design (QbD), allows for optimization of critical formulation variables to achieve reproducible particle size, entrapment efficiency, and stability. Despite prior research on lipid-based ciprofloxacin nanocarriers for localized or non-transdermal applications, there is limited evidence in the literature concerning NLCs designed for systemic transdermal delivery, highlighting the potential impact of developing a safe, effective, and patient-friendly transdermal ciprofloxacin system.

1.9 Research Aim and Objectives

To develop, optimize, and evaluate ciprofloxacin-loaded NLCs for transdermal delivery to achieve sustained systemic drug exposure.

The present study is undertaken with the following objectives:

i. To formulate and optimize ciprofloxacin-loaded nanostructured lipid carriers using Compritol® 888 ATO as the solid lipid, oleic acid as the liquid lipid, and Tween 80 as the surfactant, employing the hot homogenization method.

ii. To investigate the influence of formulation variables through a three-level, three-factor Box–Behnken design and assess the effects of lipid content, surfactant concentration, and homogenization time on key characteristics, including particle size, polydispersity index, zeta potential, and drug entrapment efficiency.

iii. To conduct a detailed characterization of the optimized NLC formulation using Fourier-transform infrared spectroscopy (FTIR), differential scanning calorimetry (DSC), transmission electron microscopy (TEM), and X-ray diffraction (XRD).

iv. To incorporate the optimized NLCs into a Carbopol-based hydrogel and evaluate its physicochemical properties, including spreadability, pH, viscosity, and storage stability.

v. To investigate the in vitro drug release, ex vivo skin permeation, and dermal compatibility of the ciprofloxacin-loaded NLC gel.

vi. To assess the antibacterial activity of the NLC gel against MRSA and compare it with that of ciprofloxacin dispersion.

1.10 Research Hypothesis

Ciprofloxacin-loaded NLCs, when formulated and optimized for transdermal delivery, will enhance systemic drug exposure, improve skin permeation, and maintain therapeutic plasma levels, while exhibiting acceptable dermal safety and antimicrobial efficacy against MRSA, compared to conventional formulations.

Chapter 2

Literature Review

2.1 Global and National Impact of Antimicrobial Resistance : A Literature Perspective

AMR is considered a major global health concern in the modern era. The World Health Organization has emphasized that AMR threatens to undermine years of progress in medical treatment and public health. This resistance can render common infections untreatable and jeopardize the efficacy of modern medical procedures, including organ transplantation, chemotherapy, and major surgical interventions (WHO, 2020) [24]. The seriousness of the crisis is highlighted by large-scale epidemiological analyses. A global assessment estimated that in 2019, antimicrobial resistance was directly responsible for about 1.27 million deaths and contributed to nearly 4.95 million additional fatalities, ranking it among the leading causes of death globally alongside HIV/AIDS and malaria [14]. Projections indicate that by 2050, AMR could result in up to 10 million deaths annually, with low- and middle-income countries experiencing the most severe impact, and a cumulative global economic burden potentially reaching 100 trillion USD [25]. The global epidemiology of AMR exhibits pronounced regional disparities. In high-income regions such as Europe, resistance rates among several key pathogens have stabilized or declined, largely due to effective antimicrobial stewardship programs,

rigorous infection control practices, and comprehensive surveillance systems. Reports from the European Centre for Disease Prevention and Control (ECDC) indicate that MRSA prevalence has decreased in multiple European Union member states over the past decade [26]. In contrast, resistance rates in Asia and Africa are increasing at an alarming pace. Studies from India report fluoroquinolone resistance exceeding 70% in *Escherichia coli*, while more than 60% of *Klebsiella pneumoniae* isolates exhibit resistance to cephalosporins (third-generation), as documented in the WHO Global Antimicrobial Resistance Surveillance System (GLASS) Report (2022) [27]. Multidrug-resistant *Klebsiella*, Acinetobacter, and MRSA are increasingly isolated from bloodstream and respiratory infections in sub-Saharan Africa, contributing to high mortality rates due to limited access to last-resort antibiotics [28].

South Asia, particularly Pakistan, bears a disproportionate burden of AMR. Unlike Europe and North America, where antibiotic sales are strictly regulated, antibiotics remain widely available over the counter in Pakistan, leading to their extensive misuse and overuse [29]. Several local studies reflect the gravity of the situation. Ali et al. reported that 45-65% of *E. coli* isolates showed resistance to fluoroquinolones, while more than 50% of *K. pneumoniae* isolates exhibited resistance against extended-spectrum cephalosporins [30]. Similarly, in tertiary care settings, *Pseudomonas aeruginosa* showed 30-50% resistance, which presents a challenge in the critical care management of patients with this infection [31]. Equally alarming is the substantial prevalence of MRSA, which has been reported to range from 36% to 61% across major Pakistani cities, including Lahore, Karachi, Islamabad, and Faisalabad. This trend reflects the escalating burden of AMR and underscores the urgent need for strengthened national surveillance and comprehensive antimicrobial stewardship programs in Pakistan [32].

On the economic and healthcare fronts, the AMR burden is high. Resistant pathogens often prolong the time of stay in hospitalization, intensive care admission, and the use of expensive second- or third-line antibiotics, such as carbapenem or glycopeptide. The World Bank estimated that if AMR is allowed to progress unabated, low-to-middle-income countries (LMICs) like Pakistan might

face a gross domestic product (GDP) reduction of 2-3.8% per year by 2050, mainly due to healthcare expenditures and productivity loss. This economic pressure adds to the clinical challenge in resource-limited healthcare systems, where diagnostic facilities and infection controls are poorly implemented [33].

Overall, the literature illustrates that AMR is not merely a microbiological problem but rather a multifaceted crisis involving clinical, economic, and societal dimensions. Although high-income countries have already managed to reverse some trends of resistance, Pakistan and other LMICs still experience a rapid rise in resistant infections, which requires immediate research into novel therapeutic strategies and delivery systems.

2.2 Methicillin-Resistant *Staphylococcus aureus*: Epidemiology and Clinical Significance

Staphylococcus aureus is an important human pathogen responsible for a wide spectrum of diseases, ranging from mild skin and soft tissue infections to serious invasive conditions such as pneumonia, osteomyelitis, endocarditis, and septicemia. The emergence of methicillin-resistant *S. aureus* (MRSA), first identified in 1961 shortly after methicillin was introduced, has made this bacterium increasingly challenging to manage in both hospital and community environments [34]. Globally, MRSA continues to contribute substantially to morbidity and mortality, with prevalence varying considerably across different regions and healthcare environments. Estimates from the CDC (2013) indicate that MRSA caused roughly 80,000 serious infections and about 11,000 deaths in the US in 2011 [35].

Although recent surveillance indicates that hospital-acquired MRSA infection rates have decreased in North America and Europe because of effective infection control and stewardship programs, rates of community-acquired MRSA strains are increasing, especially in younger, otherwise healthy individuals. In Europe, the prevalence of MRSA has started to fall over recent years in several countries, including the UK and the Netherlands [36]. However, Southern and Eastern Europe

continue to report higher rates, reaching over 25% of *S. aureus* isolates (CDC, 2013).

In marked contrast, Asian countries report persistently high rates of MRSA prevalence. In India, there have been reports from hospital-based studies of prevalence ranging from 30% to over 70% of *S. aureus* isolates, depending upon the region and population that was being evaluated [37]. Even in China, where interventions are present, MRSA rates have remained above 40% for many tertiary hospitals [38]. Similarly high rates have been documented in Middle Eastern countries, where less-than-optimal infection control practices and widespread antibiotic misuse have facilitated MRSA dissemination [39].

The situation in Pakistan is particularly concerning. Several studies conducted in diverse cities provide consistent high MRSA prevalence in both hospital and community settings. For example, one multi-center study concerning major hospitals from Lahore, Karachi, Faisalabad, and Islamabad documented MRSA rates between 36% and 61% [32]. A study conducted in tertiary care hospitals reported that over 50% of *Staphylococcus aureus* isolates were methicillin-resistant and exhibited marked resistance to ciprofloxacin, erythromycin, and aminoglycosides [29]. Community-acquired MRSA strains have also been noted in Pakistan, specifically in skin and soft tissue infections, like abscesses or cellulitis, indicating that MRSA is not confined to the hospital setting anymore [40]. The absence of a nationwide surveillance system restricts general epidemiological observations; however, the available literature keeps mentioning MRSA as one of the most common and dangerous organisms among multidrug-resistant pathogens in the country [41].

The clinical importance of MRSA is reflected by the severity of infections it causes. Rates of mortality from MRSA bacteremia, despite appropriate therapy, are as high as 20-30%. Invasive MRSA infections often require extended hospitalization, intravenous therapy with last-line antibiotics such as vancomycin or linezolid, and intensive care. Another critical factor contributing to this clinical burden is that MRSA has an astonishing ability to colonize skin, nasal passages, and medical devices, setting up persistent reservoirs for horizontal spread in healthcare settings

and the community. Biofilm development on indwelling medical devices, such as catheters and prostheses, presents a major therapeutic challenge, as bacteria embedded within biofilms can demonstrate up to a 1000-fold decrease in susceptibility to antimicrobial agents relative to planktonic cells [42].

In summary, literature evidence indicates that MRSA continues to be a highly resistant pathogen both globally and in Pakistan, thus highly contributing to morbidity, mortality, and economic burden. Its persistence in hospital and community settings, with a trend of multidrug resistance, indicates that MRSA is a critical focus for new therapeutic approaches, especially those capable of improving local delivery of drugs and overcoming resistance mechanisms.

2.3 Mechanisms of Resistance in MRSA: Literature Evidence

Multiple resistance mechanisms in MRSA collectively limit the therapeutic options (Figure 2.1). The most important driver is β-lactam resistance by the mecA/mecC genes, which encode the production of PBP2a with low affinity for β-lactams. Other drivers include overexpression of efflux pumps, like NorA; QRDR mutations in gyrA/grlA leading to high-level fluoroquinolone resistance; and development of biofilms, enhancing tolerance. Multidrug resistance is amplified through horizontal gene transfer, whereas virulence factors enhance bacterial survival and facilitate their transmission (Table 2.1) [43]. Collectively, these multidrug resistance patterns contribute to treatment failure and exacerbate the severity of clinical infections.

TABLE 2.1: Reported Mechanisms of Antibiotic Resistance in MRSA

Mechanism	**Molecular Basis**	**Clinical Impact**	**Ref**
β-lactam resistance	mecA/mecC → PBP2a with low β-lactam affinity	Failure of all penicillin and cephalosporins	[44]
Efflux pumps	NorA/NorB/MdeA extrude fluoroquinolones and dyes	Reduced ciprofloxacin efficacy	[45]

Table 2.1 continued from previous page

Mechanism	Molecular Basis	Clinical Impact	Ref
QRDR mutations	Ser84Leu (gyrA), Ser80Phe (grlA)	High-level ciprofloxacin resistance	[46]
Biofilm formation	icaADBC → extracellular matrix barrier	100-1000× increased tolerance to antibiotics	[47]
Horizontal gene transfer	Plasmids, SCCmec, transposons	Dissemination of multidrug resistance	[48]
Virulence factors (PVL)	Toxin-producing CA-MRSA strains	High transmissibility and persistence	[49]
Emerging resistance	VISA, linezolid resistance	Limited treatment options	[50]

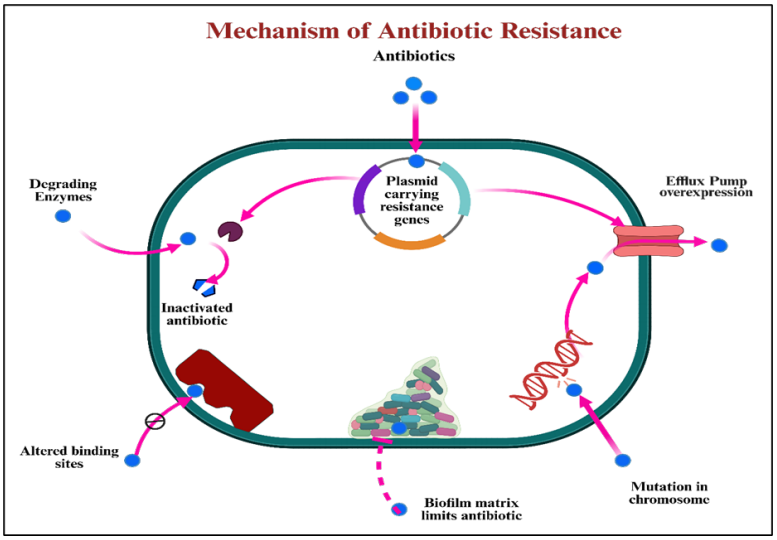

FIGURE 2.1: Major mechanisms of bacterial antibiotic resistance.

2.4 Ciprofloxacin in Antibacterial Therapy: Pharmacology, Resistance and Clinical Limitations

Ciprofloxacin is a second-generation fluoroquinolone that has emerged as one of the most extensively used synthetic antibiotics because of its broad-spectrum activity, ease of oral administration, and optimal pharmacokinetic profile. Ciprofloxacin exerts its bactericidal effect by inhibiting DNA gyrase (topoisomerase II) and

topoisomerase IV, enzymes essential for DNA replication, transcription, and repair. This dual mechanism enables potent activity against a broad range of Gram-negative and Gram-positive bacteria, including *Staphylococcus aureus*, *Escherichia coli*, *Klebsiella pneumoniae*, and *Pseudomonas aeruginosa* [51].

Ciprofloxacin is efficiently absorbed following oral administration, exhibiting a bioavailability of around 70% and achieving peak plasma levels within 1-2 hours. The drug is distributed widely into tissues, including the skin, lungs, and urinary tract. It is partially metabolized in the liver before being eliminated by the kidneys. Standard doses vary depending on the type of infection and range from 250-750 mg taken orally twice daily to 200-400 mg given intravenously every 12 hours. Topical forms, such as eye and ear drops, are commonly used for localized infections; however, despite their potential, transdermal delivery of ciprofloxacin remains underexplored for skin and soft tissue infections [52].

Despite its broad-spectrum activity and clinical importance, ciprofloxacin has several limitations related to its pharmacokinetics and physicochemical properties. It is classified as Class IV in the Biopharmaceutics Classification System, indicating that it has low water solubility and poor permeability [53]. Ciprofloxacin resistance has emerged as a critical problem worldwide. The problem is further compounded by the clinical limitations of ciprofloxacin therapy. The oral and IV administration can result in gastrointestinal, neurological, and musculoskeletal side effects, adding to the warnings provided by the FDA regarding fluoroquinolone safety [48]. Moreover, high systemic doses are often required to treat resistant infections, further increasing the risk of toxicity [54]. In addition, localized delivery-like topical/transdermal application for skin and soft tissue infections suffers from poor penetration through the stratum corneum with the conventional gel or cream formulation of ciprofloxacin [55].

This evidence shows that ciprofloxacin, though a mainstay in antibacterial treatment, faces problems with efficacy against MRSA and is limited in its use via conventional delivery. Thus, the need for novel delivery techniques is urgent. NLCs may offer advantages when used in topical gels with respect to skin penetration, sustained release, and restoration of antibacterial activity against resistant strains.

2.5 Conventional Drug Delivery Systems for Antibiotics: Limitations

Antibiotics such as ciprofloxacin have traditionally been administered through oral, intravenous (IV), intramuscular, and topical routes. Each route has contributed significantly to the management of bacterial infections, though important pharmacological and clinical limitations restrict their utility against resistant pathogens such as MRSA.

2.5.1 Oral Administration

Oral ciprofloxacin remains the most common route due to its convenient dosing and ∼70% bioavailability. However, oral formulations are associated with several drawbacks. Food and drug interactions (e.g., with antacids, iron, and calcium supplements) significantly reduce absorption. Furthermore, systemic administration often leads to side effects such as gastrointestinal upset, tendinopathy, and neurological disturbances, which have prompted FDA black-box warnings for fluoroquinolones [56]. Critically, oral administration fails to achieve sufficient concentrations for resistant MRSA infections, necessitating alternative delivery approaches [57].

2.5.2 Intravenous Administration

Intravenous therapy provides rapid and predictable plasma concentrations and is used for severe systemic infections. However, IV administration requires hospitalization, sterile procedures, and trained personnel, making it costly and inconvenient for long-term therapy. Repeated dosing can also lead to systemic toxicity, including renal and hepatic impairment. Moreover, IV antibiotics have limited ability to penetrate biofilms and poorly vascularized tissues, restricting their effectiveness against chronic MRSA infections [58].

2.5.3 Topical Formulations Creams, Ointments, Conventional Gels

Topical therapy is attractive for localized infections, as it avoids systemic toxicity and delivers drugs directly to the infection site. Ciprofloxacin ointments and gels have been evaluated for skin and soft tissue infections, but clinical outcomes remain unsatisfactory. The major challenge is the stratum corneum, the outermost skin barrier, which restricts hydrophilic drug permeation. Ciprofloxacin's moderate lipophilicity (log P ∼0.28) limits its passive diffusion, resulting in insufficient dermal concentrations for MRSA eradication. Conventional topical gels also suffer from burst release, instability, and poor sustained delivery [59].

These limitations highlight the urgent need for alternative delivery strategies capable of improving ciprofloxacin penetration, prolonging its release, and restoring its antibacterial activity against resistant strains. Nanostructured lipid carriers (NLCs) represent one such promising platform.

2.6 Advances in Nanotechnology for Antimicrobial Delivery

Nanotechnology serves as a promising strategy for addressing the challenges of conventional drug delivery systems. By engineering drugs at the nanoscale (1-1000 nm), nanoparticles can modify pharmacokinetics, improve solubility, prolong circulation time, and enhance tissue penetration. In infectious diseases, nanocarriers have been extensively explored to enhance antimicrobial efficacy, reduce toxicity, and bypass resistance mechanisms [18]

2.6.1 Liposomes

First described more than 50 years ago, liposomes have become increasingly popular as a means of improving the therapeutic outcome of drugs, owing to their

inherent capacity to encapsulate both hydrophilic and lipophilic antibiotics in their spherical, lipid bilayer vesicles, thus mimicking biological membranes and providing a targeted drug delivery system with an enhanced therapeutic index for combating antimicrobial resistance [60]. Because liposomal formulations are biocompatible and biodegradable, they have been studied for enhancing antibiotic treatments, especially for intracellular infections, biofilms, and drug-resistant bacterial strains [61]. Liposomes can improve intracellular antibiotic delivery by fusing with bacterial membranes, increasing uptake into infected macrophages, and penetrating bacterial biofilms.

There are several pharmaceutical advantages to using liposomes for antibiotic delivery, including increased solubility (especially for poorly water-soluble drugs), targeted delivery (e.g., accumulation at sites of infection via passive or active targeting), decreased systemic toxicity, protection of drugs from degradation, sustained drug release, and modification of the surface by PEGylation or ligand conjugation to extend circulation time and increase selectivity for bacteria [62]. Despite these benefits, liposomes have some drawbacks that limit their usefulness. Because liposomes are vulnerable to oxidation, hydrolysis, and drug leakage, instability is a serious issue. Additionally, they have short circulation durations and are quickly eliminated from the body by mononuclear phagocyte systems. Large-scale manufacture of liposomal formulations is also difficult due to the need for complex and costly manufacturing procedures. Hydrophilic antibiotics typically have low encapsulation efficiency, and drug leakage during storage can lessen the effectiveness of treatment [63].

2.6.2 Polymeric Nanoparticles

In biomedical applications, nanoparticles have drawn significant attention, especially for controlled drug release and antimicrobial therapy. Nanocapsules and nanospheres are examples of polymeric nanoparticles (PNPs), which are made from various polymers and range in size from 10 to 1000 nm. The polymers used to prepare nanoparticles should be non-toxic and non-antigenic; consequently,

they should be biocompatible with the host cells. Additionally, PNPs must be biodegradable within the human body. Biodegradation has a major impact on the pharmacokinetic profile of the nanocarrier due to its sustained release properties, nanoscale dimensions and compatibility with diverse cell types and tissues [64]. Delivering antibiotics directly to infection sites using nanoparticles offers a compelling strategy for lowering the required drug dose while still achieving effective treatment. This approach hinges on the sustained release capabilities of nanoparticles. Two common types of delivery carriers are nanospheres and nanocapsules. Nanospheres, lacking oil, feature a polymer matrix designed for consistent drug retention. Nanocapsules, on the other hand, possess an oily interior surrounded by a polymer shell, providing a space where medications can either dissolve or bind [65].

PNPs, a class of colloidal carriers, are frequently synthesized from polymers such as poly (lactic-co-glycolic acid) (PLGA), chitosan, and polycaprolactone (PCL). These nanocarriers are engineered to mediate regulated drug diffusion, augment drug stability, and enhance antibiotic dispersibility [66]. PNPs exhibit several distinctive properties advantageous for the delivery of antimicrobial agents. Firstly, PNPs can be synthesized from a broad spectrum of monomers, enabling precise modulation of their degradation kinetics and overall robustness. Secondly, through the selection of appropriate synthetic methodologies, such as controlled polymerization techniques like reversible addition-fragmentation chain transfer (RAFT), particulate attributes, including size, shell thickness, zeta potential, and the incorporation of functional groups, can be meticulously tailored. Polymeric nanoparticles can interact with the bacterial cell envelope through either passive or active targeting mechanisms. Passive targeting is fundamentally dependent on particle dimensions and the capacity of polymeric nanoparticles to generate pores that compromise the integrity of the microbial membrane structure [67]. The adaptable nature of PNPs permits their optimization for targeted delivery, ensuring effective permeation into resistant bacterial colonies, biofilms, and infected tissues. Notably, polymeric nanoparticles provide exceptional drug entrapment efficiency, particularly for lipophilic antibiotics, facilitating controlled and prolonged drug release [68].

Due to their flexible structure, surface modifications are possible, allowing for site-specific targeting via charge-switching or ligand conjugation. PNPs are ideal for systemic and localized antibiotic therapies because of their biodegradability, which provides low toxicity and safe metabolism. Additionally, some formulations exhibit enhanced biofilm penetration, which boosts the effectiveness of medications against persistent infections [69].

PNPs development is often a technically challenging process that calls for meticulous optimization of preparation methods, surfactants, and polymer types. Low encapsulation efficiency is still a problem, especially for hydrophilic antibiotics, necessitating ion pairing, polymer blending, or nanoprecipitation. Comprehensive biocompatibility evaluations are necessary because certain polymers may cause cytotoxicity or immunological reactions.

Furthermore, slow drug release might delay therapeutic action, specifically in the case of acute infections, which makes it challenging to eradicate bacteria promptly [70].

Additionally, resistance mechanisms including efflux pumps and dense biofilm matrices can still reduce efficacy, which has stimulated research into alternative lipid-based nanocarriers, particularly NLCs.

2.6.3 Dendrimers

Dendrimers, essentially highly branched nanoscale polymers, exhibit a distinctive tree-like architecture featuring a central core, multiple layers of branching units, and terminal functional groups. Owing to this organized structure, dendrimers function as efficient carriers for antibiotic delivery. They enhance properties such as drug solubility and stability, and facilitate improved cellular uptake, making them valuable tools in pharmaceutical applications [71]. A diverse range of dendrimer families, including poly-amidoamine (PAMAM), poly-propylene imine (PPI), and phosphorus-containing dendrimers, have been investigated for their antimicrobial applications. Among these, PAMAM dendrimers have garnered the

most substantial attention due to their precisely defined architecture and readily adaptable surface functionalities, while PPI dendrimers and phosphorus dendrimers have demonstrated potential for enhanced biocompatibility and reduced toxicity profiles [72]. Their inherent multivalency facilitates precise drug encapsulation, achieved either through covalent linkage or entrapment within internal cavities, thereby enabling targeted therapeutic intervention for bacterial infections. The clearly defined molecular structure of dendrimers confers additional benefits, such as modulated drug release and the capacity to permeate biofilms and extracellular bacterial colonies that are inaccessible to conventional antibiotics [73].

In comparison to traditional nanocarriers, dendrimer-based drug delivery systems present several compelling advantages. Antibiotic encapsulation at the molecular level ensures accurate and efficacious drug loading, thereby enhancing the therapeutic index of a wide spectrum of antimicrobial compounds. Moreover, the capability to modify terminal functionalities with specific ligands empowers dendrimers to achieve targeted delivery, directing antibiotics exclusively to the site of bacterial infection [61]. Their superior tissue penetration at the nanoscale enables access to challenging locations, such as intracellular bacterial colonies and biofilms. Dendrimers can also mediate prolonged drug release, thereby mitigate systemic adverse effects and reduce dosing frequency. Consequently, these combined attributes position dendrimers as a promising alternative to conventional antibiotic formulations [74]. Recent investigations further emphasize their aptitude in disrupting bacterial biofilms and delivering antibiotics to intracellular reservoirs of bacteria, including MRSA, *Pseudomonas aeruginosa*, and *Chlamydia*, where traditional formulations frequently exhibit therapeutic failure [75].

Dendrimers have several drawbacks that prevent them from being used in clinical settings, despite their benefits. Because of their potent cationic nature, higher-generation dendrimers (G$\geq$4) may cause hemolytic toxicity and harm biological membranes. Multiple-step, complex synthesis processes raise production costs and make large-scale manufacturing difficult. Furthermore, surface modifications of dendrimers are frequently necessary to enhance biocompatibility and avoid undesired interactions with non-target cells [76]. Their low biodegradability could cause them to accumulate in the body, requiring techniques for safe metabolism

and elimination. Moreover, non-specific interactions between biological systems and dendrimers may result in unexpected cytotoxic effects, necessitating additional optimization for clinical application [77]. Since the FDA has not yet approved any dendrimer antibiotic formulation, the translational gap is another significant limitation. Surface modification techniques like PEGylation, sugar conjugation, or carboxylation are commonly investigated to improve safety and biocompatibility and reduce cytotoxicity. Although dendrimers show special benefits for the delivery of antibiotics, toxicity and scalability issues prevent their clinical application [78].

2.6.4 Solid Lipid Nanoparticles

Solid lipid nanoparticles (SLNs) are an advanced drug delivery system made up of a combination of hydrophilic and lipophilic emulsifying agents, along with biodegradable lipids such as fatty acids, waxes, steroids, mono-, di-, and triglycerides. This composition enhances drug stability and systemic availability, facilitates sustained or regulated release, and minimizes associated toxicity. SLNs are usually between 10 and 1000 nm in size, which makes them ideal for delivering drugs to specific sites. Their nano size makes it easier for medications to be absorbed and penetrate, especially those with poor aqueous solubility [79]. Both lipophilic and hydrophilic drugs can be incorporated into SLNs, providing a wide range of medical applications. Additionally, several administration routes, including oral, intravenous, transdermal, pulmonary, and rectal delivery, have been studied [80]. SLNs, which are composed of solid lipid matrices like tristearin and Compritol, are stabilized by surfactants to preserve their structural integrity. Antibiotics are encapsulated in the lipid core of SLNs, which increases their therapeutic efficacy by shielding them from enzymatic degradation. SLNs are a promising alternative for treating drug-resistant infections because of their small size and lipid composition, which allow them to readily penetrate bacterial biofilms and infected tissues [81].

SLNs have several advantages when it comes to the delivery of antibiotics. One of

their primary benefits is that they are produced without the incorporation of organic solvents, which makes the process safer and more environmentally friendly. Additionally, by providing a tunable release of the medication, SLNs minimize the probability of systemic side effects and reduce frequent dosing. Additionally, they improve the solubility and absorption of antibiotics that have poor aqueous solubility, increasing their bioavailability. Additionally, because of their biocompatibility and biodegradability, SLNs are appropriate for long-term therapeutic applications. SLNs can be produced at a commercial scale for clinical applications through high-pressure homogenization techniques [82]. In addition to oral and intravenous routes, SLNs have been investigated for topical applications in skin and burn infections, ocular delivery for keratitis, and intranasal administration in bacterial meningitis. Recent studies also highlight the benefits of polymer-coated SLNs (e.g., chitosan, PEGylated systems) for prolonged circulation and improved mucoadhesion [83].

Despite their advantages, SLNs face certain limitations. Drug expulsion during storage is a major concern, as lipid crystallization can lead to leakage of encapsulated antibiotics, reducing their effectiveness. They also have a low loading capacity, particularly for hydrophilic drugs, with encapsulation efficiencies often below 5% [84]. Some lipid formulations may induce cytotoxicity or immune responses, requiring careful selection of lipid components. Additionally, complex manufacturing processes and scalability challenges can hinder widespread clinical adoption [85].

2.6.5 Recent Evidence from Comparative Studies

Recent advancements show that NLCs improve the activity of antibiotics on both sensitive and resistant bacterial strains significantly [86]. Notably, the NLCs using the rationally selected lipids (glyceryl monostearate, oleic acid, and soy lecithin) enhanced ceftriaxone solubility fivefold [87]. In vitro, studies confirmed that ciprofloxacin and oxacillin-loaded NLCs have two- to four-fold increased antimicrobial performance against methicillin-resistant *Staphylococcus aureus* (MRSA). The oxacillin-NLC formulation also altered bacterial membranes and induced DNA

mutations, resulting in the downregulation of several proteins, including enolase and ornithine carbamoyl transferase. The particle size of NLCs varied between 86 to 255 nm with zeta potential between 19.5 and +2. 4 mV. A slightly positive charge was found to facilitate electrostatic interactions with the negatively charged bacterial membrane and improve drug uptake [88]. The polymyxin B-loaded NLCs with surface modification demonstrated 2-3-fold enhanced bacterial killing and no appreciable cytotoxicity against fibroblast cells [89].

Despite these benefits, several difficulties still need to be addressed. Rifampicin-loaded NLCs showed a 20% drug loss after three months of storage due to lipid crystallization, which is another formulation stability issue [90]. Methods such as high-pressure homogenization (HPH) enable the scalable production of nanomedicines, but may introduce variability in particle size [91]. As shown in Figure 2.2, NLCs are better than SLNs and compete well with liposomes regarding drug loading, stability, and biocompatibility. While dendrimers allow highly specific targeting, polymer-based nanoparticles are particularly advantageous for achieving prolonged and regulated drug release. Selecting the most suitable nanocarrier depends on the antibiotic's physicochemical characteristics, the intended site of action, and whether clinical priorities favor targeted delivery or prolonged therapeutic effects.

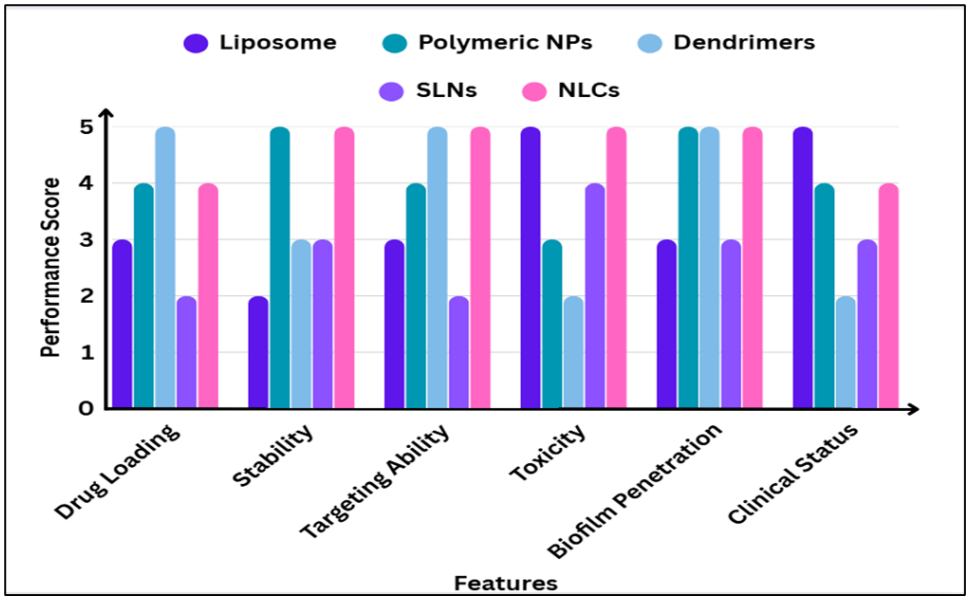

FIGURE 2.2: Comparison of drug loading, stability, targeting ability, toxicity, biofilm penetration, and clinical status of major nanocarrier systems, highlighting the favorable overall performance of NLCs.

2.7 Nanostructured Lipid Carriers as Advanced Platforms for Antibiotic Delivery

Introduced by Müller et al. in 1999-2000, NLCs represent an improved generation of lipid-based nanoparticles designed to overcome SLN limitations, including inadequate drug loading and storage-related drug loss. The inclusion of both solid and liquid lipids, along with surfactants, allows NLCs to achieve enhanced drug loading, stability, and sustained release [92]. These properties make NLCs very appealing for the delivery of antibiotics, as challenges like poor solubility, rapid degradation, and drug resistance require the use of novel carrier systems.

Over time, these structural imperfections inhibit drug expulsion and enhance their ability to absorb more drug molecules. The resulting nanoparticles, which are usually 10-500 nm in size, exhibit excellent stability and controlled release properties and can encapsulate both hydrophilic and lipophilic drugs [93]. These advantages have made NLCs highly effective antibiotic carriers. They enhance therapeutic efficacy against resistant bacterial strains by boosting bioavailability, prolonging release, and potentially circumventing bacterial defenses.

2.7.1 Composition of NLCs

The three main ingredients that are typically used in the formulation of NLCs are emulsifiers or surfactants, liquid lipids (oils), and solid lipids. Solid lipids like tristearin, cetyl palmitate, stearic acid, or glyceryl behenate provide a rigid framework that stabilizes the carrier and maintains the integrity of the nanoparticles. The solid base is supplemented with liquid lipids like oleic acid, medium-chain triglycerides, or squalene. Because the highly ordered crystalline structure of solid lipids is disrupted when liquid lipids are added, the lipid matrix becomes imperfect [94]. These imperfections serve as empty spaces that could trap more drug molecules, thereby improving the drug's loading capacity and preventing it from being expelled during storage. The third essential element is an emulsifier or surfactant, such as phospholipids, Tween, Poloxamers, or bile salts.

They improve the dispersion of the nanoparticles in aqueous environments, stabilize them, and prevent aggregation. The solid and liquid lipids ratio is essential for determining the final properties of the NLCs, including stability, particle size and entrapment efficiency. A higher proportion of liquid lipid usually enhances drug incorporation; however, a sufficient amount of solid lipid content ensures rigidity and controlled release behavior [95].

Because of their distinct advantages over SLNs resulting from their unique composition, NLCs are a better option for administering antibiotics in clinical applications. Figure 2.3 illustrates the structural composition of NLCs.

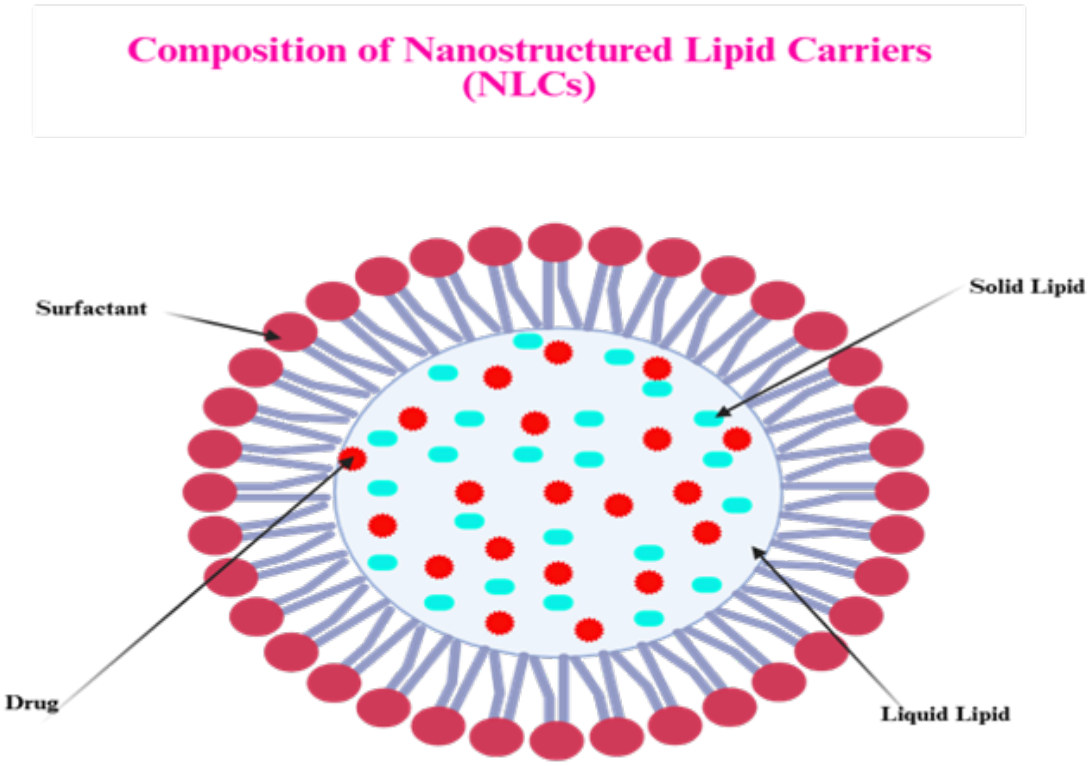

FIGURE 2.3: Structural Composition of NLCs.

2.7.2 Common Excipients Used in NLCs

The formulation of NLCs relies on a combination of lipids (solid and liquid), surfactants, and stabilizers, each contributing specific functional roles. These excipients help maintain particle stability, enhance drug loading, and modulate drug release

characteristics. Table 2.2 summarizes common excipients used in NLCs and their functional roles.

TABLE 2.2: Common Excipients Used in NLCs

Excipient Type	**Examples**	**Functional Role in NLCs**	**Ref**
Solid lipids	Behenic acid, Cetyl palmitate, Compritol® 888 ATO (glyceryl behenate), Glyceryl monostearate, Glyceryl distearate, Glyceryl tristearate, Palmitic acid, Precirol® ATO 5, Stearic acid, Tripalmitin	Provide matrix structure; control drug release; enhance stability; promote sustained delivery & occlusion	[96]
Liquid lipids	Oleic acid, Labrasol® , Miglyol® 812, Capryol® 90, Isopropyl myristate, and Labrafac™ PG	Induce structural irregularities, enhance drug encapsulation, and minimize drug leakage and improve entrapment efficiency	[97]
Surfactants	Tween-80 (polysorbate-80), Poloxamer 188, Cremophor® EL, Span® 20	Reduce interfacial tension; stabilize dispersion; prevent aggregation; favor nanosized particle formation	[98]
Co-surfactants / stabilizers	Lecithin, PEG-400, Transcutol® P	Improve wettability; enhance solubilization; increase entrapment efficiency; improve formulation stability	[99]

2.7.3 Role of Selected Excipients Used in the Formulation

Specific excipients used in their formulation strongly influence the performance and structural attributes of NLCs. For this study, Compritol® 888 ATO as a solid lipid, oleic acid as a liquid lipid, and Tween-80 as a surfactant were used based on documented compatibility and functional contributions to enhancing the stability of nanoparticles, drug loading, and dermal delivery.

Compritol® 888 ATO was selected because of its high melting point, biocompatibility, and ability to form a stable lipid matrix supporting controlled release. The

long-chain fatty acid structure allows strong lipid packing, while still retaining flexibility within the NLC matrix, enhancing sustained release and occlusion. The occlusive effect reinforces skin hydration, improving the drug permeation deeper into the skin [100].

Oleic acid is a widely used liquid lipid that was incorporated to create structural imperfections within the lipid matrix, thereby enhancing drug loading and minimizing drug leakage during storage. This compound is indeed a well-established skin penetration enhancer because it disrupts the ordered arrangement of stratum corneum lipids, thus improving transdermal transport. Its amphiphilic nature enhances the solubilization and incorporation of ciprofloxacin, thus supporting effective encapsulation [101].

Tween-80 was used as a surfactant, lowering the interfacial tension between the lipid and aqueous phases, which in turn helped in stabilizing the dispersion. Its high HLB value favors a uniform, nanosized particle and avoids aggregation. The surfactant facilitates better wettability and solubilization of the drug to improve the entrapment efficiency and the stability of the formulation [102].

Collectively, these excipients were chosen based on their synergistic capability for enhancing the physicochemical characteristics, skin permeation potential, and overall therapeutic performance of ciprofloxacin-loaded NLCs.

2.7.4 Classification of NLCs

Depending on the arrangement of their lipid matrix, NLCs are categorized into three primary types: imperfect (Type I), multiple (Type II), and amorphous (Type III) [103].

2.7.4.1 Type I: Imperfect NLCs

Imperfect-type NLCs are produced by blending solid lipids with liquid lipids, like fatty acids or triglycerides. This process intentionally disrupts the typical crystalline order found in solid lipids, introducing irregularities within the structure.

These imperfections play a critical role; they serve as additional sites for drug accommodation, thereby improving drug loading efficiency. Drug molecules encapsulated within NLCs may exist in an amorphous state or as molecular dispersions throughout the lipid matrix. In terms of drug release, NLCs characteristically provide an initial moderate burst release, which is then followed by a more sustained and controlled release phase. The exact release behavior is predominantly impacted by factors such as the proportion of solid to liquid lipids and the overall crystallinity of the carrier system. These carriers have proven particularly useful for hydrophobic drugs with low solubility, such as curcumin and paclitaxel. Their incorporation significantly reduces drug loss during storage and enhances drug entrapment efficiency, both critical factors for maintaining therapeutic effectiveness. It should be noted, though, that excessive addition of liquid lipids may destabilize the structure and cause phase separation, compromising system performance. Still, when appropriately formulated, these carriers can substantially improve drug incorporation and bioavailability [104].

The visual presentation of this type is depicted in Figure 2.4 (Type I)

2.7.4.2 Type II: Multiple NLCs

Multiple-type NLCs, described as "oil-in-solid lipid-in-water" systems, are characterized by a higher concentration of liquid lipids embedded within a solid lipid matrix. When the concentration of liquid lipids surpasses their solubility threshold, small oil compartments emerge inside the matrix, serving as reservoirs for lipophilic drugs. This design enhances drug encapsulation efficiency compared to more conventional drug delivery systems. Notably, the release of drugs from these internal reservoirs is extended over time, as the active compounds diffuse gradually through the solid lipid barrier. This sustained-release mechanism reduces premature drug leakage and supports long-term drug retention, which is particularly advantageous for unstable drugs that necessitate controlled delivery, such as antifungals, retinoids, and antibiotics. It is essential to carefully optimize the solid and liquid lipids ratio; an excessive quantity of liquid lipid may disrupt the integrity of the matrix and destabilize the system. Ultimately, these NLCs offer

significant benefits for chronic therapies that require continuous and prolonged drug action [105]. Figure 2.4 (Type II) depicts a schematic representation of this structural configuration.

2.7.4.3 Type III: Amorphous NLCs

Amorphous-type NLCs bypass the issue of lipid crystallization by incorporating excipients such as hydroxy octacosanyl hydroxystearate and medium-chain triglycerides. This approach creates a disordered, amorphous matrix without long-range structural order. As a result, drug molecules remain stable and are less likely to be expelled during storage, an obvious advantage, particularly for sensitive compounds. Drugs are distributed quite evenly throughout this amorphous structure, providing a uniform, controlled release and minimizing undesirable burst effects. This characteristic makes amorphous NLCs especially suitable for challenging drugs like peptides or antioxidants. Although the formulation process can be more complex compared to traditional systems, the reliability and therapeutic potential of these NLCs make them a compelling option for advanced drug delivery [106]. Figure 2.4 (Type III) illustrates the schematic configuration of this amorphous NLC structure.

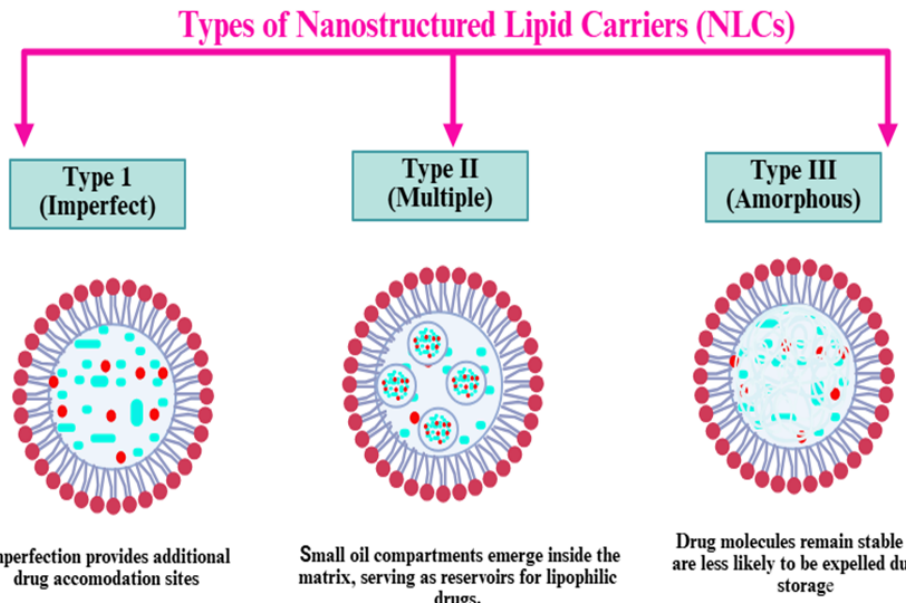

FIGURE 2.4: Schematic illustration of NLC types: (Type I) imperfect crystal, (Type II) multiple, and (Type III) amorphous, showing differences in lipid matrix arrangement and drug accommodation.

2.7.5 Techniques for the Preparation of NLCs

NLCs can be produced through a range of well-established techniques, with the selection of a particular method guided by the physicochemical properties of the API, the composition of the lipid matrix, surfactant characteristics, the intended route of administration, and considerations for large-scale manufacturing. Among these approaches, high-pressure homogenization (HPH) is regarded as suitable for industrial production and can be implemented in either hot or cold homogenization modes, depending on the formulation requirements. Hot homogenization involves heating the lipid-drug mixture above the lipids melting point and dispersing it into a hot surfactant solution, followed by high-pressure processing and cooling to form NLCs ideal for lipophilic drugs but unsuitable for thermolabile compounds. Cold homogenization, on the other hand, minimizes thermal degradation by processing the cooled and pulverized lipid-drug matrix at low temperatures, though it yields a broader particle size distribution [107]. The microemulsion technique utilizes a warm microemulsion of lipid, surfactant, and aqueous phase, which is dispersed in cold water to precipitate NLCs; it is simple and reproducible but limited by high surfactant requirements and scalability concerns [108]. The emulsification-solvent evaporation technique involves dissolving the lipid and drug in an organic solvent, dispersing this solution into an aqueous phase containing surfactants, and subsequently evaporating the solvent to generate NLCs. This technique is particularly suitable for thermolabile and hydrophilic drugs; however, it is generally unsuitable for parenteral applications due to the potential toxicity associated with residual solvents [109]. Ultrasonication employs high-frequency vibrations to reduce droplet size in a hot surfactant solution, forming NLCs upon cooling; it is cost-effective for lab-scale production but poses risks of metal contamination and overheating [110]. Solvent injection involves rapidly adding lipids dissolved in a water-miscible solvent to an aqueous surfactant solution, triggering nanoparticle formation via solvent diffusion. Despite its efficiency, the method is limited by difficulties in solvent elimination and scaling up [111]. Additional methods include the use of double emulsions (W/O/W) for hydrophilic drugs, as well as spray drying and freeze drying for powder conversion and oral delivery. Phase inversion, which

relies on temperature shifts in emulsions, is also employed. For antibiotic formulations, solvent-free methods such as HPH, microemulsion, and ultrasonication are preferred to preserve drug activity and minimize toxicity. Sterile manufacturing or post-process sterilization is essential for parenteral and ophthalmic applications, and the choice of method must align with drug stability, entrapment efficiency, release kinetics, and regulatory standards [112]. Figure 2.5 depicts a diagrammatic representation of the key techniques utilized for the preparation of NLCs. Examples of antibiotic-loaded NLCs formulations and their applications are presented in Table 2.3.

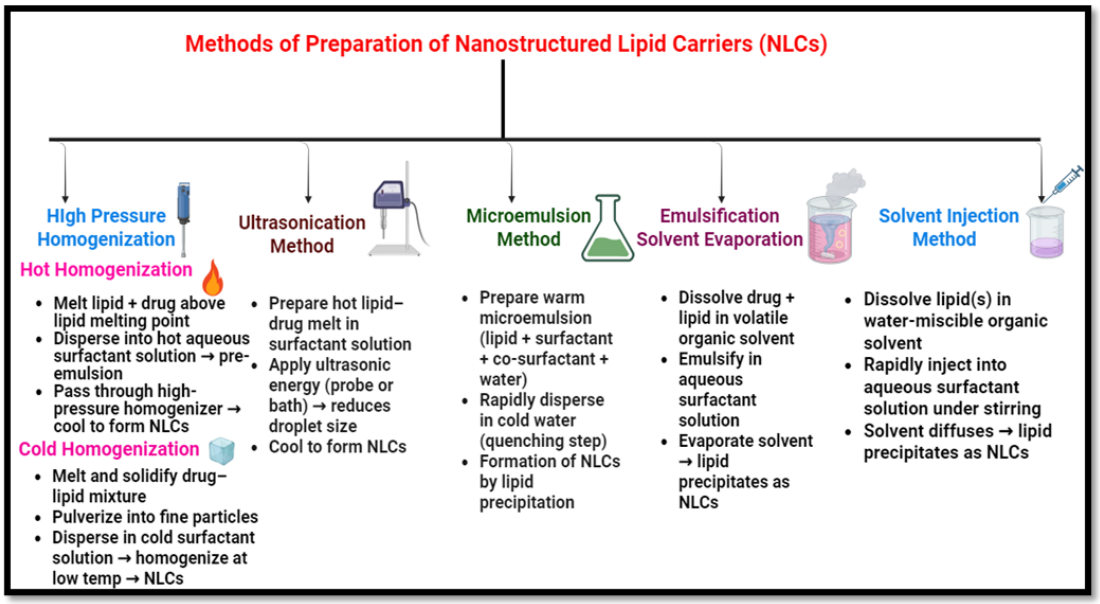

FIGURE 2.5: Schematic overview of principal fabrication approaches used for NLCs.

TABLE 2.3: Antibiotic-Loaded NLCs

NLC Formulations	**Application**	**Key Findings**	**Improvement**	**Ref**
Ciprofloxacin / Rolipram NLCs	MRSA bacteremia	Enhanced antibacterial activity, sustained release, and improved survival in mice.	∼2× antibacterial activity	[113]
PEGylated Trimethoprim / Sulfamethoxazole NLCs	MRSA infection	Reduced renal/hepatic toxicity, targeted delivery to infection sites.	Reduced off-target toxicity	[114]

Table 2.3 continued from previous page

NLC Formulations	Application	Key Findings	Improvement	Ref
Sodium Colistimethate / Amikacin NLCs	Pseudomonas wound infections	Functionalized dermal substitutes showed potent antibacterial effects.	Not specified	[115]
Clarithromycin NLCs	Helicobacter pylori infection	Improved gastric stability and mucosal adhesion, enhanced eradication efficacy.	Enhanced gastric residence	[116]
Vancomycin NLCs	MRSA biofilm infections	Improved biofilm permeation and sustained drug release were observed relative to the unencapsulated drug.	3× efficacy in biofilm model	[117]
Rifampicin NLCs	Tuberculosis therapy	Increased lung bioavailability (3.5-fold) and reduced dosing frequency.	Reduced dosing frequency	[118]
Tobramycin NLCs	Cystic fibrosis (lung delivery)	Improved transport across biological barriers enhanced local efficacy.	Improvement Compared to Free Drug	[119]
Azithromycin NLCs	Chlamydial infections	Prolonged drug release, improved intracellular targeting.	∼2× antibacterial activity	[120]
Ciprofloxacin-DNase NLCs	Pseudomonas aeruginosa biofilms	Synergistic biofilm disruption enhanced antibiotic penetration.	Reduced off-target toxicity	[121]
Silver Sulfadiazine NLCs	Burn wound infections	Sustained antimicrobial action, accelerated wound healing.	Not specified	[122]

2.8 Advantages of NLCs in Antibiotic Delivery

2.8.1 Enhanced Drug Loading and Stability

The combination of liquid and solid lipids within the matrix causes imperfections in the crystalline structure, thereby increasing the space for drug entrapment.

This design enhances drug loading and minimizes drug expulsion during storage, significantly improving the formulation's stability [123].

2.8.2 Improved Bioavailability and Controlled Release

The solubility and permeability of antibiotics can be increased by NLCs, ultimately increasing the bioavailability. This design ensures a continuous release of the drug, enabling it to remain at the desired therapeutic levels for prolonged periods and consequently reducing dosing frequency [124].

2.8.3 Targeted Delivery and Reduced Toxicity

Surface modification of NLCs for targeting specific tissues or sites of infection (PEGylation). For instance, PEGylated NLCs containing trimethoprim / sulfamethoxazole showed augmented antibacterial activity against MRSA and diminished renal and hepatic toxicity in vivo [125].

2.8.4 Efficacy Against Biofilms

NLCs have demonstrated the ability to penetrate bacterial biofilms, a significant advantage given that these structures often exhibit substantial resistance to traditional antibiotics. Their ability to deliver antibiotics directly into the biofilms can significantly enhance the antimicrobial efficacy, targeting biofilm-related resistance mechanisms [126]. As shown in Figure 2.6, NLCs can infiltrate the biofilm and bypass efflux pumps, while conventional antibiotics are ejected or blocked.

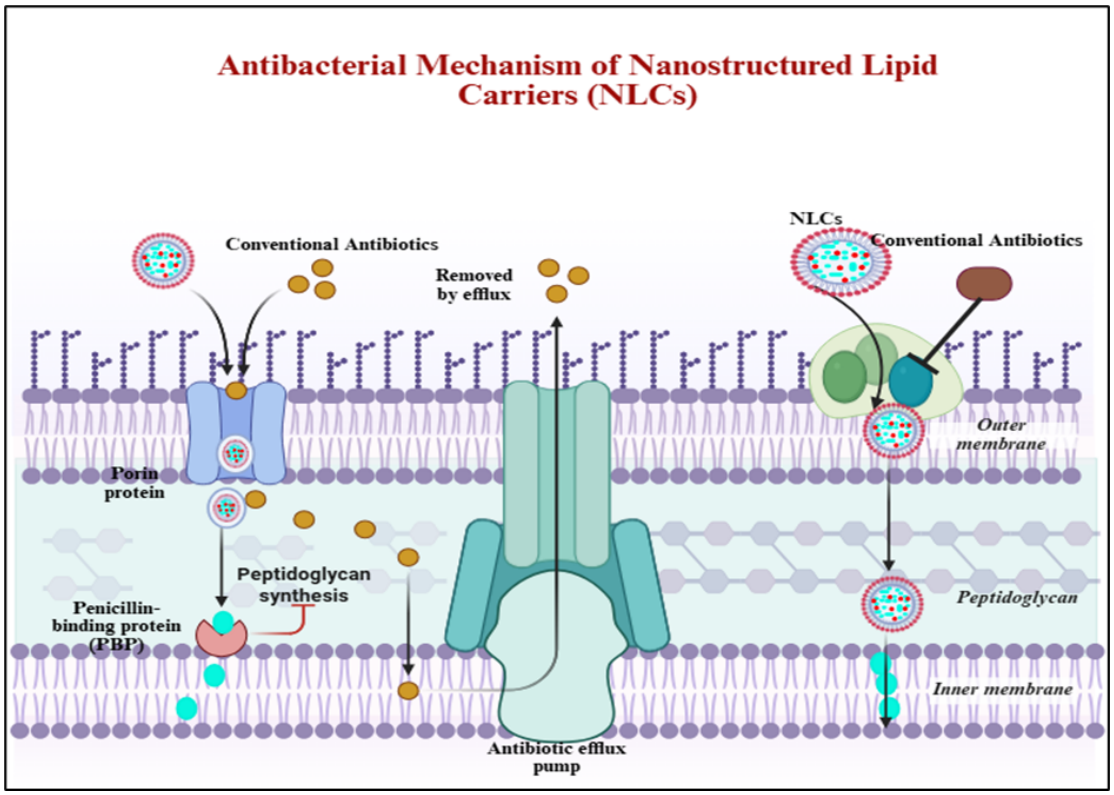

FIGURE 2.6: Schematic comparison of biofilm penetration by free antibiotics and antibiotic-loaded NLCs, highlighting enhanced penetration and antibacterial efficacy with NLCs.

2.9 Mechanisms of Enhanced Antibacterial Action via Transdermal NLCs

NLCs boost the antibacterial activity of drugs by circumventing biological and physicochemical barriers in topical delivery. Their small size facilitates interaction with the stratum corneum and penetration into deeper skin layers, while the mixed lipid matrix increases drug encapsulation and enables sustained release at infected tissues. Lipids like oleic acid disrupt the structure of the stratum corneum, improving permeability and facilitating deeper diffusion. Solid lipids, such as Compritol, enhance skin hydration, further aiding drug permeation [127].

Encapsulating antibiotics in NLCs protects them from degradation and increases

their stability, particularly for drugs like ciprofloxacin, which often has poor permeability in standard formulations. The sustained release from NLCs helps maintain therapeutic concentrations over time, which improves bacterial killing and reduces the risk of resistance. Overall, NLCs significantly enhance both topical drug delivery and antibacterial efficacy compared to conventional formulations [128].

2.10 Carbopol Gel and Nanogel-Based Drug Delivery Systems

Topical gels are important semisolid dosage forms used to deliver therapeutic agents directly to the skin for local or transdermal effects. Among the various polymeric gels, Carbopol® is particularly popular due to its excellent viscosity, bioadhesive properties, and user-friendly characteristics. Carbopol is a synthetic polymer composed of acrylic acid units arranged in a three-dimensional, cross-linked network, which swells and forms a gel structure upon neutralization. Additionally, Carbopol gels are non-greasy and cosmetically appealing, making them ideal for dermatological formulations [129].

Incorporating lipid-based nanoparticles, such as NLCs, into Carbopol gels creates nanogels that enhance drug delivery and localization while ensuring sustained release. This approach ensures longer skin retention of the drug, resulting in enhanced clinical performance. Studies indicate that Carbopol-based nanogels enhance the dermal delivery of antibiotics, reduce systemic exposure, and minimize irritation, making them especially beneficial for treating superficial infections and resistant pathogens [130].

2.11 Literature Gap

AMR represents a major global health challenge, MRSA classified as a critical-priority bacteria by the World Health Organization in 2017. Management of

MRSA infections is complicated by poor drug penetration, systemic toxicity associated with high-dose therapy, and rapid emergence of resistance. In Pakistan, over 60% of hospital-acquired infections are attributed to MRSA, highlighting the need for alternative therapeutic approaches. Over the last twenty years, nanotechnology-driven drug delivery systems, especially NLCs, have attracted considerable interest because of their high drug-loading potential, biocompatibility, physical stability, and capacity to improve drug penetration through the skin. Ciprofloxacin-loaded NLCs, as reported in several studies, typically demonstrate nanometric particle sizes (<200 nm), high encapsulation efficiency (>80%), sustained drug release for up to 48 hours, and improved antibacterial activity compared with free ciprofloxacin [131–133]. Despite these promising attributes, existing literature continues to exhibit critical limitations that must be addressed to advance the clinical translation of these systems.

i. Limited focus on MRSA - Most of the studies investigated ciprofloxacin NLCs against *E. coli* or non-resistant strains.

ii. Lack of Optimized Formulations: Though ciprofloxacin NLCs have been reported, no systematic optimizations using advanced statistical designs like Box-Behnken Design have been performed.

iii. Despite promising vitro performance, many NLC systems have not progressed beyond suspension formulations, restricting their clinical relevance. Formulation into a Carbopol-based gel represents a practical strategy to enhance stability, application convenience, and patient compliance.

iv. Lack of thorough evaluation: Most of the reports restrict themselves to in vitro characterization and antibacterial assays, with limited information about ex vivo skin permeation, in vivo safety studies concerning skin irritation, and stability studies, which are vital data for translational potential.

v. Lack of regional context: Despite the high prevalence of MRSA in South Asia, no study to date has systematically developed and characterized a ciprofloxacin-loaded NLC gel specifically intended for transdermal delivery against MRSA infections in this region.

These limitations thus underpin the need for a ciprofloxacin-loaded NLC gel that is systematically optimized, clinically applicable, and well-characterized for transdermal application.

Chapter 3

Material and Methods

3.1 Materials

The active pharmaceutical ingredient (API) ciprofloxacin was provided by Bio-Labs (Pvt.) Ltd., Pakistan. The screening lipids Geleol™ (glyceryl monostearate), Precirol® ATO 5 (glyceryl palmitostearate), Capryol® 90 (propylene glycol monocaprylate), and Labrafac™ PG (propylene glycol dicaprylocaprate) were obtained from their respective manufacturers, with Compritol® 888 ATO (glyceryl behenate) provided as a complimentary research sample through the manufacturer's academic program (Gattefossé, France). Oleic acid and Tween-80 were obtained from Sigma-Aldrich. Eucalyptus oil, dimethyl sulfoxide (DMSO), and triethanolamine (TEA), were sourced from BioShop Canada Inc. Sodium chloride, disodium hydrogen phosphate, and methanol were procured from Merck. Carbopol® 940, isoeucalyptol, and other analytical-grade reagents were supplied by Sigma-Aldrich through authorized distributors. Distilled water was prepared internally using the purification system at the Capital University of Science and Technology (CUST), Islamabad, and all chemicals and excipients were of pharmaceutical or analytical grade, used directly without further purification.

3.2 Animals and Ethical Approval

All procedures were approved by the Research Ethics Committee, Faculty of Pharmacy, CUST, Islamabad (Approval No.: REC/FoP/F2025/04), and followed national and institutional guidelines for laboratory animals. Adult New Zealand White rabbits (*Oryctolagus cuniculus*), weighing 1.8–2.2 kg, were maintained under controlled temperature (22 ± 2 °C), humidity (55 ± 5%), and a 12-hour light/dark cycle, with free access to standard feed and water.

3.3 Methods

3.3.1 Lipid Screening and Selection

A preliminary screening of several solid and liquid lipids as potential ingredients for the formulation of ciprofloxacin-loaded NLCs was done according to previously reported method with slight modification [134]. The screening was conducted by adding 1 mg of ciprofloxacin (at a time) to 250 mg of each lipid and the resulting mixture was then heated to around 80 ± 2 ^{o}C under stirring at 2000 rpm to melt the lipid. Compritol® 888 ATO, Stearic acid, Geleol™, Precirol® ATO 5 were among the solid lipids tested; Oleic acid, Capryol® 90, and Labrafac™ PG were among the liquid lipids. The drug solubility was evaluated visually when a clear solution was obtained without any drug crystals. The process was carried out repeatedly until drug saturation was achieved. Lipids that completely solubilized ciprofloxacin without the formation of visible crystals were considered compatible and selected for further formulation development. All experimental procedures were executed in triplicate, with observations carefully recorded.

3.3.2 Preparation of Ciprofloxacin-Loaded NLCs

A hot homogenization technique was used to prepare ciprofloxacin-loaded NLCs, with minor modifications to a previously published method [135].

The formulation was prepared using a total of 400 mg of lipids, composed of both solid (Compritol 888 ATO) and liquid (oleic acid) lipids. Solid lipids accounted for 60–80% of the total, with the remainder being liquid lipids. Ciprofloxacin (0.3% w/v) was added to the melted lipid mixture, which was maintained at 85 °C with continuous stirring. The aqueous phase, containing Tween-80 at 1–3% w/w (relative to total lipids), was heated to the same temperature and gradually added to the lipid phase under stirring. This mixture was then subjected to high-speed homogenization at 25,000 rpm for 5–15 minutes. Finally, the ciprofloxacin-loaded NLC dispersion was allowed to cool slowly to room temperature (Figure 3.1).

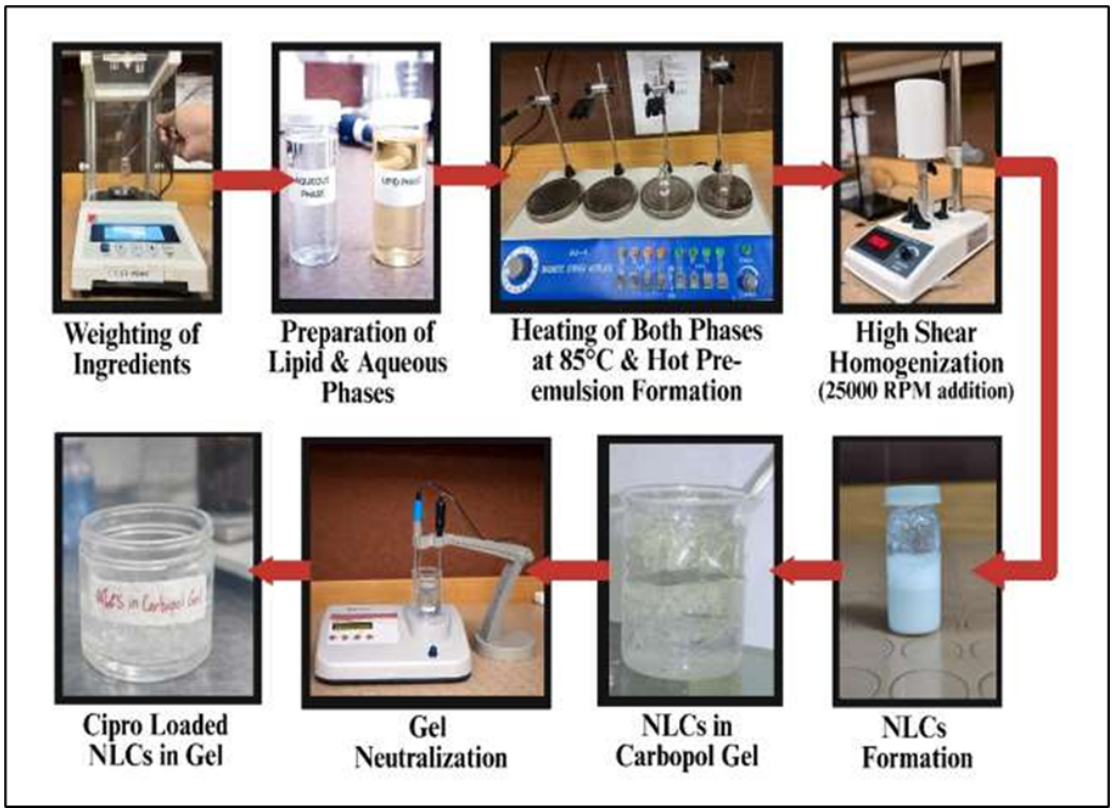

FIGURE 3.1: Schematic diagram of the homogenization method for preparation of ciprofloxacin-loaded NLCs.

3.3.3 Experimental Design and Optimization

Design-Expert® software (Version 10.0, State-Ease Inc., Minneapolis, USA) was employed to optimize the formulation using a three-level, three-factor Box–Behnken design (BBD).

The factors investigated were as follows: Solid lipid content (as a percentage of total lipid), between 60% and 80%; surfactant concentration (as a percentage w/w of total lipid), between 1% and 3%; and homogenization time, between 5 and 15 min [136].

The experimental design consisted of 17 runs (12 factorial runs and 5 center points to assess variability and model adequacy), and the measured responses were particle size (nm), entrapment efficiency (% EE), zeta potential (mV), and polydispersity index (PDI).

This model included interaction and quadratic terms to assess antagonistic or synergistic effects on the measured responses, and Response Surface Methodology (RSM) was employed to examine the effects of individual and combined factors on particle size, PDI, zeta potential, and EE.

Numerical point prediction was used to choose the optimal formulation, which maximized EE and maintained a stable zeta potential while minimizing particle size and PDI [137, 138].

For preparation and optimization of ciprofloxacin-loaded NLCs, independent and dependent variables used in the Box–Behnken design are presented in Table 3.1.

TABLE 3.1: Independent and dependent variables employed in the Box–Behnken design for the preparation and optimization of ciprofloxacin-loaded NLCs.

Factors	Level used		
Independent Variable	**Low (-1)**	**Medium (0)**	**High (+1)**
A=Solid Lipid (% of Total Lipid)	60	70	80
B=Surfactant (%w/w)	1	2	3
C=Homogenization Time (min)	5	10	15
Dependent Variable		**Goal**	
R1=Particle Size (nm)		Minimize	
R2 = Poly Dispersity Index (PDI)		Minimize	
R3= Zeta Potential (mV)		Maximize	
R4= Entrapment Efficiency (%)		Maximize	

3.4 Characterization of Ciprofloxacin - Loaded NLCs

3.4.1 Measurement of Particle Size, Polydispersity Index and Zeta Potential

Ciprofloxacin-loaded NLCs were evaluated for particle size (Z), PDI, and zeta potential using dynamic light scattering (DLS). A suitable volume of NLC dispersion was diluted in deionized water, and a Zetasizer Nano ZS (Malvern Instruments, UK) was used to examine it at 25°C [139].

3.4.2 Determination of Entrapment Efficiency

The entrapment efficiency (%EE) of ciprofloxacin-loaded NLCs was calculated by ultrafiltration to separate the entrapped drug from the free drug. The ciprofloxacin-loaded NLCs were pelleted by centrifuging a 0.5 mL sample of the NLC suspension at 14,000 × g at 4°C for 20 min, leaving unentrapped ciprofloxacin in the supernatant. The supernatant was carefully collected using 0.45 μm membrane filter to remove any remaining lipid particles. The amount of unentrapped ciprofloxacin in the filtered supernatant was quantified by measuring absorbance at 275 nm by UV spectrophotometry using equation 1.

$$\% \; EE = \left[\frac{W_t \; - \; W_s}{W_t}\right] \times 100 \tag{3.1}$$

% EE represents the entrapment efficiency.

W_t represent the total amount of ciprofloxacin used in the NLCs.

W_s It is the amount of free drug present in the supernatant [140].

3.4.3 Transmission Electron Microscopy Analysis

The surface morphology and structural features of ciprofloxacin-loaded NLCs were examined using transmission electron microscopy (TEM). A small amount of diluted NLC dispersion was placed onto a carbon-coated copper grid and allowed to settle for 1–2 minutes. Excess liquid was gently removed with filter paper, and the grid was then negatively stained with a 1% (w/v) phosphotungstic acid solution (pH 7.0) to enhance contrast. After air-drying at room temperature, images were captured at various magnifications using a TEM instrument (e.g., JEOL JEM-2100, Japan) [141].

3.4.4 X-ray Diffraction Analysis

X-ray diffraction (XRD) analysis was conducted to examine the solid-state characteristics of ciprofloxacin, the selected lipid excipients, their physical mixture, and the optimized ciprofloxacin-loaded NLCs (F1). Prior to analysis, all samples were finely ground and evenly mounted on glass sample holders. X-ray diffraction (XRD) patterns were recorded using a Bruker D8 Advance diffractometer (Bruker, Germany) with a Cu Ka radiation source (θ = 1.5406 Å) operating at 40 kV and 30 mA. Samples were scanned over a 2θ range of 5° to 60° with a step size of 0.02° and a scanning rate of 2° per minute. The resulting diffraction patterns were analyzed to identify the presence, disappearance, or shifting of characteristic peaks, which could indicate modifications in the crystalline nature of ciprofloxacin upon formulation into the NLC system [142].

3.4.5 Differential Scanning Calorimetry Analysis

Differential scanning calorimetry (DSC) was employed to investigate the thermal effect and compatibility of ciprofloxacin with the lipid excipients. Samples of 5-10 mg were sealed in aluminum pans, while an empty pan served as a reference. DSC analysis was conducted on a PerkinElmer STA 6000/8000 (USA) under nitrogen

at 20 mL/min, with the temperature ramped from 30 °C to 350 °C at 10 °C/min [143].

3.4.6 Fourier Transform Infrared Spectroscopy

FTIR analysis was carried out to detect possible interactions between ciprofloxacin and the NLC excipients. Samples were mixed with KBr, compressed into discs, and scanned from 4000 to 400 cm^{-1} at 4 cm^{-1} resolution using a PerkinElmer FTIR spectrometer (USA). Alterations in peak position, intensity, or disappearance were interpreted as evidence of drug excipient interaction and successful drug encapsulation [144].

3.5 In Vitro Drug Release Study and Drug Release Kinetics

The in vitro release of ciprofloxacin from the NLC formulation was investigated using the dialysis bag method. Dialysis membranes with a molecular weight cut-off of 10 kDa were pre-soaked in distilled water overnight. The NLC dispersion was placed inside the pre-soaked dialysis bag, which was then sealed and immersed in 250 mL of phosphate-buffered saline (PBS, pH 7.4) containing 0.1% Tween-80 to maintain sink conditions [145].

The system was stirred continuously at 100 rpm using a magnetic stirrer and maintained at 37 ± 0.5 °C. Samples of 5 mL were collected at predetermined time intervals up to 24 hours and immediately replaced with an equal volume of fresh, pre-warmed PBS. Each sample was filtered through a 0.45 μm membrane and analyzed spectrophotometrically at 275 nm [146].

To assess the release kinetics, the cumulative release data were fitted to zero-order, first-order, Higuchi, and Korsmeyer–Peppas models. The model with the highest correlation coefficient (R^2) was considered the best fit. For the Korsmeyer–Peppas

model, the release exponent (n) was calculated to provide insight into the mechanism of drug release from the NLCs. All experiments were performed in triplicate, and the results are presented as mean ± standard deviation [147].

3.6 Preparation of Ciprofloxacin-Loaded NLC-Based Carbopol Gel

The ciprofloxacin-loaded NLC gel was prepared by a slightly modified method reported in the literature [148]. Briefly, Carbopol 940 (1.0% w/w) was dispersed in distilled water under continuous stirring and allowed to hydrate completely in the dark. Iso-eucalyptol was incorporated as a skin penetration enhancer. A transparent gel base was obtained by neutralizing the hydrated Carbopol dispersion with 0.5% (w/v) triethanolamine.

The optimized ciprofloxacin-loaded NLC dispersion, containing 0.3% w/v drug, was gradually incorporated into the gel base with gentle stirring. The total volume of the formulation was made up of distilled water. For comparison, a plain ciprofloxacin gel (0.3% w/v) was prepared by directly dispersing the drug in the Carbopol gel containing iso-eucalyptol [149–151].

3.6.1 Macroscopic and Organoleptic Properties, pH and Rheology

To prepare a topical formulation, the optimized ciprofloxacin-loaded NLCs were incorporated into a 1.0% (w/w) Carbopol 940 gel base. The gel was evaluated at room temperature for appearance, uniformity, consistency, and any signs of separation. The surface pH of the gel was measured using a digital pH meter (PHS-25CW, BANTE Instruments, China), calibrated with standard buffer solutions of pH 4, 7, and 10. Measurements were performed at 25 ± 1 °C, allowing the electrode to stabilize for 30 seconds, and each reading was recorded in triplicate [152].

Gel viscosity was determined using a Brookfield DV2T viscometer (Spindle S64) across a shear rate of 0.1-1.5 rpm at 25 ± 0.5 °C. Spreadability was tested by placing 350 mg of gel on a fixed glass plate (10 × 5 cm), followed by dropping a 5.75 ± 0.05 g plate from 5 cm. The diameter of the spread gel after 60 seconds was measured to determine its ease of application [153].

3.6.2 Ex Vivo Skin Permeation Study

Ex vivo skin permeation of the optimized ciprofloxacin-loaded NLC gel was carried out using a Franz diffusion cell (2.54 cm^2 diffusion area). Excised full-thickness skin from healthy New Zealand White rabbits was cleaned of subcutaneous fat and pre-equilibrated in PBS (pH 7.4) for 1 hour. The skin was positioned between donor and receptor chambers, with the stratum corneum facing the donor side. The receptor compartment contained PBS (pH 5.5), maintained at 37 ± 0.5 °C, and stirred continuously. A measured dose of either NLC gel or plain gel was applied to the donor side, and receptor samples were collected at predetermined times, replaced immediately with fresh buffer. Cumulative drug permeation per unit area was plotted over time, and steady-state flux (J ss) was calculated using equation 2 from the slope of the linear region to evaluate permeation efficiency [154].

$$Jss = \frac{\triangle Q}{A \triangle t} \tag{3.2}$$

In this formula, $\triangle$Q indicates the cumulative drug permeated at steady state (μg), A is the effective diffusion surface (2.54 cm^2), and it represents the time (h) corresponding to the linear steady-state phase. The enhancement ratio (ER) was calculated by dividing the flux of the NLC gel by that of the plain gel using equation 3.

$$ER = \frac{Jss\ (NLCs\ gel)}{Jss\ (Plain\ gel)} \tag{3.3}$$

All experiments were conducted in triplicate, and data are presented as mean ± standard deviation. Statistical significance between the NLC gel and plain gel was evaluated using an unpaired two-tailed t-test, with $p < 0.05$ considered significant.

3.6.3 In Vivo Dermal Compatibility Study

The dermal safety of the optimized ciprofloxacin-loaded NLC gel was tested using healthy adult New Zealand White rabbits (*Oryctolagus cuniculus*) in accordance with OECD Guideline 404 [155, 156].

The study protocol was approved by the Research Ethics Committee, Faculty of Pharmacy, Capital University of Science and Technology, Islamabad (Approval No.: REC/FoP/F2025/04), and all procedures were performed following institutional and national animal welfare regulations.

Nine rabbits were randomly divided into three groups of three animals each: a test group treated with the ciprofloxacin-loaded NLC gel, a positive control group treated with 0.8% w/v sodium lauryl sulfate solution, and a negative control group receiving a plain gel without active drug or NLCs. Animals were housed under standard environmental conditions (temperature 22 ± 2 °C, relative humidity 55 ± 5%, 12-hour light/dark cycle) with free access to food and water.

The dorsal area of each rabbit was shaved 24 hours before the experiment to expose intact skin. A 6.5 cm^2 area was selected for formulation application, and 100 mg of each gel was spread evenly on the marked site using a sterile spatula.

The test areas were covered with an occlusive patch to ensure consistent contact. Skin reactions were assessed at 24-, 48-, and 72-hour post-application. Erythema and edema were scored according to the Draize scale (0 = no reaction, 3 = severe reaction), and the Primary Irritation Index (PII) was calculated using equation 4:

$$PII = (sum\ of\ eruthma + edema\ score) \div (No.of\ animals \times No.of\ readings) \tag{3.4}$$

Based on OECD guidelines, any formulation with a PII value less than 0.5 was considered non-irritant to the skin [157]. Throughout the study, the rabbits were carefully monitored for changes in behavior, signs of discomfort, or any systemic adverse effects. The procedures did not require anesthesia or any invasive interventions [158].

3.7 Antibacterial Evaluation

3.7.1 MRSA Clinical Isolate Source and Verification

A clinical isolate of methicillin-resistant *Staphylococcus aureus* (MRSA) was employed in the present study. The isolate was obtained from IDC Diagnostic Laboratory, Chandni Chowk, Rawalpindi, Pakistan, with ethical approval granted by the Research Ethics Committee, Faculty of Pharmacy, Capital University of Science and Technology, Islamabad (Approval No. REC/FoP/F2025/04). Identification of the isolate as S. aureus was confirmed using standard phenotypic characterization, including Gram staining, catalase activity, and coagulase production. Methicillin resistance was phenotypically verified in accordance with Clinical and Laboratory Standards Institute (CLSI) M100 recommendations using the cefoxitin (30 μg) disc diffusion method [159].

3.7.2 Antibacterial Activity Well Diffusion Method

The antibacterial activity of the developed formulations was evaluated against a clinical isolate of methicillin-resistant *Staphylococcus aureus* (MRSA) obtained from IDC Diagnostic Laboratory using the agar well diffusion method. A standardized bacterial suspension equivalent to 0.5 McFarland was uniformly spread onto Mueller–Hinton agar (MHA) plates. Wells of 6 mm diameter were aseptically created in the agar. To facilitate uniform diffusion of gel-based formulations through the agar matrix, each sample was first dispersed in dimethyl sulfoxide

(DMSO) using established procedures. The final concentration of DMSO was maintained below 10% (v/v) to avoid antimicrobial interference.

Two sets of experimental plates were prepared. The first set contained solvent control (S), ciprofloxacin (API) dispersion (B), and ciprofloxacin-loaded NLC gel formulations (A1-A3), while the second set comprised solvent control (S), ciprofloxacin (API) dispersion (B), and blank NLC gel formulations (A1-A3). A volume (100 μL) of each sample was introduced into the respective wells. The plates were incubated at 37 °C for 24 hours, after which the zones of inhibition (ZOI) were measured in millimeters using a digital caliper. The solvent control showed no inhibition, confirming that the DMSO concentration used did not affect bacterial growth. All tests were performed in triplicate, and the results are presented as mean ± standard deviation. Differences between multiple groups were analyzed using one-way ANOVA followed by Tukey's post-hoc test, with $p < 0.001$ considered statistically significant [160].

3.8 Stability Study

The physical stability of the optimized NLC gel was evaluated following ICH guidelines. Samples were stored under refrigerated (4 ± 2 °C), ambient (25 ± 2 °C), and accelerated (40 ± 2 °C, 75 ± 5% RH) conditions in tightly sealed, light-resistant containers. Evaluations were performed at 0, 1, 2, and 3 months to monitor changes in visual appearance, pH, and viscosity. Formulations were considered stable if no observable changes occurred, viscosity remained within ±10% of the initial value, and pH deviation did not exceed 0.5 units [161].

3.9 Statistical Analysis

All data were analyzed using SPSS Statistics version 26.0 (IBM, USA). Comparisons between groups were performed using one-way analysis of variance (ANOVA)

followed by Tukey's post hoc test. Differences were considered statistically significant at $p < 0.05$. Results are presented as mean ±â standard deviation (SD, n = 3).

Chapter 4

Results and Discussion

4.1 Lipid Screening and Selection

The solubility of ciprofloxacin in the lipid matrix is a critical factor for achieving efficient drug loading in NLCs. During preliminary lipid screening, several solid lipids including Stearic acid, Geleol™, and Precirol® ATO 5 exhibited immediate turbidity upon the addition of 1 mg of ciprofloxacin, indicating limited solubility.

In contrast, Compritol® 888 ATO showed gradual solubilization, remaining clear with 1-3 mg of drug and only turning turbid at 4 mg, suggesting moderate drug-lipid compatibility. Among the liquid lipids tested, Oleic acid displayed the highest solubilizing potential, remaining transparent up to 3 mg of ciprofloxacin, whereas Capryol® 90 and Labrafac™ PG became turbid at the first 1 mg of drug. Based on these results, Compritol® 888 ATO and Oleic acid were selected as the solid and liquid lipids, respectively. This combination is anticipated to provide a stable lipid matrix, enhance drug solubilization, and support high drug loading in NLCs while maintaining their structural integrity (Table 4.1) [133, 162].

Table 4.1: Solubility of ciprofloxacin in melted solid and liquid lipids

Lipid	**Ciprofloxacin (mg)**	**Visual Observation**
Stearic acid	1	Turbid
Geleol™	1	Turbid

Table 4.1 continued from previous page

Lipid	Ciprofloxacin (mg)	Visual Observation
Precirol® ATO 5	1	Turbid
Compritol® 888 ATO	1	Clear
Compritol® 888 ATO	2	Clear
Compritol® 888 ATO	3	Clear
Compritol® 888 ATO	4	Slightly turbid
Oleic acid	1	Clear
Oleic acid	2	Clear
Oleic acid	3	Clear
Oleic acid	4	Slightly turbid
Capryol® 90	1	Turbid
Labrafac™ PG	1	Turbid

4.2 Optimization of Ciprofloxacin-Loaded NLCs by Box-Behnken Design

A three-level, three-factor Box-Behnken design was employed to investigate the effects of solid lipid percentage (A), surfactant concentration (B), and homogenization time (C) on the physicochemical properties of ciprofloxacin-loaded NLCs. A total of seventeen experimental runs, including five center points, were designed using Design-Expert® software. The responses evaluated for each formulation included particle size (PS), polydispersity index (PDI), zeta potential (ZP), and drug entrapment efficiency (%EE). The particle size of the prepared formulations ranged from 104.3 to 328.8 nm, PDI from 0.2311 to 0.3920, zeta potential from -14.75 to -34.39 mV, and EE from 61.04 to 87.85%. The observed and predicted responses are presented in Table 4.2, while Table 4.3 summarizes the statistical model parameters. The high R^2 values (0.9982-0.9998), adjusted R^2 values (0.9942-0.9996), and predicted R^2 values (0.9939-0.9989) confirmed excellent model fitting. Model p-values (<0.0001) indicated significance, whereas the lack-of-fit p-values (>0.05) demonstrated non-significant lack-of-fit, confirming adequacy of the quadratic model.

TABLE 4.2: Box-Behnken design matrix with observed and predicted responses for ciprofloxacin-loaded NLCs

Independent	**Variables**				**Dependent**	**Variables**					
					Observed	**Responses**			**Predicted**	**Responses**	
Run	**Solid Lipid**	**Surfactant**	**Homogenization Time**	**Particle Size**	**Poly Dispersity Index**	**Zeta Potential**	**Entrapment Efficiency**	**Particle Size**	**Polydispersity Index**	**Zeta Potential**	**Entrapment Efficiency**
	(%of Total Lipid)	(B)	(C)	nm	(PDI)	(ZP) mV	%	nm	(PDI)	(ZP) mV	% EE
		%w/w	min	Y1	Y2	Y3	Y4	Y1	Y2	Y3	Y4
F1	70	2	10	137.7	0.263	-27.9	87.85	137.8	0.2639	-27.44	87.51
F2	80	3	10	156.9	0.2311	-34.39	88.14	157.28	0.2297	-34.43	86
F3	70	3	15	104.3	0.2339	-33.68	86.33	103.54	0.2341	-33.8	86.59
F4	70	2	10	136.9	0.2632	-26.9	87.9	137.8	0.2639	-27.44	87.51
F5	60	1	10	328.8	0.3837	-14.75	61.04	328.4	0.3851	-14.71	61.18
F6	70	3	5	142.9	0.2551	-32.18	84.72	143.89	0.2549	-32.19	84.61
F7	70	1	5	246.7	0.392	-15.3	63.21	247.5	0.3918	-15.18	62.95
F8	60	3	10	224.8	0.2432	-30.22	79.44	224.23	0.2446	-30.05	79.43
F9	60	2	15	143.9	0.2549	-29.6	81.12	145.27	0.2533	-29.65	80.87
F10	80	2	15	104.4	0.2327	-33.1	84.59	104.8	0.2339	-32.94	84.47
F11	70	2	10	137.2	0.264	-27.99	86.99	137.8	0.2639	-27.44	87.51

Table 4.2 continued from previous page

Independent Variables					Dependent Variables Observed Responses				Predicted Responses		
Run	**Solid Lipid** (%of Total Lipid)	**Surfactant** (B) %w/w	**Homogenization Time** (C) min	**Particle Size** nm Y1	**Poly Dispersity Index** (PDI) Y2	**Zeta Potential** (ZP) mV Y3	**Entrapment Efficiency** % Y4	**Particle Size** nm Y1	**Polydispersity Index** (PDI) Y2	**Zeta Potential** (ZP) mV Y3	**Entrapment Efficiency** % EE Y4
F12	80	1	10	296.7	0.3578	-17.16	63.37	297.29	0.3564	-17.33	63.38
F13	70	2	10	137.8	0.266	-26.99	86.89	137.8	0.2639	-27.44	87.51
F14	60	2	5	176.1	0.281	-26.87	76.77	175.7	0.2798	-27.03	76.89
F15	80	2	5	119.5	0.2538	-30.79	83.79	118.13	0.2555	-30.74	84.04
F16	70	2	10	139.2	0.2635	-27.42	87.93	137.8	0.2639	-27.44	87.51
F17	70	1	15	245.1	0.3642	-18.4	65.28	244.11	0.3644	-18.39	65.39

TABLE 4.3: Model fitting parameters, p-values and lack-of-fit for NLC responses

Response	**Particle Size (nm)**	**PDI**	**Zeta Potential (mV)**	**Entrapment Efficiency (%)**
R^2	0.9998	0.9995	0.9982	0.9991
Adjusted R^2	0.9996	0.9942	0.9959	0.9979
Predicted R	0.9981	0.9989	0.9939	0.9954
Model p-value	<0.0001	<0.0001	<0.0001	<0.0001
Lack of Fit	0.1255	0.1158	0.8936	0.744
SD	1.28	0.0018	0.4066	0.4554
%CV	0.728	0.6349	1.52	0.5712

R^2 = Coefficient of determination; Adjusted R^2 = adjusted coefficient of determination; Predicted R^2 = predicted coefficient of determination; p-value < 0.05 indicates a significant model; Lack of fit p-value > 0.05 indicates a non-significant lack of fit.

4.2.1 Polynomial Equations

The effect of formulation variables on the responses was analyzed using quadratic polynomial equations with A, B, and C representing solid lipid percentage, surfactant concentration, and homogenization time, respectively.

4.2.1.1 Particle Size - Y_1

Particle size (Y_1) decreased with increasing solid lipid and surfactant levels, as described by equation 4.1:

$$\begin{aligned} Y_1 = {} & 137.77 - 24.51A - 61.04B - 10.94C - 8.96AB \\ & + 4.27AC - 9.24BC + 32.62A^2 + 81.41B^2 \\ & - 34.42C^2 \end{aligned} \tag{4.1}$$

4.2.1.2 PDI - Y_2

Polydispersity index (Y_2) was similarly influenced, with surfactant concentration showing the most significant reduction (equation 4.2):

$$\begin{aligned} Y_2 = {} & 0.2639 - 0.0109A - 0.0668B - 0.0120C \\ & + 0.0034AB + 0.0012AC + 0.0016BC \\ & - 0.0078A^2 + 0.0479B^2 - 0.0005C^2 \end{aligned} \tag{4.2}$$

4.2.1.3 Zeta Potential - Y_3

Zeta potential (Y_3) became more negative with increasing lipid and surfactant content, indicating enhanced stability (equation 4.3):

$$\begin{aligned} Y_3 = {} & -27.44 - 1.75A - 8.11B - 1.21C - 0.44AB \\ & + 0.10AC + 0.40BC - 0.95A^2 + 4.262B^2 \\ & - 1.70C^2 \end{aligned} \tag{4.3}$$

4.2.1.4 Entrapment Efficiency - Y_4

Entrapment efficiency (Y_4) improved with higher surfactant levels and longer homogenization times, as reflected in equation 4.4:

$$\begin{aligned} Y_4 = {} & 87.51 + 2.69A + 10.72B + 1.10C + 1.59AB \\ & - 0.89AC - 0.12BC - 3.92A^2 - 10.6B^2 \\ & - 20.3C^2 \end{aligned} \tag{4.4}$$

Positive coefficients indicate a synergistic (direct) effect of a factor, while negative coefficients represent an antagonistic (inverse) effect. The interaction and quadratic terms highlight non-linear relationships between formulation components.

4.3 Effect of Independent Factors on Responses

4.3.1 Particle Size - Y_1

Particle size ranged between 104.3 and 328.8 nm. The 3D response surface plots (Figure 4.1A-C) revealed that both solid lipid percentage and surfactant concentration had strong, interactive effects on particle size, while homogenization time had a relatively minor impact. Increasing the solid lipid content initially decreased particle size due to improved lipid packing, but excessive solid lipid caused aggregation and viscosity-induced growth. Elevated surfactant levels reduced particle size by lowering interfacial tension and improving dispersion stability, with minimal improvement beyond 2% [104, 163]. The optimized formulation (F1), 70% solid lipid, 2% surfactant, 10 min homogenization) yielded a particle size of 137.7 nm, closely matching the predicted 137.8 nm.

4.3.2 Particle Size - Y_2

PDI values (0.2311-0.3920) indicated a narrow size distribution across batches. As shown in Figure 4.1D-F, increasing surfactant concentration significantly reduced PDI by enhancing steric stabilization, while higher solid lipid content slightly increased heterogeneity due to elevated viscosity. Homogenization time had minimal influence. The optimized NLCs (F1) exhibited a PDI of 0.2630, in close agreement with the predicted 0.2639, confirming excellent uniformity and model reliability [84].

4.3.3 Zeta Potential - Y_3

Zeta potential varied between -14.75 and -34.39 mV, reflecting good electrostatic stability. The 3D plots (Figure 4.1G-I) demonstrated that increasing solid lipid and surfactant concentrations increased the magnitude of the negative charge, attributed to anionic fatty acid residues and polar head groups of Tween-80 [164, 165].

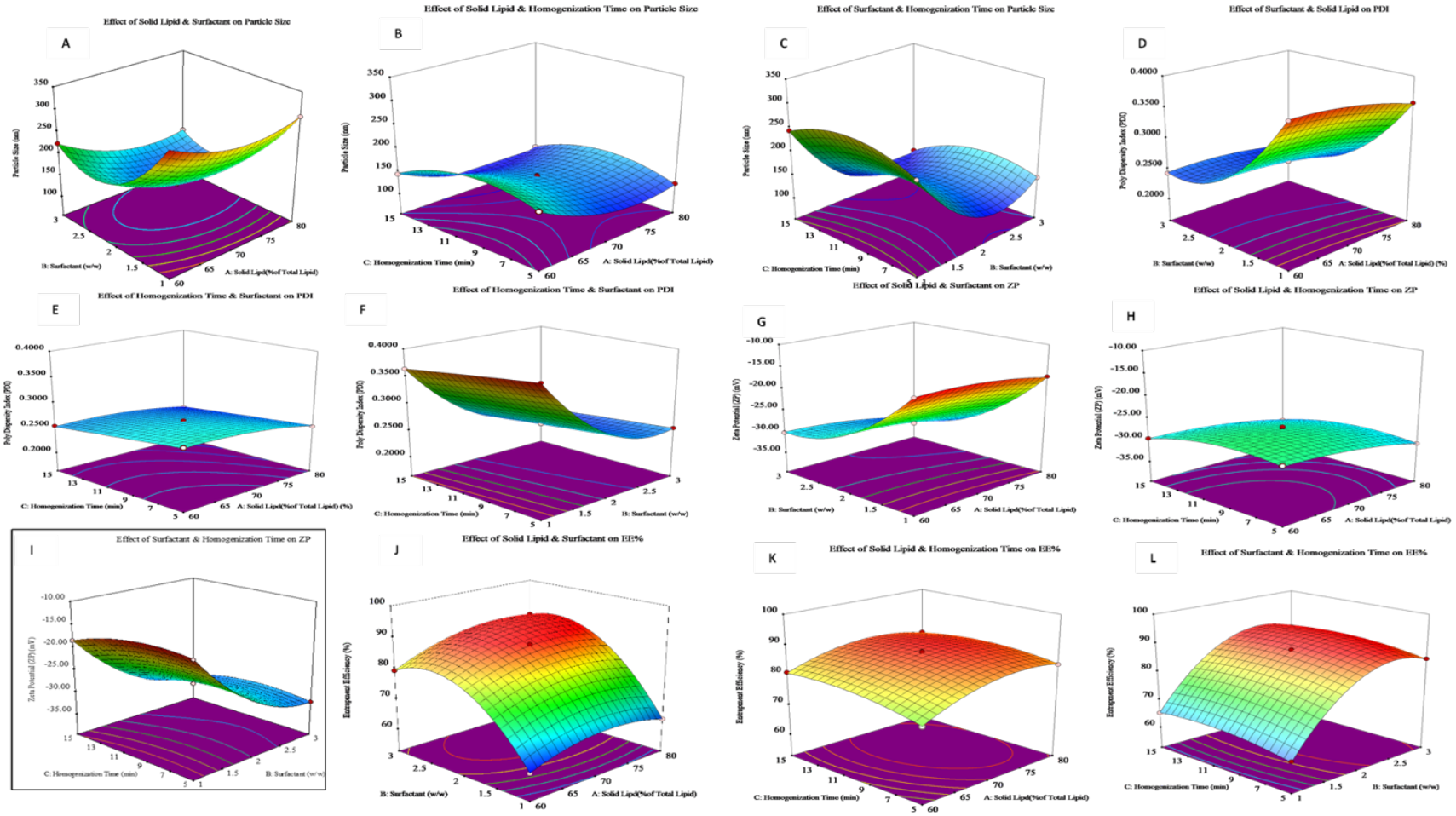

FIGURE 4.1: 3D response surface graphs indicating the interactive effects of solid lipid concentration, surfactant concentration, and homogenization time on particle size (A-C), polydispersity index (PDI) (D-F), zeta potential (ZP) (G-I), and entrapment efficiency (%EE) (J-L) of ciprofloxacin-loaded NLCs optimized using a Box-Behnken design.

Homogenization time slightly influenced ZP, possibly through surface orientation effects. The optimized formulation (F1) displayed a zeta potential of -27.90 mV, consistent with the predicted -27.44 mV.

4.3.4 Entrapment Efficiency - Y_4

Entrapment efficiency ranged from 61.04 to 87.85%. The 3D surface plots (Figure 4.1A-C) indicated that EE increased with higher surfactant concentration, likely due to improved solubilization of ciprofloxacin within the lipid matrix. Solid lipid percentage enhanced EE up to 70%, beyond which encapsulation decreased because of reduced liquid lipid fraction. Moderate homogenization favored drug incorporation, whereas prolonged homogenization caused slight drug leakage [166]. The optimized formulation (F1) achieved an EE of 87.85%, in close agreement with the predicted 87.51%, confirming the reliability of the optimization process.

4.4 Model Validation and Optimization

Comparison of observed and predicted responses (Table 4.2) demonstrated minimal deviation, validating the accuracy of the quadratic model. The desirability function identified F1 as the optimized formulation, composed of a 70:30 solid-to-liquid lipid ratio, 2% Tween-80, and 10 min of homogenization. The optimized formulation exhibited a particle size of 137.7 nm, a polydispersity index (PDI) of 0.263, a zeta potential of 27.90 mV, and an entrapment efficiency (EE) of 87.85%. The predicted and experimental values showed close agreement, confirming the robustness of the Box Behnken optimization.

The observed trends are consistent with previous reports on NLC systems, where particle size and PDI are primarily governed by surfactant concentration and lipid ratio, zeta potential is influenced by lipid composition and interfacial charge, and EE depends on the balance between lipids (solid & liquid). The response surface plots clearly demonstrate the synergistic and interactive effects of formulation

variables on each response [167, 168]. The optimized formulation and its statistical confirmation are summarized in Tables 4.4.

TABLE 4.4: Confirmation table of optimized formulation with statistics

Analysis	Predicted Mean	Predicted Median	Observed	Std Dev	n	SE Pred	95% PI low	Data Mean	95% PI high
Particle Size (nm)	137.8	137.8	137.7	1.3	3	1.4	134.5	137.7	141.1
Polydispersity Index (PDI)	0.2639	0.2639	0.263	0.0018	3	0.002	0.2593	0.263	0.2686
Zeta Potential (ZP) (mV)	-27.44	-27.44	-27.9	0.41	3	0.45	-28.49	-27.9	-26.39
Entrapment Efficiency (%)	87.512	87.512	87.85	0.45544	3	0.498905	86.3323	87.15	88.6917

4.5 Characterization of Ciprofloxacin - Loaded NLCs

4.5.1 Particle Size, Polydispersity Index and Zeta Potential of Optimized Formulation

The optimized formulation exhibited a particle size of 137.7 nm, a polydispersity index (PDI) of 0.263, a zeta potential of 27.90 mV, and an entrapment efficiency (EE) of 87.85% as shown in Figure 4.2.

The nanoscale particle size confirms the efficiency of the hot homogenization process and the optimized ratio of solid lipid (Compritol 888 ATO) and liquid lipid (oleic acid) in producing fine, stable lipid particles.

The smaller particle size enhances the surf ace area available for drug release and facilitates deeper skin penetration when applied topically [21].

The presence of Tween-80, a nonionic surfactant, contributed to the reduction of interfacial tension, leading to uniform droplet breakdown during homogenization and stabilization of the dispersion [169].

A PDI value below 0.3 indicates a homogeneous particle population with minimal aggregation, suggesting excellent reproducibility and stability of the system.

A PDI value below 0.3 indicates a homogeneous particle population with minimal aggregation, suggesting excellent reproducibility and stability of the system. This narrow size distribution reflects the effective control of formulation parameters predicted by the Box-Behnken model. Comparable PDI ranges have been reported for optimized NLCs incorporating ciprofloxacin and other drugs [164].

The zeta potential of -27.90 mV demonstrates adequate electrostatic repulsion between particles, preventing flocculation and indicating good colloidal stability. The negative charge likely arises from ionized free fatty acids (oleic acid) and the adsorption of the surfactant layer onto the lipid surface. As reported in previous studies, NLCs with zeta potential values exceeding ±25 mV is considered physically stable due to sufficient repulsive forces.

As reported in previous studies, NLCs with zeta potential values exceeding ±25 mV is considered physically stable due to sufficient repulsive forces.

Furthermore, the steric stabilization offered by Tween-80 adds a protective mechanism against aggregation, supporting the formulation's long-term physical stability [151, 170].

Overall, the optimized ciprofloxacin NLC formulation exhibited an ideal balance of small particle size, low polydispersity index, and negative zeta potential, confirming the success of the optimization strategy and suitability for stable topical delivery.

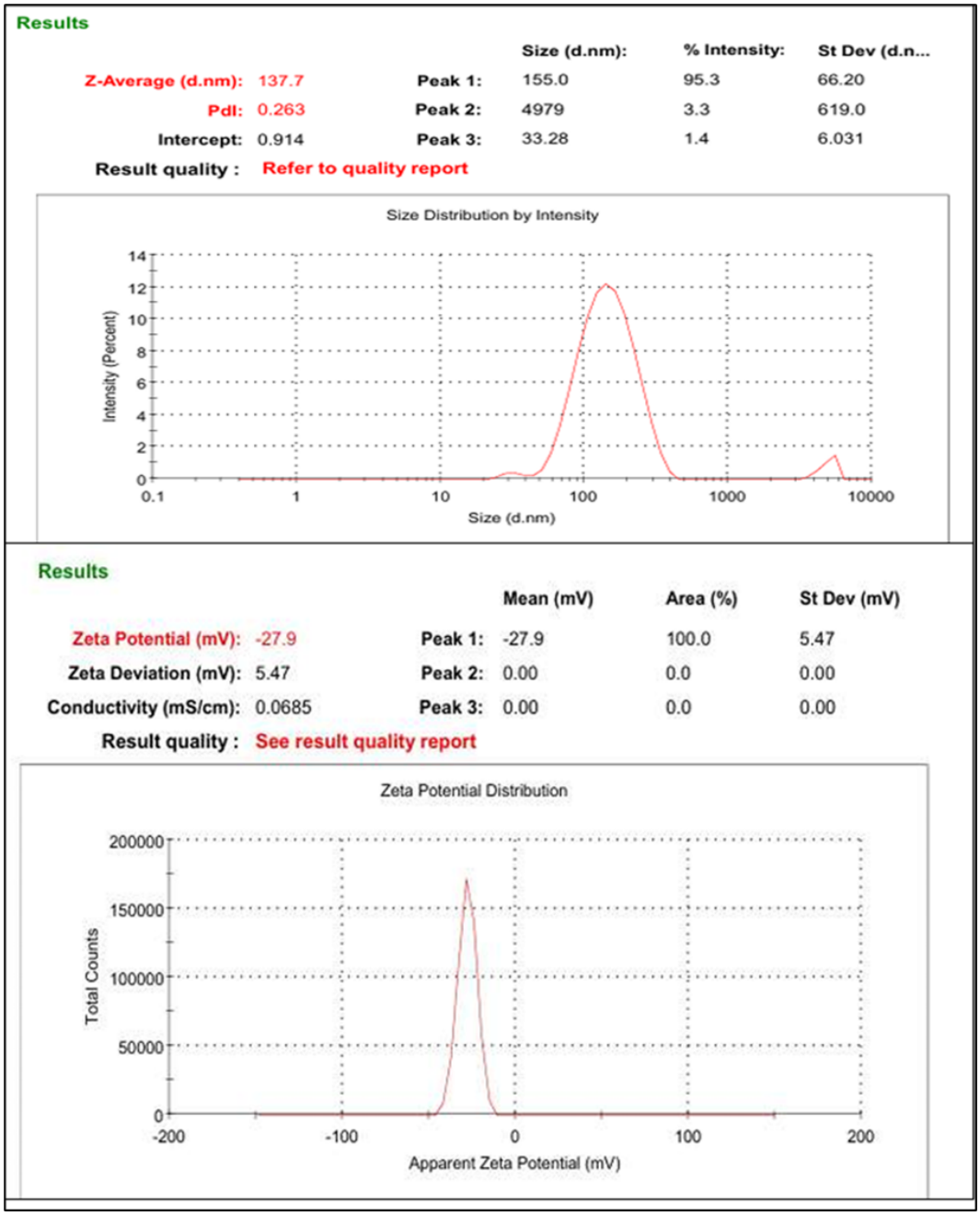

FIGURE 4.2: Z-Average, PDI, and zeta potential of the optimized ciprofloxacin-loaded NLCs, confirming nanoscale size, uniform distribution, and robust colloidal stability.

4.5.2 Entrapment Efficiency

The entrapment efficiency (EE) of the developed ciprofloxacin-loaded NLCs ranged from 61.04% to 87.85%, as shown in Table 4.2. The variation in EE among formulations reflected the influence of lipid composition, surfactant concentration,

and homogenization time. An increase in the solid lipid fraction (Compritol) generally improved EE up to an optimum level, as the solid lipid matrix provided structural rigidity and sufficient space for drug accommodation.

However, a further increase in solid lipid concentration tended to decrease EE, possibly due to enhanced crystallinity that limited the amorphous regions required for drug entrapment. Surfactant concentration also exhibited a pronounced effect on EE.

Moderate levels of Tween-80 promoted higher drug retention within the lipid matrix by reducing interfacial tension and improving dispersion stability, while excessive surfactant might increase drug solubilization in the aqueous phase, thereby lowering encapsulation.

Homogenization time influenced EE indirectly by affecting particle formation kinetics; moderate homogenization favored efficient drug incorporation, whereas prolonged homogenization could lead to drug expulsion from the lipid core due to thermal stress [171].

The optimized formulation (F1; 70:30 solid-to-liquid lipid ratio, 2% Tween-80, 10 min homogenization) demonstrated the highest EE (87.85 ± 0.62%), closely matching the predicted value (87.51%). The high EE can be attributed to the synergistic balance between Compritol and oleic acid, forming a partially disordered lipid matrix that enhances drug accommodation.

This phenomenon has been widely reported, where the incorporation of liquid lipids into solid matrices generates imperfections that trap lipophilic drugs more efficiently and minimize leakage during emulsification and cooling [172].

Overall, these findings confirm that the lipid-to-surfactant ratio and process conditions play significant roles in determining the entrapment performance of NLCs. The results align with previous studies where optimized lipid blends and surfactant levels significantly improved the encapsulation efficiency of antibiotics and other bioactive agents [163, 173].

4.5.3 Transmission Electron Microscopy

A transmission electron microscopy (TEM) analysis was conducted using a Hitachi High-Tech Corp. HT7800 model on the optimized formulation of ciprofloxacin-loaded NLCs. The micrographs presented in Figure 4.3 reveal a population of spherical nanoparticles with smooth surfaces and well-defined boundaries, captured at a magnification of 10,000× (scale bar: 1.0 μm), showing that the particles are well dispersed on the substrate with no significant aggregation. This indicates effective steric stabilization by Tween 80 and good compatibility of the lipid matrix, which consists of Compritol and oleic acid. The particle size measured by TEM was in the nanometric range, consistent with the size obtained through dynamic light scattering (DLS). The slight difference in particle size may be due to the variations between hydrodynamic measurements in DLS and the dry-state imaging in TEM. The spherical shape and uniform distribution of the nanoparticles are advantageous for topical and transdermal drug delivery, as they promote close contact with the skin surface and facilitate passage through the stratum corneum. Overall, the TEM results support the development of ciprofloxacin-loaded NLCs with appropriate morphology, consistent size, and structural integrity, enhancing their potential for improved dermal drug delivery systems [174, 175].

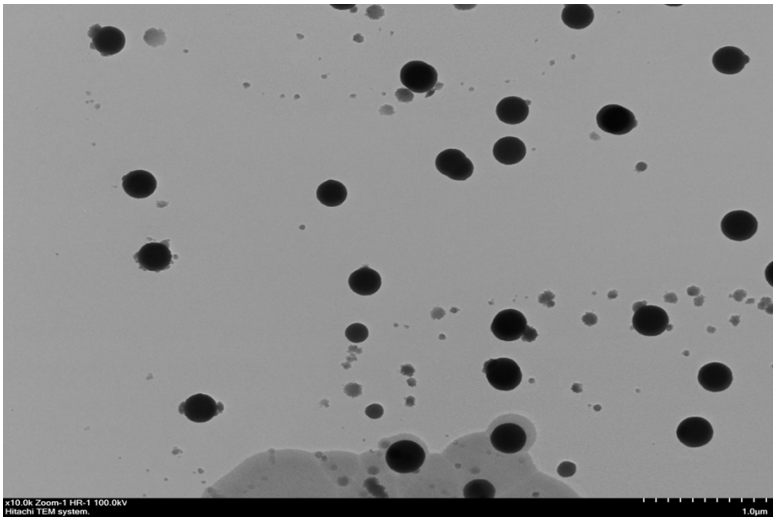

FIGURE 4.3: TEM images of ciprofloxacin - loaded NLCs. (A) Low magnification (×10,000) showing uniformly dispersed spherical nanoparticles (scale bar: 1 μm). (B) High magnification highlighting individual particles <200 nm with smooth surfaces (scale bar: 200 nm).

4.5.4 X-ray Diffraction Analysis

X-ray diffraction (XRD) analysis was conducted to assess the crystalline nature and potential solid-state interactions among the individual components, ciprofloxacin, Compritol 888 ATO, their physical mixture, and optimized ciprofloxacin-loaded NLCs (Figure 4.4). The findings provide insight into entrapment efficiency, molecular dispersion, and transformation of the drug in the lipid matrix.

XRD pattern of pure ciprofloxacin exhibited distinct diffraction peaks at 2θ values of approximately 8.7°, 11.2°, 14.9°, 20.7°, 25.3°, 26.6°, 29.3°, and 32.5°, indicating a predominantly crystalline structure. These peaks are consistent with previous reports and demonstrate the well-ordered lattice structure of ciprofloxacin in its pure form [176, 177]. The crystalline state is typical for ciprofloxacin anhydrous or hemihydrate forms and contributes to its poor aqueous solubility.

Compritol 888 ATO exhibited a dominant sharp peak at approximately $2\theta = 21.3°$, along with a smaller peak at ∼23.5°, which are characteristic of its semi-crystalline lipidic structure. These peaks correspond to the crystalline arrangement of glyceryl behenate (its major component) [178, 179]. The semi-crystalline nature of Compritol confers a key impact on the structural matrix of the lipid carrier system.

The XRD pattern of the physical mixture retained the major crystalline peaks of ciprofloxacin, with similar 2θ values, although peak intensities were slightly diminished and appeared broader. The characteristic Compritol peak at 21.3° remained observable but with reduced intensity. These results suggest that no significant interaction or complexation occurred between the drug and lipid in the physical mixture. The reduction in peak sharpness may indicate weak physical interactions or slight packing disruptions [180, 181].

In contrast, the XRD pattern of the final ciprofloxacin-loaded NLC formulation revealed a complete absence of ciprofloxacin's crystalline peaks and a broad, diffuse halo, indicating a transition from a crystalline to an amorphous or molecularly dispersed state. The disappearance of characteristic Compritol and ciprofloxacin

peaks confirms that both have undergone structural reorganization due to incorporation into the lipid matrix. The presence of Tween 80 (surfactant) and oleic acid (liquid lipid) likely disrupted the lipid lattice, enhancing drug solubilization and stabilizing the amorphous dispersion. This transformation is highly favorable for improving drug solubility and bioavailability [180].

The XRD results collectively demonstrate that ciprofloxacin transitions from a crystalline to an amorphous form when incorporated into the NLCs. The absence of characteristic peaks from both ciprofloxacin and Compritol in the NLC formulation confirms successful molecular dispersion of the drug. This amorphization is beneficial for increasing dissolution rate, stability, and bioavailability, key goals in lipid-based drug delivery systems.

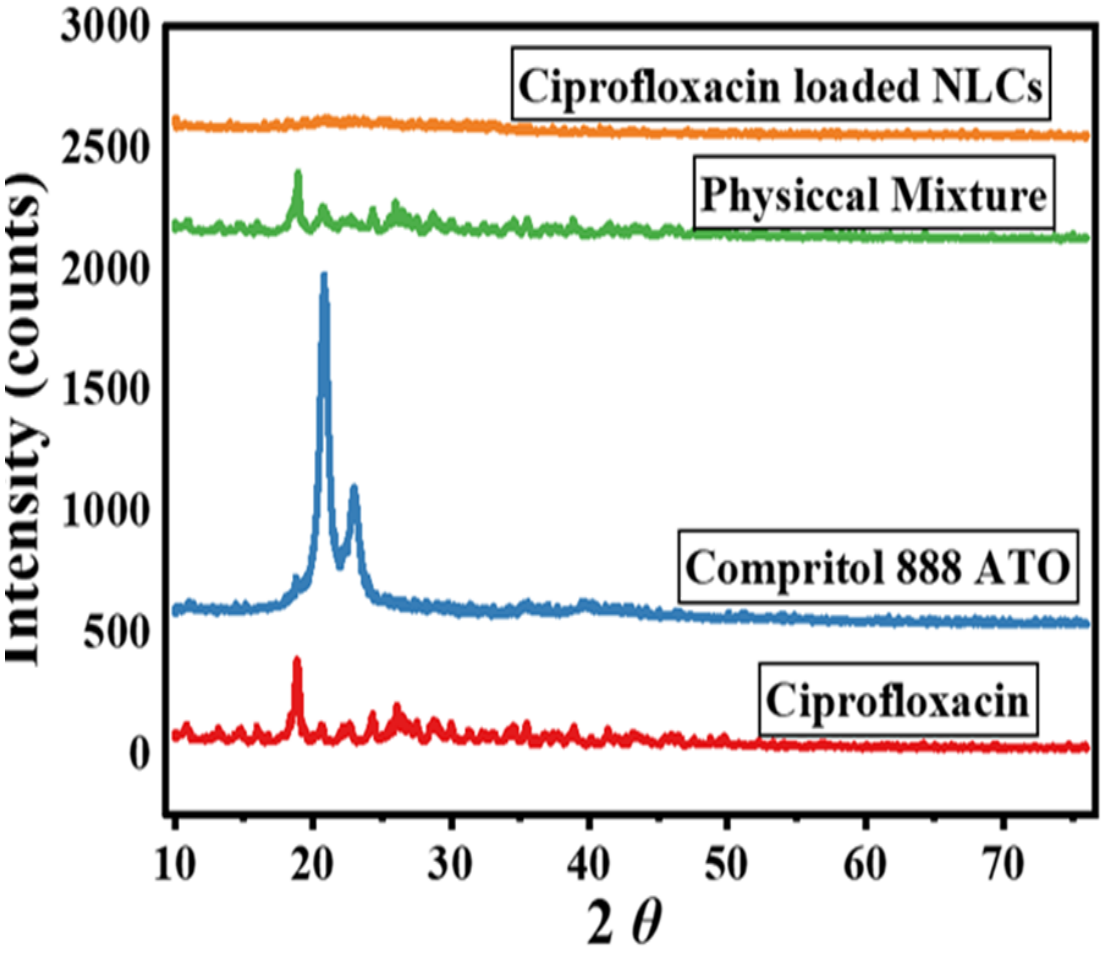

FIGURE 4.4: XRD diffractogram of (A) ciprofloxacin, (B) Compritol 888 ATO, (C) physical mixture, (D) ciprofloxacin-loaded NLCs.

4.5.5 Differential Scanning Calorimetry

The thermal behavior, crystallinity, and compatibility of ciprofloxacin with the lipid excipients used in the NLC formulation were evaluated using differential scanning calorimetry (DSC), and the resulting thermograms are shown in Figure 4.5A-E. Pure ciprofloxacin (Figure 4.5A) exhibited two characteristic endothermic transitions: a small event around 150-170°C associated with dehydration or polymorphic relaxation, followed by a sharp, intense melting peak near 310-330°C, confirming its highly crystalline nature as previously described in the literature [182].

Compritol® 888 ATO (Figure 4.5B) showed a single well-defined melting endotherm at approximately 70-80°C, consistent with its crystalline long-chain glyceride structure [183].

In contrast, oleic acid (Figure 4.5C) exhibited no sharp transitions due to its liquid state at room temperature, displaying only minor baseline fluctuations typical of low-crystallinity fatty acids [184].

Tween 80 (Figure 4.5D) exhibited a broad, shallow thermal drift with no distinct melting peak, confirming its amorphous nature. A small rise near 250-300°C corresponded to the onset of thermal degradation, consistent with earlier reports on polysorbate surfactants [185].

In contrast, the graph of the ciprofloxacin-loaded NLCs (Figure 4.5E) did not display the characteristic ciprofloxacin melting peak at 310-330°C; instead, only broad, low-intensity transitions due to the lipid matrix were observed. The disappearance of the drug's crystalline melting endotherm indicates that ciprofloxacin is no longer present in crystalline form within the formulation but has been converted into an amorphous or molecularly dispersed state within the lipid matrix.

This behavior reflects strong drug-lipid interactions and is a key indicator of successful encapsulation, improved miscibility, and reduced drug crystallinity, findings that align with previous reports on NLC systems where lipid matrices promote molecular dispersion of incorporated drugs [186, 187].

Overall, the DSC results confirm effective incorporation of ciprofloxacin into the NLC system and validate the suitability of the selected lipid excipients for producing a thermally stable formulation with enhanced compatibility and reduced crystallinity.

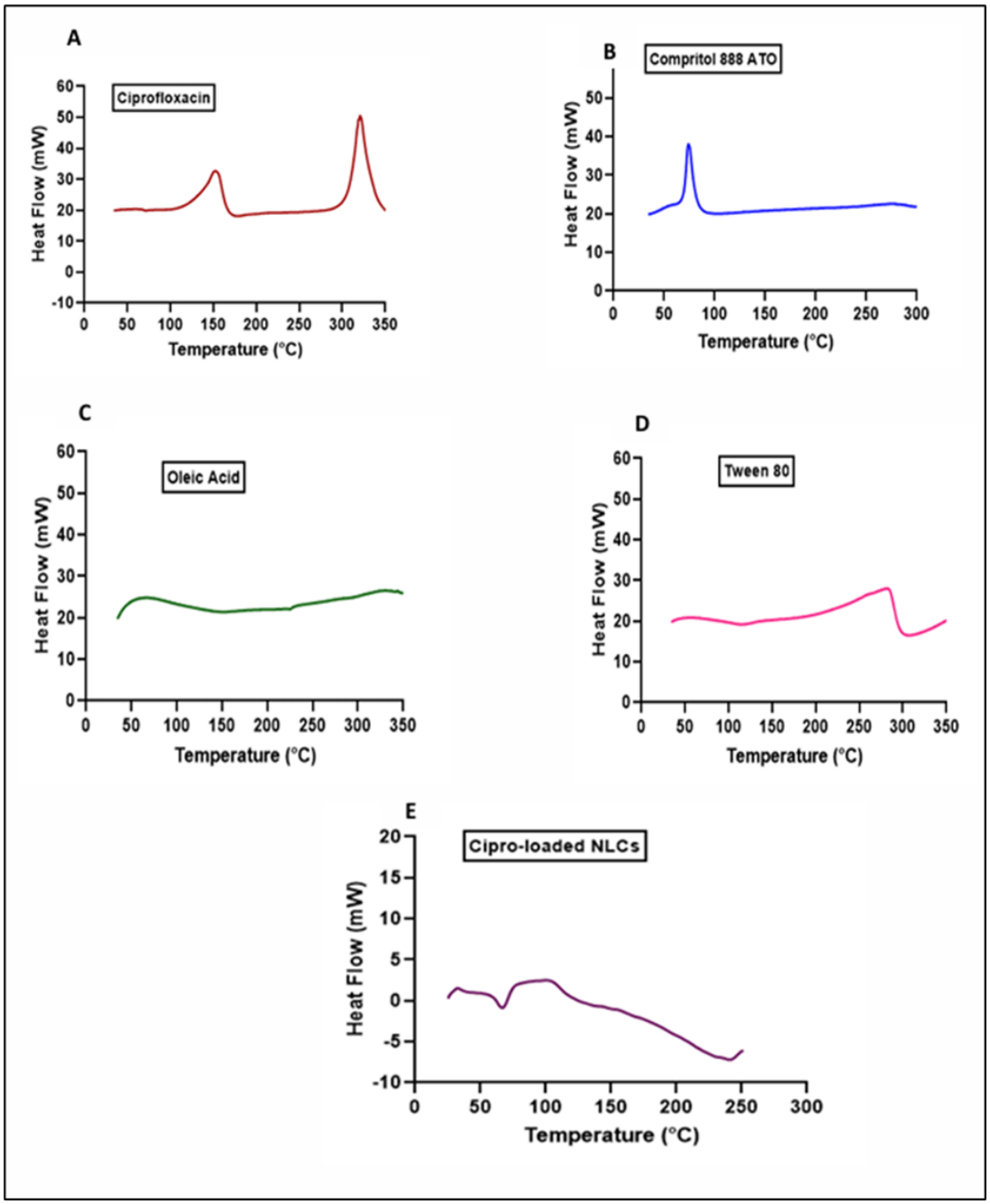

FIGURE 4.5: Differential scanning calorimetry (DSC) thermograms of (A) pure ciprofloxacin, (B) Compritol® 888 ATO, (C) oleic acid, (D) Tween 80, and (E) the optimized ciprofloxacin-loaded NLC formulation.

4.6 Fourier - Transform Infrared Spectroscopy

The Fourier transform infrared (FTIR) spectra of ciprofloxacin, excipients (Compritol ® 888 ATO, oleic acid and Tween 80), physical mixture and the optimized ciprofloxacin-loaded NLCs are shown in Figure 4.6A-F.

The pure ciprofloxacin spectrum (Figure 4.6A) showed distinctive absorption peaks at approximately 3500-3400 cm^{-1} (O-H/N-H stretching vibrations), 1715 cm^{-1} (C=O stretching of carboxylic acid), 1620 cm^{-1} (C=O stretching of quinolone group), 1450 cm^{-1} (C-N stretching), and 1040 cm^{-1} (C-F stretching). These bands are in good agreement with reported data, confirming the structural integrity of ciprofloxacin [188, 189].

Compritol® 888 ATO (Figure 4.6B) showed strong bands at 2915 cm^{-1} and 2848 cm^{-1} due to $-CH_2/-CH_3$ stretching vibrations and a sharp peak at 1732 cm^{-1} corresponding to the ester carbonyl (C=O) of the triglyceride structure [190, 191].

Oleic acid (Figure 4.6C) presented a broadened band attributed to -OH stretching vibrations around 3000-3500 cm^{-1} and a C=O stretching vibration near 1710 cm^{-1}, typical of free fatty acids [192].

Tween-80 (Figure 4.6D) exhibited characteristic peaks at 2920 cm^{-1} (C-H stretching) and 1100-1150 cm^{-1} (C-O-C stretching of ether linkages) [193].

The physical mixture (Figure 4.6E) displayed almost all principal peaks of ciprofloxacin and the excipients with slight reductions in intensity, indicating no chemical incompatibility between components [181].

However, in the NLC formulation spectrum (Figure 4.6F), most of the distinct ciprofloxacin peaks were either broadened or disappeared, and no sharp or new peaks were observed. This broadening and flattening of characteristic bands reflect complete drug entrapment in the lipid matrix and conversion of ciprofloxacin into an amorphous form. The disappearance of distinct ciprofloxacin peaks indicates uniform drug incorporation within the lipid matrix, with no detectable crystalline drug phase [132].

The reduction or disappearance of characteristic ciprofloxacin bands, such as the C=O stretching at 1715 cm^{-1} and the C-F band around 1040 cm^{-1}, suggests that the drug molecules are well accommodated within the lipid network through weak intermolecular hydrogen bonding and van der Waals interactions. The lipid matrix (solid lipid + liquid lipid + surfactant) provides an amorphous microenvironment that masks the crystalline peaks of drug [194].

This observation aligns with reports that incorporation of liquid lipids like oleic acid into solid lipids such as Compritol leads to partial lattice disorder, producing less-ordered matrices capable of trapping drug molecules in an amorphous or molecularly dispersed form. The presence of Tween-80 further stabilizes the system by preventing crystallization during cooling. Similar FTIR findings have been reported for ciprofloxacin and other hydrophilic drugs encapsulated in lipid-based nanocarriers, confirming physical entrapment without chemical modification [195].

The absence of new peaks or major shifts further demonstrates the chemical stability of ciprofloxacin in the NLC formulation, as no covalent interactions occurred during the homogenization or emulsification process. The disappearance of sharp crystalline peaks and appearance of broader, diffuse bands collectively indicate reduced lipid crystallinity, enhanced amorphous character, and efficient drug incorporation, features that directly contribute to the sustained-release behavior observed in subsequent in vitro studies [196].

The NLC formulation exhibited a non-Fickian (anomalous) diffusion mechanism ($n = 0.5663$), indicating that a combination of diffusion and lipid matrix erosion governs drug release. This pattern is typical for NLCs with higher solid-to-liquid lipid ratios, where the compact lipid matrix slows release while amorphous regions facilitate controlled diffusion [197].

Collectively, the FTIR results confirmed that ciprofloxacin was successfully incorporated within the NLC matrix without chemical degradation or interaction. The disappearance of sharp peaks in the formulation spectrum provides strong evidence of molecular dispersion and amorphization, which are desirable for stable, sustained-release topical formulations.

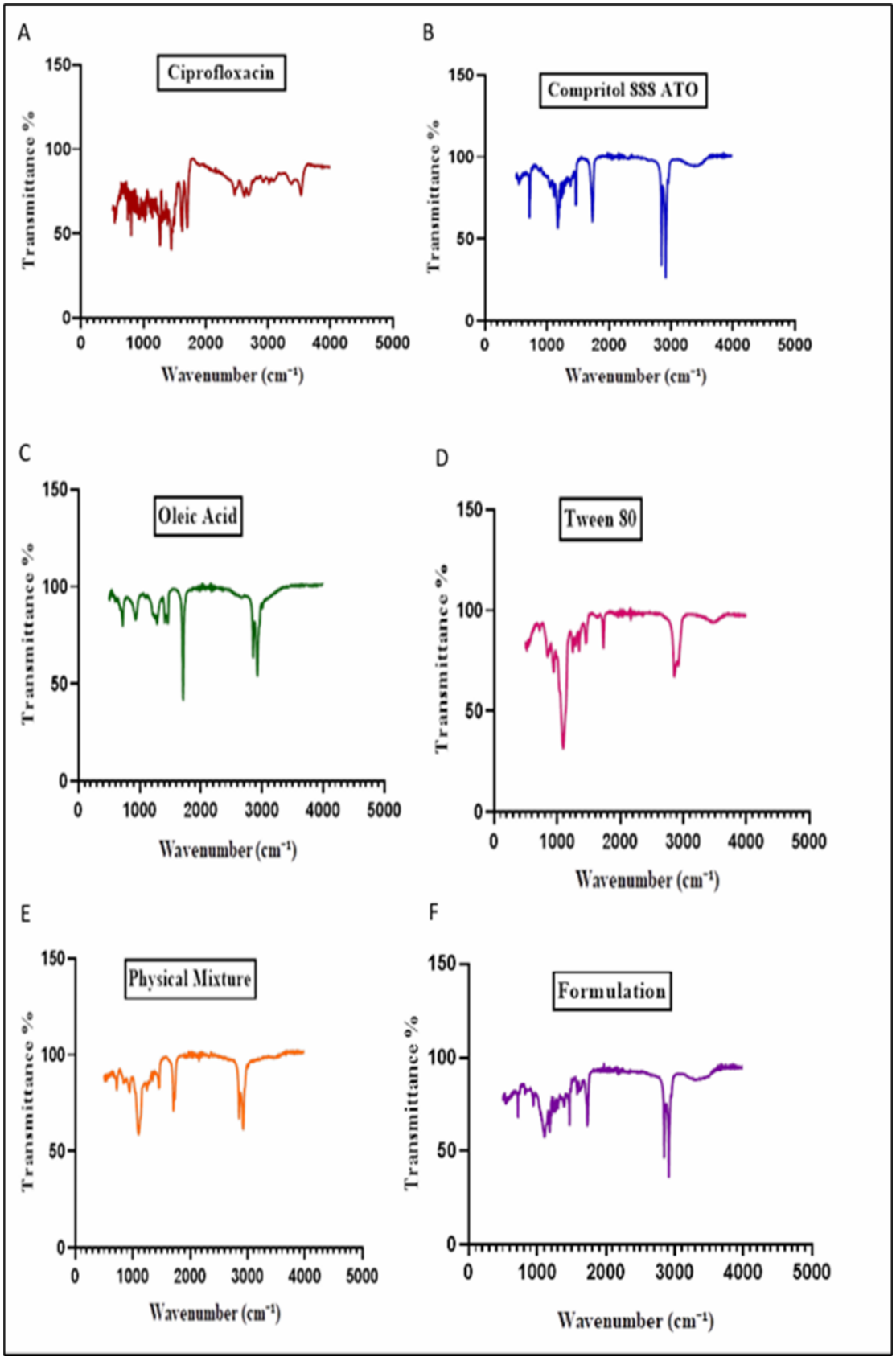

FIGURE 4.6: FTIR spectra of (A) ciprofloxacin, (B) Compritol ® 888 ATO, (C) oleic acid, (D) Tween-80, (E) physical mixture, and (F) ciprofloxacin-loaded NLCs.

4.7 Evaluation of In-Vitro Drug Release and Kinetic Modeling

In vitro drug release was evaluated in phosphate-buffered saline (PBS, pH 7.4) using a dialysis membrane method to compare the release profile of ciprofloxacin from the optimized NLC formulation with that of the plain drug dispersion. The cumulative percentage release data is presented in Figure 4.7.

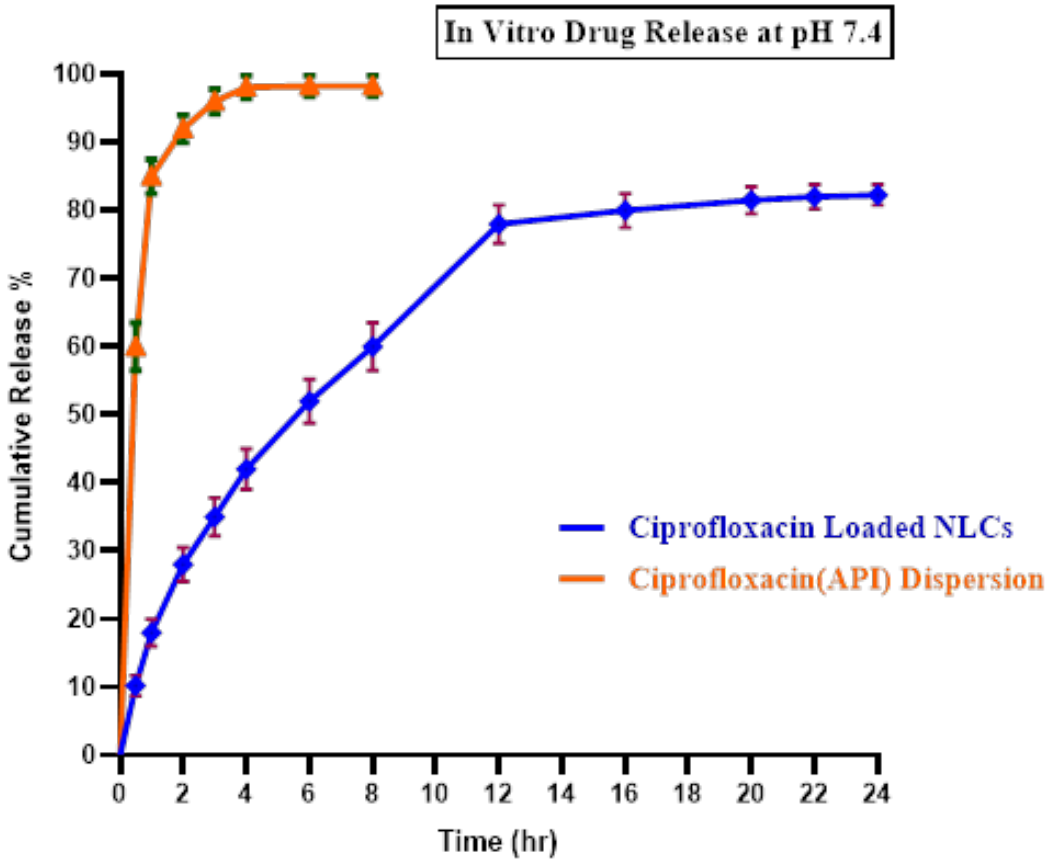

FIGURE 4.7: Cumulative in-vitro release profiles of ciprofloxacin from the optimized ciprofloxacin-loaded NLCs and the plain drug dispersion in phosphate-buffered saline (PBS, pH 7.4). Values are expressed as mean ± standard deviation (n = 3).

The ciprofloxacin dispersion exhibited a rapid release, achieving near-complete drug liberation (≈ 98.3 %) within 6-8 hours which is consistent with previous reports demonstrating fast dissolution of ciprofloxacin dispersions under similar conditions [198]. In contrast, the NLC formulation displayed a biphasic release pattern, with an initial burst of roughly 22% within the first hour, followed by a

sustained release phase lasting up to 24 hours, achieving a cumulative drug release of approximately 83%. This extended release is likely due to the combination of solid and liquid lipids, which create a partially disordered lipid matrix that can encapsulate the drug and slow its diffusion, thereby maintaining prolonged drug availability [131].

The initial burst in NLCs can be attributed to desorption of surface-associated drug, whereas the sustained release reflects the gradual diffusion of ciprofloxacin from the lipid matrix. The prolonged release confirms that the developed NLC system effectively modulates drug delivery, likely due to the combination of Compritol and oleic acid, which together form an imperfect crystalline matrix capable of accommodating the drug and retarding its release [133].

To investigate the release mechanism of ciprofloxacin from the NLCs, the release data were fitted to zero-order, first-order, Higuchi, and Korsmeyer-Peppas kinetic models. The correlation coefficients (R^2) for each model are summarized in Table 4.5. Among the models tested, the Korsmeyer-Peppas model exhibited the highest correlation ($R^2 = 0.9932$) with a release exponent (n) of 0.5663, indicating non-Fickian (anomalous) diffusion. These results indicate that ciprofloxacin release is governed by a combination of diffusion through the lipid matrix and gradual relaxation or erosion of the carrier structure [199].

The high correlation coefficient obtained for the Higuchi model ($R^2 = 0.9472$) highlights the dominant contribution of diffusion to the release process. Furthermore, the release exponent (n) falling between 0.45 and 0.89 confirms anomalous (non-Fickian) transport, consistent with earlier findings on ciprofloxacin release from NLCs [200].

TABLE 4.5: Kinetic model fitting for ciprofloxacin release from NLCs

Release Model	**R^2**	**n**
Zero-order	0.8336	
First-order	0.6585	
Higuchi	0.9472	
Korsmeyer-Peppas	0.9932	0.5663

4.8 Evaluation of Ciprofloxacin-NLC Gel

4.8.1 Physical and Rheological Evaluation of Ciprofloxacin - Loaded NLC Gel

The optimized gel was transparent and homogeneous with no visible aggregates, lumps, or phase separation, which reflected the effective dispersion of the NLCs in the polymeric matrix. Table 4.6 depicts the results for the characterization parameters. The pH of the surface of the gel was found to be 6.52 ± 0.01, within the physiological skin pH range, which could minimize irritation and ensure good compatibility with the stratum corneum. Rheological analysis by a Brookfield DV2T viscometer showed pseudoplastic behavior, which is favorable in topical preparations since it allows easy spreadability upon the application of stress, with the preservation of structural integrity at rest. Viscosity at 0.5 rpm was 73,400 ± 180 cP, high enough to ensure no runoff and provide prolonged skin contact. The spreadability of the gel, determined by a modified glass plate method, was 5.97 ± 0.12 cm, indicating that the gel is spreadable with low mechanical force and thus can be applied evenly. High spreadability enhances patient compliance, ensuring drug is uniformly distributed on the surface of the skin [201, 202].

TABLE 4.6: Physicochemical attributes and rheological behavior of ciprofloxacin-Loaded NLC gel

Parameter	**Measured Value (Mean ± SD)**	**Observation / Implication**
Appearance	Translucent, homogeneous	Stable formulation with no visible aggregates or phase separation, indicating uniform NLC dispersion
pH	6.52 ± 0.05	Falls within the physiological skin pH range, supporting dermal compatibility
Viscosity (0.5 rpm)	73,400 cP ± 180	Appropriate consistency for topical use; demonstrates shear-thinning behavior beneficial for spreadability
Rheology	Pseudoplastic (non-Newtonian)	Ensures ease of application while maintaining retention on the skin surface

Table 4.6 continued from previous page

Parameter	**Measured Value (Mean ± SD)**	**Observation / Implication**
Spreadability	5.97 cm ± 0.12	Facilitates uniform application with minimal force, enhancing patient compliance

4.8.2 Ex Vivo Skin Permeation of Ciprofloxacin - Loaded NLC Gel

The ex vivo permeation study indicates a substantial enhancement in the transdermal delivery performance of the ciprofloxacin-loaded NLC gel relative to the plain ciprofloxacin gel (active pharmaceutical ingredient in gel) (Figure 4.8, Table 4.7). The cumulative permeation at 2 hours (Q_2h) was higher for the plain gel (486.14 $\mu g/cm^2$) owing to a rapid burst release. By contrast, the NLC gel exhibited a lower early permeation (341.34 $\mu g/cm^2$), which is consistent with its controlled-release profile and aligns with previously reported lipid-based nanocarrier behavior [203]. However, within 4 hours, the permeation trajectories of the two formulations diverged markedly ($p < 0.01$ at each time point). The NLC gel demonstrated a continuous, nearly linear permeation phase from 2-12 hours ($R^2 = 0.995$), achieving a cumulative permeation of 617.72 $\mu g/cm^2$ at 4 hours and progressing to 1,151.57 $\mu g/cm^2$ by 24 hours, in agreement with sustained diffusion patterns observed in NLC-mediated dermal delivery systems [204]. In contrast, the plain gel reached an early plateau at approximately 737.01 $\mu g/cm^2$ after 6 hours, with negligible further permeation, thereafter 753.54 $\mu g/cm^2$ at 24 hours ($p < 0.001$). The sustained permeation fraction from 4-24 hours was 45.2% for the NLC gel versus 10.7% for plain gel, corresponding to a 4.2-fold improvement in extended delivery. Flux analysis corroborated these observations: the NLC formulation showed a significantly higher steady-state flux ($J\_ss = 75.5$ $\mu g/cm^2/h$) than plain gel (24.7 $\mu g/cm^2/h$), yielding an enhancement ratio (ER) of 3.05 (Table 4.6). The prolonged time to 50% release ($T_{50}\% = 3.7$ h versus 1.8 h), reduced burst release, higher release efficiency (72.3% vs. 38.5%), and greater cumulative permeation collectively suggest that the ciprofloxacin-loaded NLCs modulate

release through dual lipid-matrix diffusion and nanocarrier-mediated skin penetration [205]. The 33.7% higher total permeation observed for the NLC gel ($p < 0.001$) is attributed to enhanced follicular uptake, improved skin partitioning, and controlled drug release from the Compritol-oleic acid lipid blend. Overall, the permeation profile confirms that the ciprofloxacin-loaded NLC gel constitutes a superior transdermal delivery system able to sustain drug transport across the skin while minimizing the burst release, an important attribute for the prolongation of antibacterial therapy.

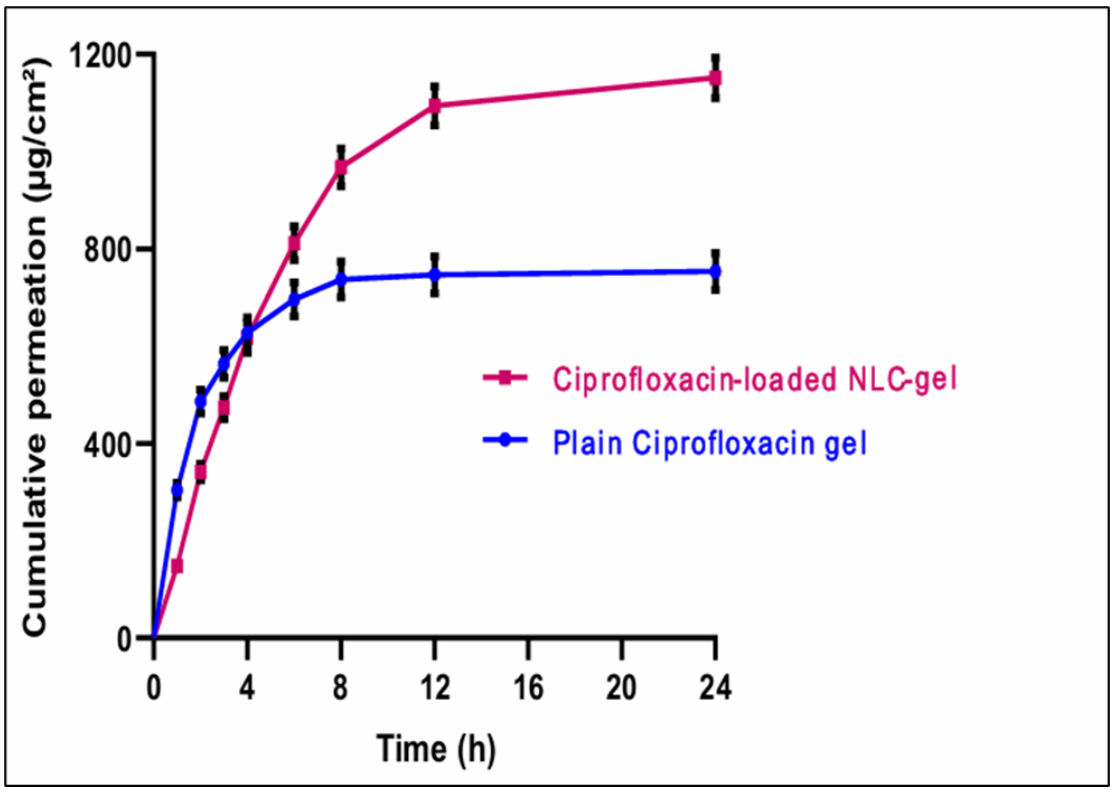

FIGURE 4.8: Enhanced 24 h permeation of ciprofloxacin from NLC-gel versus plain gel (mean ± SD, n=3).

TABLE 4.7: Ex vivo permeation parameters of ciprofloxacin from NLC gel versus conventional gel (n = 3)

Assessment Parameter	**Plain cipro gel**	**Cipro-loaded NLC-gel**	**p-value**	**Significance**
Q_{24} ($\mu g/cm^2$)	753.54÷2.35	1151.5 ± 3.2.2	<0.001	***
Jss ($\mu g/cm^2/h$)	24.7±1.08	75.5±1.95	<0.001	***
Enhancement Ratio (ER, 24 h)	1 (Reference)	3.05	——-	——

Note: Skin permeation performance was characterized by cumulative drug transport over 24 hours (Q_{24}) and steady-state flux (J_{ss}). Data are reported as mean ± SD (n = 3). Comparisons between groups were conducted using an unpaired Student's t-test, and differences reaching *p < 0.001 were regarded as significant when compared with the plain gel.

4.8.3 Skin Irritation Test

The ciprofloxacin-loaded NLC gel exhibited excellent dermal compatibility, with no observable erythema or edema across all evaluation time point (24, 48, or 72 h) (Table 4.8).

These findings indicate that the developed formulation is well tolerated upon topical application. In contrast, the 0.8% w/v sodium lauryl sulfate (positive control) elicited marked irritation responses, including moderate to severe erythema accompanied by mild edema, thereby confirming the sensitivity of the irritation model.

No adverse skin reactions were observed in the negative control group (plain gel), further supporting the inherent safety of the formulation components (Figure 4.9) [206].

The Primary Irritation Index (PII) for the ciprofloxacin-loaded NLC gel was calculated as 0.00, classifying the formulation as non-irritant according to OECD criteria (PII < 0.5). This absence of irritation is attributable to the biocompatible lipid matrix comprising Compritol ® and oleic acid, together with the non-ionic surfactant Tween 80, which is known for its low irritancy and favorable interaction with the skin barrier.

Statistical analysis revealed no significant differences in erythema or edema scores between the NLC gel and the negative control ($p > 0.05$). Conversely, a highly significant difference was observed when compared with the positive control group ($p < 0.001$), confirming that the developed NLC gel lacks irritant potential and is suitable for topical administration [207].

TABLE 4.8: Dermal irritation response following topical administration of cipro floxacin - loaded NLC gel, positive control and plain gel in New Zealand White rabbits

Experimental Group	Rabbit ID	Erythema score (24 h)	Edema score (24 h)	Combined score (24 h)	Erythema score (48 h)	Edema score (48 h)	Combined score (48 h)	Erythema score (72 h)	Edema score (72 h)	Combined score (72 h)
Ciprofloxacin - loaded NLC gel	1	0	0	0	0	0	0	0	0	0
(Test group)	2	0	0	0	0	0	0	0	0	0
	3	0	0	0	0	0	0	0	0	0
Mean ± SD	—	0.00 ± 0.00	0.00 ± 0.00	0.00 ± 0.00	0.00 ± 0.00	0.00 ± 0.00	0.00 ± 0.00	0.00 ± 0.00	0.00 ± 0.00	0.00 ± 0.00
Positive control (0.8% SLS)	4	3.00	2.00	5.00	2.00	1.00	3.00	1.00	1.00	2.00
	5	3.00	2.00	5.00	3.00	2.00	5.00	1.00	0.00	1.00
	6	2.00	2.00	4.00	1.00	1.00	2.00	0.00	1.00	1.00
Mean ± SD	—	2.66 ± 0.05	2.00 ± 0.04	4.66 ± 1.27	2.00 ± 0.04	1.33 ± 0.01	3.33 ± 0.58	0.66 ± 0.01	0.66 ± 0.01	1.32 ± 0.01
Plain gel	7	0	0	0	0	0	0	0	0	0
(negative control)	8	0	0	0	0	0	0	0	0	0
	9	0	0	0	0	0	0	0	0	0
Mean ± SD	—	0.00 ± 0.00	0.00 ± 0.00	0.00 ± 0.00	0.00 ± 0.00	0.00 ± 0.00	0.00 ± 0.00	0.00 ± 0.00	0.00 ± 0.00	0.00 ± 0.00

Note: All data are expressed as mean ± SD (n = 3). Group comparisons were carried out using one-way analysis of variance followed by Tukey's multiple comparison procedure, with statistical significance defined at $p < 0.05$. Erythema and edema were graded according to the Draize scale, and the total irritation score represents the sum of both parameters. SLS: sodium lauryl sulfate.

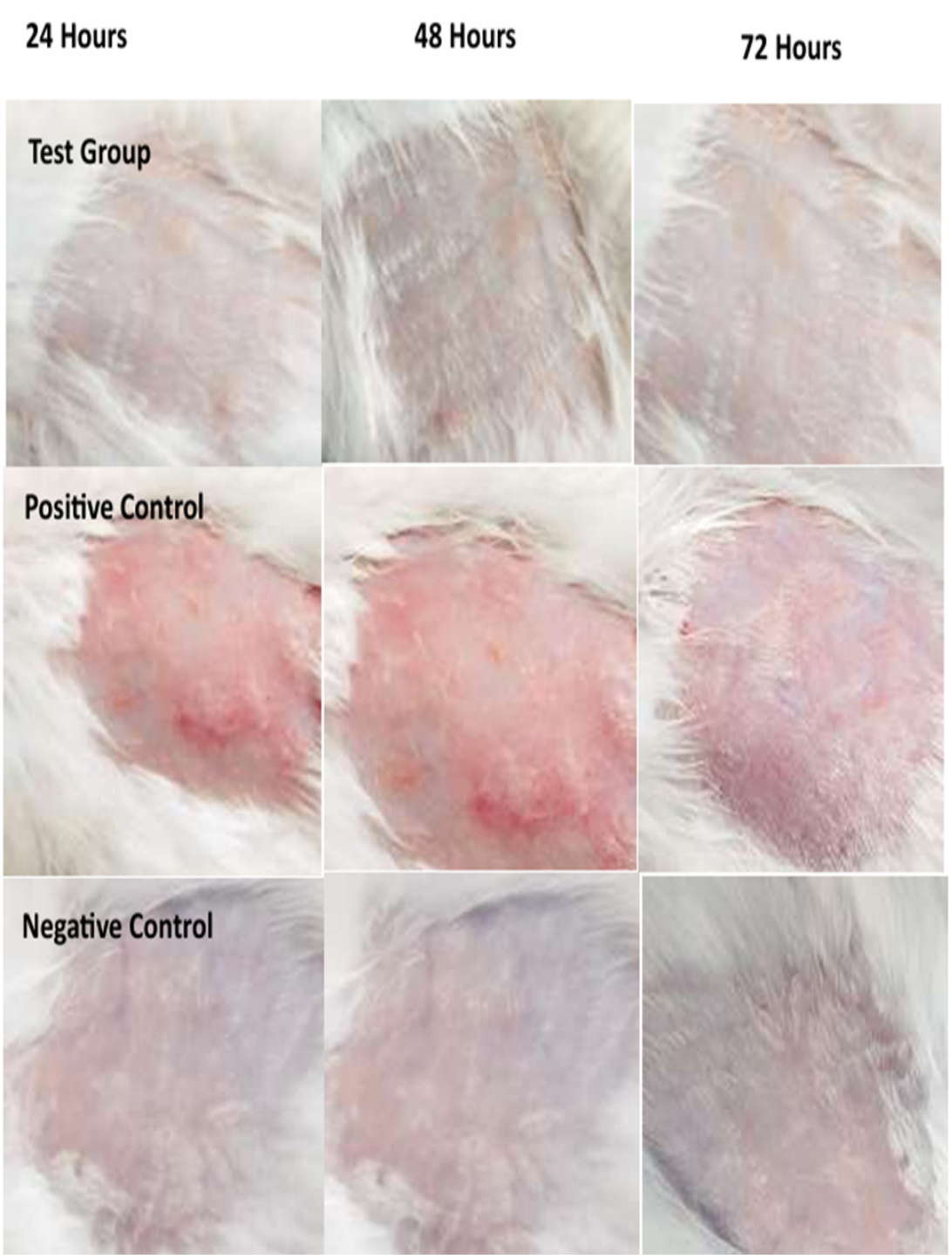

FIGURE 4.9: Comparison of dermal irritation scores at 24, 48, and 72 hours for the ciprofloxacin-loaded NLC gel, positive control (0.8% SLS), and negative control (plain gel).

4.9 Antibacterial Activity

The ciprofloxacin-loaded NLC-gel exhibited a significantly higher inhibitory effect compared with both ciprofloxacin (API) dispersion and blank NLC gel at the

tested time points (12 and 24 h). Representative plates and corresponding graphs are presented in Figure 4.10.

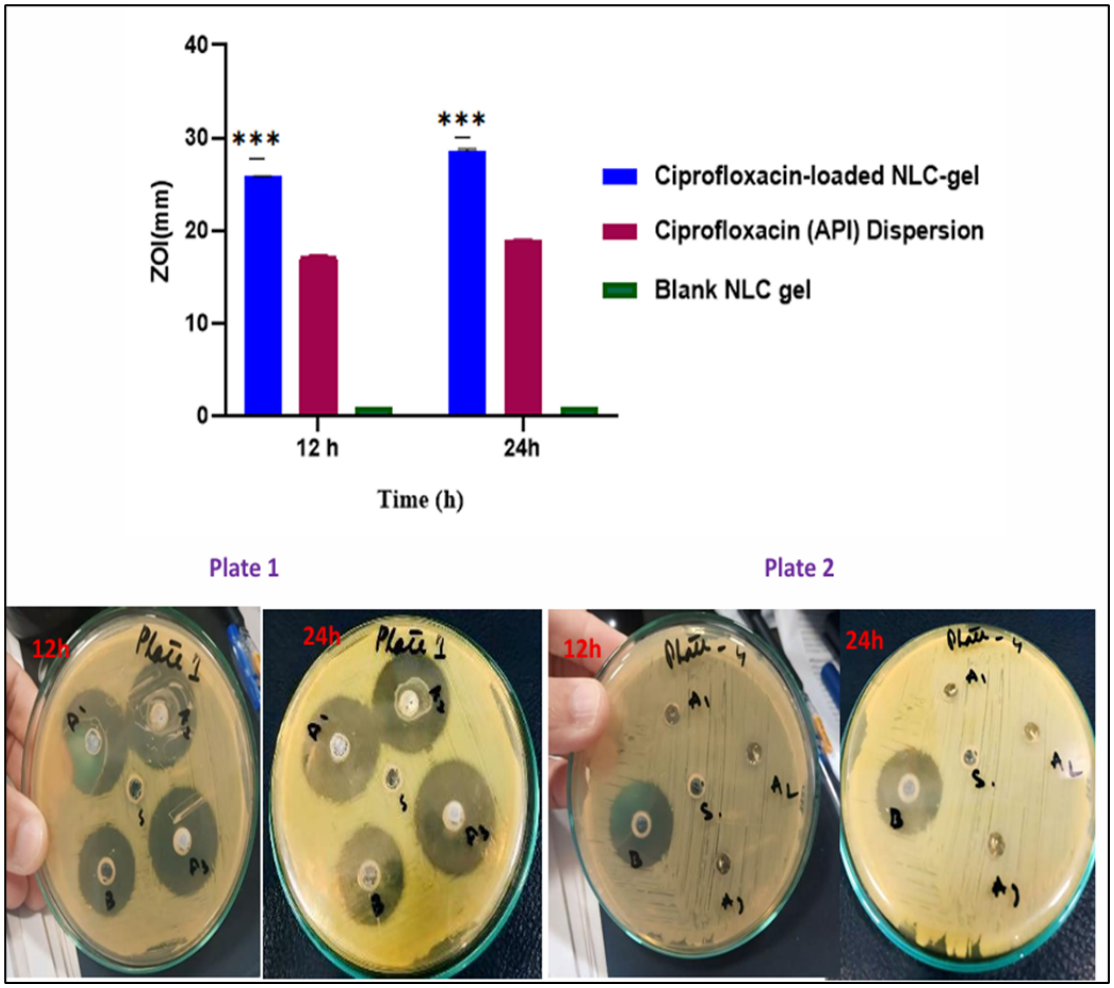

FIGURE 4.10: Antibacterial activity of ciprofloxacin - loaded NLC-gel against MRSA determined by agar well diffusion at 12 h and 24 h. Results are presented as mean ± SD (n = 3). Ciprofloxacin-loaded NLC - gel showed significantly larger zones of inhibition compared with ciprofloxacin dispersion and blank NLCs, confirming enhanced efficacy due to sustained drug release (*$p < 0.001$).

At 12 h, the mean ZOI for ciprofloxacin-loaded NLC-gel was 25.80 ± 0.10 mm, while for ciprofloxacin dispersion, it was 16.2 ± 0.21 mm and 1.0 mm for blank-NLC. After 24 h, ciprofloxacin-loaded NLC-gel further increased ZOI to 28.55 ± 0.25 mm, while ciprofloxacin dispersion reached 19.0 ± 0.20 mm, and blank-NLC remained inactive. One-way ANOVA coupled with Tukey's multiple comparison analysis confirmed the superior antibacterial performance of the ciprofloxacin-loaded NLC gel at both points relative to the ciprofloxacin dispersion and blank NLCs (***$p < 0.001$).

Agar plate images support the quantitative measurements of ZOI. Plate 1 (12 h, 24 h) shows wells with ciprofloxacin-loaded NLC-gel (A1–A3) exhibiting larger zones, while the Ciprofloxacin Dispersion (B) displays smaller zones, and the solvent control (S) shows no inhibition. Plate 2 (12 h, 24 h) demonstrates blank NLC gel (A1–A3) with no inhibitory zones, which assures that the excipients themselves do not possess any intrinsic antibacterial activity, and the effect observed was due to ciprofloxacin delivery.

The improved antibacterial activity of ciprofloxacin-loaded NLCs can, therefore, be directly related to its enhanced in vitro permeation profile. NLCs allow for better and prolonged drug release, which provides higher local concentrations of ciprofloxacin at the site of infection. This may improve deeper diffusion into the bacterial culture and result in a stronger inhibition effect. In addition, nanoparticles may assist in continuous drug diffusion through the agar medium, thereby increasing their effectiveness against MRSA. Similar trends have been reported in the literature, where nano-based carriers were shown to sustain higher localized drug concentrations and exhibit enhanced antibacterial efficacy against resistant pathogens [114, 140, 208].

The overall results thus indicate that the ciprofloxacin-loaded NLC-gel significantly outperformed the plain ciprofloxacin gel in the inhibition of MRSA growth, and the observed correlation between enhanced permeation and antibacterial efficacy supports the therapeutic potential of NLC-based topical formulations. The lack of antibacterial activity associated with blank NLC gel confirms that excipients themselves do not contribute to antimicrobial effects, and the resultant activity arises due to the ciprofloxacin delivery system [88, 209].

4.10 Stability Studies of Ciprofloxacin - Loaded NLC Gel

The optimized gel showed good physical stability throughout the experimental period, with no signs of phase separation, precipitation, or discoloration, which

reflects its good physical integrity. The initial pH of the NLC gel was 6.52 ± 0.01, and no significant deviation (±0.5 units) was observed during three months of storage across all conditions. Under accelerated conditions, there was a slight decrease in pH over the three-month period, to 6.28 ± 0.03, but this was still within the stability limit. Viscosity measurement confirmed the structural integrity of the gel network. At both refrigerated and ambient conditions, viscosity decreased by less than 5%, while at 40∘C there was a gradual decrease, with a maximum viscosity drop of 3.96% following three months of storage. More importantly, the gel maintained its pseudoplastic character, indicating the integrity of the inner structure of NLCs and Carbopol 940 network was preserved. The reduction in viscosity upon increase of temperature is attributed to the relaxation of the polymeric network chains and the attenuated hydrogen bonding interactions due to thermal stress [201, 210].

As demonstrated in Table 4.9, the optimized formulation was stable for all tested storage conditions in terms of its physicochemical and rheological attributes, indicating that it may be stored long term before administration.

TABLE 4.9: Stability parameters of ciprofloxacin - loaded NLC gel at ICH conditions up to 3 months

Month	**Storage Temp**	**Physical Appearance**	**pH** (mean ± SD)	**Viscosity** (cP, mean ± SD)	% **Viscosity Variation**
1	4°C	Transparent, uniform	6.50 ± 0.01	73,400 ± 180	-0.41
1	25°C	Transparent, uniform	6.48 ± 0.02	72,950 ± 200	-0.62
1	40°C	Transparent, uniform	6.42 ± 0.03	71,900 ± 210	-2.05
2	4°C	Transparent, uniform	6.49 ± 0.02	73,100 ± 175	-0.41
2	25°C	Transparent, uniform	6.46 ± 0.02	72,600 ± 180	-1.1
2	40°C	Transparent, uniform	6.35 ± 0.03	71,100 ± 200	-3.1
3	4°C	Transparent, uniform	6.48 ± 0.02	72,900 ± 170	-0.68

Table 4.9 continued from previous page

Month	**Storage Temp**	**Physical Appearance**	**pH** (mean ± SD)	**Viscosity** (cP, mean ± SD)	% **Viscosity Variation**
3	25°C	Transparent, uniform	6.44 ± 0.03	72,000 ± 180	-1.9
3	40°C	Transparent, uniform	6.28 ± 0.03	70,500 ± 200	-3.96

Chapter 5

Conclusion and Future Recommendations

5.1 Conclusion

Ciprofloxacin-loaded NLCs were successfully developed and optimized as a transdermal delivery system. The optimized NLCs exhibited nanoscale particle size, high entrapment efficiency, and favorable physicochemical stability, ensuring efficient drug incorporation within the lipid matrix. Ex vivo permeation studies demonstrated enhanced skin penetration and sustained drug release, while in vivo dermal assessments confirmed good tolerance and safety. The formulation also maintained antibacterial efficacy against MRSA, indicating its potential to overcome pharmacokinetic limitations of conventional ciprofloxacin therapy. Overall, this study establishes a systematic, Box-Behnken guided NLC platform as a promising strategy for transdermal delivery of ciprofloxacin and other poorly soluble antibiotics, addressing key challenges associated with antimicrobial resistance and improving therapeutic outcomes.

5.2 Future Recommendations

Ciprofloxacin-loaded NLCs offer a promising strategy for transdermal drug delivery; however, further investigations are required to advance this platform toward clinical application. While preclinical assessments demonstrate effective skin permeation, controlled release behavior, and acceptable dermal tolerability, clinical studies in human subjects are necessary to establish pharmacokinetic profiles, systemic exposure, therapeutic efficacy, and immunological safety. Such evaluations are critical for defining optimal dosing regimens, confirming long-term safety, and meeting regulatory requirements for clinical translation.

Beyond ciprofloxacin, the NLC platform exhibits substantial versatility and may be adapted for the delivery of other therapeutic agents. Antibiotics with poor aqueous solubility and limited membrane permeability, particularly those classified as Biopharmaceutics Classification System (BCS) Class IV, may benefit from incorporation into lipid-based transdermal systems to address the limitations of conventional oral administration.

Moreover, given the increasing global burden of multidrug-resistant infections, future research may explore the co-encapsulation of synergistic antimicrobial agents or combination therapies to enhance antibacterial efficacy while potentially reducing the emergence of resistance.

Comprehensive stability assessment is essential to support further development and potential commercialization. Long-term and accelerated stability studies under controlled environmental conditions, including variations in temperature, humidity, and light exposure, are required to ensure the retention of physicochemical integrity, drug content uniformity, and performance characteristics of both NLC dispersions and their hydrogel formulations.

In parallel, formulation refinement strategies such as surface functionalization, ligand-mediated targeting, or polyethylene glycol (PEG) modification may be investigated to enhance delivery efficiency and minimize non-specific interactions.

Advancements in transdermal delivery technologies may further improve the performance of NLC-based systems. Integration with physical or chemical enhancement techniques, including microneedle-assisted delivery, iontophoresis, or optimized penetration enhancers, may facilitate increased drug transport across the skin barrier and allow therapeutic plasma concentrations to be achieved at reduced doses. Additionally, mechanistic investigations focusing on nanoparticle–skin interactions, including alterations in stratum corneum lipid organization and intracellular uptake pathways, would provide valuable insight for rational system optimization.

Finally, the application of NLC-based transdermal platforms may be extended to other therapeutic classes, including antiviral, anti-fungal, and anti-inflammatory agents with limited oral bioavailability. The incorporation of systematic development approaches, such as Quality by Design (QbD), may support the creation of robust, scalable, and reproducible formulations, thereby enhancing the clinical relevance and translational potential of transdermal nanocarrier systems.

Bibliography

[1] A. Estany-Gestal, A. Salgado-Barreira, and J. M. Vazquez-Lago, "Antibiotic use and antimicrobial resistance: A global public health crisis," *Antibiotics*, vol. 13, no. 9, p. 900, 2024.

[2] C. J. L. Murray *et al.*, "Global burden of bacterial antimicrobial resistance in 2019: A systematic analysis," *The Lancet*, vol. 399, no. 10325, pp. 629–655, 2022.

[3] T. Mustafa *et al.*, "Regional and national trends in consumption of antimicrobials in pakistan; pre and post-covid (2019–2021)," *Clinical Infectious Diseases*, vol. 77, no. Supplement_7, pp. S569–S577, 2023.

[4] Z. Ullah, S. Ahmad, and H. Y. Mahsood, "Antimicrobial resistance (amr) in pakistan: A growing crisis," *Gomal Journal of Medical Sciences*, vol. 23, no. 1, 2025.

[5] J. Li *et al.*, "Methicillin-resistant staphylococcus aureus (mrsa): Resistance, prevalence, and coping strategies," *Antibiotics*, vol. 14, no. 8, p. 771, 2025.

[6] A. Habib and A. Qadir, "Frequency and antibiotic susceptibility pattern of community-associated methicillin-resistant staphylococcus aureus (ca-mrsa) in uncomplicated skin and soft tissue infections," *Journal of the College of Physicians and Surgeons Pakistan*, vol. 32, pp. 1398–1403, 2022.

[7] M. M. Idrees *et al.*, "Prevalence of meca- and mecc-associated methicillin-resistant staphylococcus aureus in clinical specimens, punjab, pakistan," *Biomedicines*, vol. 11, no. 3, p. 878, 2023.

[8] U. Tasneem *et al.*, "Co-occurrence of antibiotic resistance and virulence genes in methicillin resistant staphylococcus aureus (mrsa) isolates from pakistan," *African Health Sciences*, vol. 22, no. 1, pp. 486–495, 2022.

[9] H. Lade and J.-S. Kim, "Molecular determinants of β-lactam resistance in methicillin-resistant staphylococcus aureus (mrsa): An updated review," *Antibiotics*, vol. 12, no. 9, p. 1362, 2023.

[10] P. Gauba and A. Saxena, "Ciprofloxacin properties, impacts, and remediation," *CABI Reviews*, 2023.

[11] S. Hansmann, Y. Miyaji, and J. Dressman, "An in silico approach to determine challenges in the bioavailability of ciprofloxacin, a poorly soluble weak base with borderline solubility and permeability characteristics," *European Journal of Pharmaceutics and Biopharmaceutics*, vol. 122, pp. 186–196, 2018.

[12] R. Leclercq, "Mechanisms of resistance to macrolides and lincosamides: Nature of the resistance elements and their clinical implications," *Clinical Infectious Diseases*, vol. 34, no. 4, pp. 482–492, 2002.

[13] S. Hassanzadeh *et al.*, "Epidemiology of efflux pumps genes mediating resistance among staphylococcus aureus; a systematic review," *Microbial Pathogenesis*, vol. 139, p. 103850, 2020.

[14] C. J. L. Murray *et al.*, "Global burden of bacterial antimicrobial resistance in 2019: A systematic analysis," *The Lancet*, vol. 399, no. 10325, pp. 629–655, 2022.

[15] M. A. Juma *et al.*, "Whole genome sequencing-based characterization and determination of quinolone resistance among methicillin-resistant and methicillin-susceptible s. aureus isolates from patients attending regional referral hospitals in tanzania," *BMC Genomics*, vol. 25, no. 1, p. 1130, 2024.

[16] S. Badawy *et al.*, "Toxicity induced by ciprofloxacin and enrofloxacin: Oxidative stress and metabolism," *Critical Reviews in Toxicology*, vol. 51, no. 9, pp. 754–787, 2021.

[17] V. P. Chavda, *Nanobased Nano Drug Delivery: A Comprehensive Review*, 2019, pp. 69–92.

[18] R. Y. Pelgrift and A. J. Friedman, "Nanotechnology as a therapeutic tool to combat microbial resistance," *Advanced Drug Delivery Reviews*, vol. 65, no. 13-14, pp. 1803–1815, 2013.

[19] J. K. Patra *et al.*, "Nano based drug delivery systems: Recent developments and future prospects," *Journal of Nanobiotechnology*, vol. 16, no. 1, p. 71, 2018.

[20] J. Ponnusamy and S. Gopal, "Nanostructured lipid carriers: Enhancing delivery of poorly soluble drugs," *Current Nanomaterials*, 2025.

[21] R. Müller, M. Radtke, and S. Wissing, "Nanostructured lipid matrices for improved microencapsulation of drugs," *International Journal of Pharmaceutics*, vol. 242, no. 1-2, pp. 121–128, 2002.

[22] C.-L. Fang, S. A. Al-Suwayeh, and J.-Y. Fang, "Nanostructured lipid carriers (nlcs) for drug delivery and targeting," *Recent Patents on Nanotechnology*, vol. 7, no. 1, pp. 41–55, 2013.

[23] E. B. Souto *et al.*, "Physicochemical and biopharmaceutical aspects influencing skin permeation and role of sln and nlc for skin drug delivery," *Heliyon*, vol. 8, no. 2, 2022.

[24] World Health Organization, "Global antimicrobial resistance surveillance system (glass) report: Early implementation 2020," World Health Organization, Tech. Rep., 2020.

[25] B. Aslam and S. F. Aljasir, "Climate change and amr: Interconnected threats and one health solutions," *Antibiotics*, vol. 14, no. 9, p. 946, 2025.

[26] European Food Safety Authority and European Centre for Disease Prevention and Control, "The european union summary report on antimicrobial resistance in zoonotic and indicator bacteria from humans, animals and food in 2018/2019," *EFSA Journal*, vol. 19, no. 4, p. e06490, 2021.

[27] World Health Organization, "Global antimicrobial resistance and use surveillance system (glass) report 2022," World Health Organization, Tech. Rep., 2022.

[28] B. H. Gulumbe and A. A. Faggo, "Epidemiology of multidrug-resistant organisms in africa," *Mediterr Journal of Infection Microbes Antimicrobials*, vol. 8, no. 25, pp. 1–11, 2019.

[29] H. Bilal *et al.*, "Antibiotic resistance in pakistan: A systematic review of past decade," *BMC Infectious Diseases*, vol. 21, no. 1, p. 244, 2021.

[30] M. Afzal, "Antibiotic resistance pattern of escherichia coli and klebsiella species in pakistan: A brief overview," *Journal Microbial and Biochemical Technology*, vol. 9, pp. 277–279, 2017.

[31] S. Malik and J. Ahmed, "Antimicrobial susceptibility pattern and esbl prevalence in klebsiella pneumoniae from urinary tract infections in the north-west of pakistan," *African Journal of Microbiology...*, 2009.

[32] D. Kumar *et al.*, "The rising threat of mrsa: Antimicrobial resistance profiling of staphylococcus aureus from secondary care setting in sindh," *Pure and Applied Biology (PAB)*, vol. 14, no. 3, 2025.

[33] World Health Organization, "Antimicrobial resistance multi-partner trust fund: Forging tripartite collaboration for urgent global and country action against antimicrobial resistance (amr): Annual progress report 2020," Food & Agriculture Org., Tech. Rep., 2021.

[34] H. F. Chambers and F. R. DeLeo, "Waves of resistance: Staphylococcus aureus in the antibiotic era," *Nature Reviews Microbiology*, vol. 7, no. 9, pp. 629–641, 2009.

[35] "Antibiotic resistance threats in the united states, 2013," Tech. Rep., 2013.

[36] World Health Organization, "Analysis of antibacterial agents in clinical and preclinical development: Overview and analysis 2025," Tech. Rep., 2025.

[37] N. Mahmood *et al.*, "Mutational analysis of gyrb at amino acids: G481a & d505a in multidrug resistant (mdr) tuberculosis patients," *Journal of Infection and Public Health*, vol. 12, no. 4, pp. 496–501, 2019.

[38] Y. Guo *et al.*, "Multicenter antimicrobial resistance surveillance of clinical isolates from major hospitals—china, 2022," *China CDC Weekly*, vol. 5, no. 52, p. 1155, 2023.

[39] H. Tabaja, J. R. Hindy, and S. S. Kanj, "Epidemiology of methicillin-resistant staphylococcus aureus in arab countries of the middle east and north african (mena) region," *Mediterr Journal Hematology and Infectious Diseases*, vol. 13, no. 1, p. e2021050, 2021.

[40] A. Ullah *et al.*, "High frequency of methicillin-resistant staphylococcus aureus in peshawar region of pakistan," *SpringerPlus*, vol. 5, no. 1, p. 600, 2016.

[41] S. Abrar *et al.*, "Prevalence of extended-spectrum-β-lactamase-producing enterobacteriaceae: First systematic meta-analysis report from pakistan," *Antimicrobial Resistance & Infection Control*, vol. 7, no. 1, p. 26, 2018.

[42] A. Kaushik *et al.*, "Biofilm producing methicillin-resistant staphylococcus aureus (mrsa) infections in humans: Clinical implications and management," *Pathogens*, vol. 13, no. 1, p. 76, 2024.

[43] Y. Liu *et al.*, "Unmasking mrsa's armor: Molecular mechanisms of resistance and pioneering therapeutic countermeasures," *Microorganisms*, vol. 13, no. 8, p. 1928, 2025.

[44] H. F. Chambers, "Methicillin resistance in staphylococci: Molecular and biochemical basis and clinical implications," *Clinical Microbiology Reviews*, vol. 10, no. 4, pp. 781–791, 1997.

[45] M. Papadimitriou-Olivgeris *et al.*, "Risk factors for kpc-producing klebsiella pneumoniae enteric colonization upon icu admission," *Journal of Antimicrobial Chemotherapy*, vol. 67, no. 12, pp. 2976–2981, 2012.

[46] D. C. Hooper and G. A. Jacoby, "Mechanisms of drug resistance: Quinolone resistance," *Annals of the New York Academy of Sciences*, vol. 1354, no. 1, pp. 12–31, 2015.

[47] M. Otto, "Staphylococcal infections: Mechanisms of biofilm maturation and detachment as critical determinants of pathogenicity," *Annual Review of Medicine*, vol. 64, no. 1, pp. 175–187, 2013.

[48] S. Lakhundi and K. Zhang, "Methicillin-resistant staphylococcus aureus: Molecular characterization, evolution, and epidemiology," *Clinical Microbiology Reviews*, vol. 31, no. 4, pp. 10.1128/cmr.00 020–18, 2018.

[49] L. J. Shallcross *et al.*, "The role of the panton-valentine leucocidin toxin in staphylococcal disease: A systematic review and meta-analysis," *The Lancet Infectious Diseases*, vol. 13, no. 1, pp. 43–54, 2013.

[50] K. Hiramatsu *et al.*, "Multi-drug-resistant *Staphylococcus aureus* and future chemotherapy," *Journal of Infection and Chemotherapy*, vol. 20, no. 10, pp. 593–601, 2014.

[51] S. L. Davis, G. Delgado, Jr., and P. S. McKinnon, "Pharmacoeconomic considerations associated with the use of intravenous-to-oral moxifloxacin for community-acquired pneumonia," *Clinical Infectious Diseases*, vol. 41, no. Supplement_2, pp. S136–S143, 2005.

[52] A. M. Junkert *et al.*, "Pharmacokinetics of oral ciprofloxacin in adult patients: A scoping review," *British Journal of Clinical Pharmacology*, vol. 90, no. 2, pp. 528–547, 2024.

[53] M. N. Martinez and G. L. Amidon, "A mechanistic approach to understanding the factors affecting drug absorption: A review of fundamentals," *The Journal of Clinical Pharmacology*, vol. 42, no. 6, pp. 620–643, 2002.

[54] A. Dalhoff, "Global fluoroquinolone resistance epidemiology and implications for clinical use," *Interdisciplinary Perspectives on Infectious Diseases*, vol. 2012, no. 1, p. 976273, 2012.

[55] T. Fazal *et al.*, "Recent developments in natural biopolymer based drug delivery systems," *RSC Advances*, vol. 13, no. 33, pp. 23 087–23 121, 2023.

[56] D. J. Buehrle, M. M. Wagener, and C. J. Clancy, "Outpatient fluoroquinolone prescription fills in the united states, 2014 to 2020: Assessing the impact of food and drug administration safety warnings," *Antimicrobial Agents and Chemotherapy*, vol. 65, no. 7, pp. 10.1128/aac.00 151–21, 2021.

[57] M. Huruba *et al.*, "Survey of healthcare professionals to assess the awareness, knowledge and self-reported behavior regarding recent fluoroquinolones safety issues," *Medicine and Pharmacy Reports*, vol. 94, no. 4, p. 498, 2021.

[58] J. J. De Waele *et al.*, "Antimicrobial resistance and antibiotic stewardship programs in the icu: Insistence and persistence in the fight against resistance. a position statement from esicm/escmid/waaar round table on multi-drug resistance," *Intensive Care Medicine*, vol. 44, no. 2, pp. 189–196, 2018.

[59] R. Paliwal and S. R. Paliwal, *Nanomedicine, Nanotheranostics and Nanobiotechnology: Fundamentals and Applications*. CRC Press, 2025.

[60] H. Nsairat *et al.*, "Liposomes: Structure, composition, types, and clinical applications," *Heliyon*, vol. 8, no. 5, 2022.

[61] R. S. Kalhapure *et al.*, "Nanoengineered drug delivery systems for enhancing antibiotic therapy," *Journal of Pharmaceutical Sciences*, vol. 104, no. 3, pp. 872–905, 2015.

[62] M. Ferreira *et al.*, "Liposomes as antibiotic delivery systems: A promising nanotechnological strategy against antimicrobial resistance," *Molecules*, vol. 26, no. 7, p. 2047, 2021.

[63] J.-S. Kim, "Liposomal drug delivery system," *Journal of Pharmaceutical Investigation*, vol. 46, pp. 387–392, 2016.

[64] S. Deng *et al.*, "Polymeric nanocapsules as nanotechnological alternative for drug delivery system: Current status, challenges and opportunities," *Nanomaterials*, vol. 10, no. 5, p. 847, 2020.

[65] K. C. d. Castro, J. M. Costa, and M. G. N. Campos, "Drug-loaded polymeric nanoparticles: A review," *International Journal of Polymeric Materials and Polymeric Biomaterials*, vol. 71, no. 1, pp. 1–13, 2022.

[66] B. Lu, X. Lv, and Y. Le, "Chitosan-modified plga nanoparticles for control-released drug delivery," *Polymers*, vol. 11, no. 2, p. 304, 2019.

[67] A. K. Shakya *et al.*, "Review on plga polymer based nanoparticles with antimicrobial properties and their application in various medical conditions or infections," *Polymers*, vol. 15, no. 17, p. 3597, 2023.

[68] M.-H. Xiong *et al.*, "Delivery of antibiotics with polymeric particles," *Advanced Drug Delivery Reviews*, vol. 78, pp. 63–76, 2014.

[69] Y. Alvarado *et al.*, *Polymer Nanoparticles for the Release of Complex Molecules*, 2019, pp. 135–163.

[70] X. Li *et al.*, "Bridging the gap between fundamental research and product development of long acting injectable plga microspheres," *Expert Opinion on Drug Delivery*, vol. 19, no. 10, pp. 1247–1264, 2022.

[71] E. Abbasi *et al.*, "Dendrimers: Synthesis, applications, and properties," *Nanoscale Research Letters*, vol. 9, pp. 1–10, 2014.

[72] S. Alamos-Musre *et al.*, "From structure to function: The promise of pamam dendrimers in biomedical applications," *Pharmaceutics*, vol. 17, no. 7, p. 927, 2025.

[73] S. Mignani *et al.*, "Expand classical drug administration ways by emerging routes using dendrimer drug delivery systems: A concise overview," *Advanced Drug Delivery Reviews*, vol. 65, no. 10, pp. 1316–1330, 2013.

[74] S. Alfei and A. M. Schito, "From nanobiotechnology, positively charged biomimetic dendrimers as novel antibacterial agents: A review," *Nanomaterials*, vol. 10, no. 10, p. 2022, 2020.

[75] C. K. Ezeh and M. E. Dibua, "Anti-biofilm, drug delivery and cytotoxicity properties of dendrimers," *ADMET and DMPK*, vol. 12, no. 2, pp. 239–267, 2024.

[76] X. Li *et al.*, "Safety challenges and application strategies for the use of dendrimers in medicine," *Pharmaceutics*, vol. 14, p. 1292, 2022.

[77] J. Šebestík, M. Reiniš, and J. Ježek, *Biocompatibility and Toxicity of Dendrimers*. Springer, 2012, pp. 111–114.

[78] E. K. Apartsin, "Dendrimers for drug delivery: Where do we stand in 2023?" *MDPI*, p. 2740, 2023.

[79] K. Rajpoot, "Solid lipid nanoparticles: A promising nanomaterial in drug delivery," *Current Pharmaceutical Design*, vol. 25, no. 37, pp. 3943–3959, 2019.

[80] O. A. Madkhali, "Perspectives and prospective on solid lipid nanoparticles as drug delivery systems," *Molecules*, vol. 27, no. 5, p. 1543, 2022.

[81] L. Arana, L. Gallego, and I. Alkorta, "Incorporation of antibiotics into solid lipid nanoparticles: A promising approach to reduce antibiotic resistance emergence," *Nanomaterials*, vol. 11, no. 5, p. 1251, 2021.

[82] A. K. Jain and S. Thareja, *Solid Lipid Nanoparticles*, 2020, pp. 221–249.

[83] D. P. Gaspar and A. J. Almeida, *Surface-Functionalized Lipid Nanoparticles for Site-Specific Drug Delivery*. Springer, 2019, pp. 73–98.

[84] P. Ghasemiyeh and S. Mohammadi-Samani, "Solid lipid nanoparticles and nanostructured lipid carriers as novel drug delivery systems: Applications, advantages and disadvantages," *Research in Pharmaceutical Sciences*, vol. 13, no. 4, pp. 288–303, 2018.

[85] G. Yoon, J. W. Park, and I.-S. Yoon, "Solid lipid nanoparticles (slns) and nanostructured lipid carriers (nlcs): Recent advances in drug delivery," *Journal of Pharmaceutical Investigation*, vol. 43, pp. 353–362, 2013.

[86] D. Buldain *et al.*, "Antimicrobial activity of nanostructured lipid carriers loaded with melaleuca armillaris essential oil against staphylococcus aureus sensitive and resistant to methicillin," *Frontiers in Nanotechnology*, vol. 6, p. 1476423, 2024.

[87] S. Padhi, R. Mazumder, and S. Bisht, "Preformulation screening of lipids using solubility parameter concept in conjunction with experimental research to develop ceftriaxone loaded nanostructured lipid carriers," *Brazilian Journal of Pharmaceutical Sciences*, vol. 59, p. e21308, 2023.

[88] A. Alalaiwe *et al.*, "Synergistic anti-mrsa activity of cationic nanostructured lipid carriers in combination with oxacillin for cutaneous application," *Frontiers in Microbiology*, vol. 9, p. 1493, 2018.

[89] E. D. Rocha *et al.*, "Enhanced in vitro antimicrobial activity of polymyxin b–coated nanostructured lipid carrier containing dexamethasone acetate," *Journal of Pharmaceutical Innovation*, vol. 16, no. 1, pp. 125–135, 2021.

[90] K. S. Bhaskar and J., "Formulation and evaluation of rifampicin nanoparticles," *World Journal of Pharmaceutical Science and Research*, vol. 3, no. 5, pp. 384–393, 2024.

[91] P. Vinchhi, J. K. Patel, and M. M. Patel, *High-Pressure Homogenization Techniques for Nanoparticles*. Springer, 2021, pp. 263–285.

[92] R. H. Müller *et al.*, *Nanostructured Lipid Carriers (NLC): The Second Generation of Solid Lipid Nanoparticles*. Springer, 2016, pp. 161–185.

[93] V. R. Salvi and P. Pawar, "Nanostructured lipid carriers (nlc) system: A novel drug targeting carrier," *Journal of Drug Delivery Science and Technology*, vol. 51, pp. 255–267, 2019.

[94] R. Khutale and P. Khulbe, "Nanostructured lipid carriers (nlc): A novel drug targeting carrier system."

[95] R. Shah *et al.*, *Composition and Structure*. Springer, 2014, pp. 11–22.

[96] R. H. Müller, K. Mäder, and S. Gohla, "Solid lipid nanoparticles (sln) for controlled drug delivery–a review of the state of the art," *European Journal of Pharmaceutics and Biopharmaceutics*, vol. 50, no. 1, pp. 161–177, 2000.

[97] C. Nayak *et al.*, "Next-generation nanostructured lipid carriers: A review of latest trends and innovations," *Biomedical Materials & Devices*, 2025.

[98] G. Yoon, J. W. Park, and I.-S. Yoon, "Solid lipid nanoparticles (slns) and nanostructured lipid carriers (nlcs): Recent advances in drug delivery," *Journal of Pharmaceutical Investigation*, vol. 43, no. 5, pp. 353–362, 2013.

[99] S. Das and A. Chaudhury, "Recent advances in lipid nanoparticle formulations with solid matrix for oral drug delivery," *AAPS PharmSciTech*, vol. 12, no. 1, pp. 62–76, 2011.

[100] W. Mehnert and K. Mäder, "Solid lipid nanoparticles: Production, characterization and applications," *Advanced Drug Delivery Reviews*, vol. 64, pp. 83–101, 2012.

[101] C.-Y. Chen *et al.*, "Oleic acid-loaded nanostructured lipid carrier inhibit neutrophil activities in the presence of albumin and alleviates skin inflammation," *International Journal of Nanomedicine*, pp. 6539–6553, 2019.

[102] N. m. Izza *et al.*, "Systematic characterization of nanostructured lipid carriers from cetyl palmitate/caprylic triglyceride/tween 80 mixtures in an aqueous environment," *Langmuir*, vol. 37, no. 14, pp. 4284–4293, 2021.

[103] Q. Li *et al.*, "A review of the structure, preparation, and application of nlcs, pnps, and plns," *Nanomaterials*, vol. 7, no. 6, p. 122, 2017.

[104] J. Garg *et al.*, "Nanostructured lipid carriers: A promising drug carrier for targeting brain tumours," *Future Journal of Pharmaceutical Sciences*, vol. 8, no. 1, p. 25, 2022.

[105] B. Subramaniam, Z. H. Siddik, and N. H. Nagoor, "Optimization of nanostructured lipid carriers: Understanding the types, designs, and parameters in the process of formulations," *Journal of Nanoparticle Research*, vol. 22, no. 6, p. 141, 2020.

[106] P. Jaiswal, B. Gidwani, and A. Vyas, "Nanostructured lipid carriers and their current application in targeted drug delivery," *Artificial Cells, Nanomedicine, and Biotechnology*, vol. 44, no. 1, pp. 27–40, 2016.

[107] F. L. Luedtke *et al.*, "Optimization of high pressure homogenization conditions to produce nanostructured lipid carriers using natural and synthetic emulsifiers," *Food Research International*, vol. 160, p. 111746, 2022.

[108] M. D. Joshi, R. H. Prabhu, and V. B. Patravale, *Fabrication of Nanostructured Lipid Carriers (NLC)-Based Gels from Microemulsion Template for Delivery Through Skin*. Springer, 2019, pp. 279–292.

[109] D. Liu *et al.*, "Diclofenac sodium-loaded solid lipid nanoparticles prepared by emulsion/solvent evaporation method," *Journal of Nanoparticle Research*, vol. 13, no. 6, pp. 2375–2386, 2011.

[110] K. L. López *et al.*, "Solid lipid nanoparticles (sln) and nanostructured lipid carriers (nlc) prepared by microwave and ultrasound-assisted synthesis: Promising green strategies for the nanoworld," *Pharmaceutics*, vol. 15, no. 5, p. 1333, 2023.

[111] V.-A. Duong, T.-T.-L. Nguyen, and H.-J. Maeng, "Preparation of solid lipid nanoparticles and nanostructured lipid carriers for drug delivery and the effects of preparation parameters of solvent injection method," *Molecules*, vol. 25, no. 20, p. 4781, 2020.

[112] E. Gomaa *et al.*, "Methods for preparation of nanostructured lipid carriers," *Methods*, vol. 199, pp. 3–8, 2022.

[113] C.-C. Liao *et al.*, "Multifunctional lipid-based nanocarriers with antibacterial and anti-inflammatory activities for treating mrsa bacteremia in mice," *Journal of Nanobiotechnology*, vol. 19, pp. 1–18, 2021.

[114] S. E. Alavi *et al.*, "A pegylated nanostructured lipid carrier for enhanced oral delivery of antibiotics," *Pharmaceutics*, vol. 14, no. 8, p. 1668, 2022.

[115] C. Vairo *et al.*, "In vitro and in vivo antimicrobial activity of sodium colistimethate and amikacin-loaded nanostructured lipid carriers (nlc)," *Nanomedicine: Nanotechnology, Biology and Medicine*, vol. 29, p. 102259, 2020.

[116] M. Sharaf *et al.*, "Co-delivery of hesperidin and clarithromycin in a nanostructured lipid carrier for the eradication of helicobacter pylori in vitro," *Bioorganic Chemistry*, vol. 112, p. 104896, 2021.

[117] J. Hollis, "The development and characterization of a vancomycin nanostructured lipid carrier and evaluation of their antimicrobial properties on staphylococcus aureus," Master's thesis, University of Central Lancashire, 2024.

[118] A. C. Vieira *et al.*, "Targeted macrophages delivery of rifampicin-loaded lipid nanoparticles to improve tuberculosis treatment," *Nanomedicine*, vol. 12, no. 24, pp. 2721–2736, 2017.

[119] M. Moreno-Sastre *et al.*, "Pulmonary delivery of tobramycin-loaded nanostructured lipid carriers for pseudomonas aeruginosa infections associated with cystic fibrosis," *International Journal of Pharmaceutics*, vol. 498, no. 1-2, pp. 263–273, 2016.

[120] K. K. Abla, S. M. Hijazi, and M. M. Mehanna, "Augmented efficiency of azithromycin for mrsa ocular infections management: Limonene-based nanostructured lipid carriers in-situ approach," *Journal of Drug Delivery Science and Technology*, vol. 87, p. 104764, 2023.

[121] K. K. Patel *et al.*, "Dnase-i functionalization of ciprofloxacin-loaded chitosan nanoparticles overcomes the biofilm-mediated resistance of pseudomonas aeruginosa," *Applied Nanoscience*, vol. 10, pp. 563–575, 2020.

[122] H. A. A. El-Enin *et al.*, "Augmented silver sulfadiazine nanostructured lipid carriers impregnated collagen sponge for promoting burn wound healing," *International Journal of Biological Macromolecules*, p. 140371, 2025.

[123] N. Osman *et al.*, "Surface modification of nano-drug delivery systems for enhancing antibiotic delivery and activity," *Wiley Interdisciplinary Reviews: Nanomedicine and Nanobiotechnology*, vol. 14, no. 1, p. e1758, 2022.

[124] C. Vairo, "Antibiotic-loaded nanostructured lipid carriers (nlcs) for multiresistant respiratory tract and wound infections," Ph.D. dissertation, 2020.

[125] A. N. F. Marzaman *et al.*, "Recent advances in pharmaceutical approaches of antimicrobial agents for selective delivery in various administration routes," *Antibiotics*, vol. 12, no. 5, p. 822, 2023.

[126] A. Ahsan *et al.*, "Lipid nanocarriers-enabled delivery of antibiotics and antimicrobial adjuvants to overcome bacterial biofilms," *Pharmaceutics*, vol. 16, no. 3, p. 396, 2024.

[127] I. Chauhan *et al.*, "Nanostructured lipid carriers: A groundbreaking approach for transdermal drug delivery," *Advanced Pharmaceutical Bulletin*, vol. 10, no. 2, p. 150, 2020.

[128] N. Mennini *et al.*, "Comparison of liposomal and nlc (nanostructured lipid carrier) formulations for improving the transdermal delivery of oxaprozin: Effect of cyclodextrin complexation," *International Journal of Pharmaceutics*, vol. 515, no. 1-2, pp. 684–691, 2016.

[129] F. I. Safitri, D. Nawangsari, and D. Febrina, "Overview: Application of carbopol 940 in gel," in *International Conference on Health and Medical Sciences (AHMS 2020)*. Atlantis Press, 2021.

[130] A. Bamisaye *et al.*, "Development and characterization of pegylated ofloxacin and ciprofloxacin loaded sandbox oil based nanoemulsion and its potential for transdermal drug delivery," *Journal of Chemical Society of Nigeria*, vol. 45, no. 2, 2020.

[131] A. Youssef, N. Dudhipala, and S. Majumdar, "Ciprofloxacin loaded nanostructured lipid carriers incorporated into in-situ gels to improve management of bacterial endophthalmitis," *Pharmaceutics*, vol. 12, no. 6, p. 572, 2020.

[132] S. Dlamini *et al.*, "Enhancing activity and overcoming ciprofloxacin resistance via multifunctional nanostructured lipid carriers," *Journal of Drug Delivery Science and Technology*, p. 106933, 2025.

[133] A. S. Almarshedi *et al.*, "Development of inhalable nanostructured lipid carriers for ciprofloxacin for noncystic fibrosis bronchiectasis treatment," *International Journal of Nanomedicine*, pp. 2405–2417, 2021.

[134] P. Mura *et al.*, "Cyclodextrin complexation as a fruitful strategy for improving the performance of nebivolol delivery from solid lipid nanoparticles," *International Journal of Pharmaceutics*, vol. 668, p. 124972, 2025.

[135] P. Nnamani *et al.*, "Preparation, characterisation and in vitro antibacterial property of ciprofloxacin-loaded nanostructured lipid carrier for treatment of bacillus subtilis infection," *Journal of Microencapsulation*, vol. 36, no. 1, pp. 32–42, 2019.

[136] F. Shakeel *et al.*, "Nanoemulsions as vehicles for transdermal delivery of aceclofenac," *AAPS PharmSciTech*, vol. 8, no. 4, p. 104, 2007.

[137] S. Javed *et al.*, "Nanostructured lipid carrier system: A compendium of their formulation development approaches, optimization strategies by quality by design, and recent applications in drug delivery," *Nanotechnology Reviews*, vol. 11, no. 1, pp. 1744–1777, 2022.

[138] L. Sahoo *et al.*, "Box behnken design-enabled development of nanostructured lipid carrier transdermal patch for enhancement of bioavailability of olmesartan medoxomil," *Journal of Pharmaceutical Innovation*, vol. 17, no. 4, pp. 1405–1419, 2022.

[139] G. S. Muraca *et al.*, "Improving ciprofloxacin antimicrobial activity through lipid nanoencapsulation or non-thermal plasma on pseudomonas aeruginosa biofilms," *Journal of Drug Delivery Science and Technology*, vol. 64, p. 102644, 2021.

[140] A. Mirzaie *et al.*, "Preparation and optimization of ciprofloxacin encapsulated niosomes: A new approach for enhanced antibacterial activity,

biofilm inhibition and reduced antibiotic resistance in ciprofloxacin-resistant methicillin-resistance staphylococcus aureus," *Bioorganic Chemistry*, vol. 103, p. 104231, 2020.

[141] S. Hoeppener, *Characterization of Drug Delivery Systems by Transmission Electron Microscopy*. Cham: Springer International Publishing, 2024, pp. 191–209.

[142] D. Sonawane and V. Pokharkar, "Quercetin-loaded nanostructured lipid carrier in situ gel for brain targeting through intranasal route: Formulation, in vivo pharmacokinetic and pharmacodynamic studies," *AAPS PharmSciTech*, vol. 25, no. 2, p. 30, 2024.

[143] L. Montenegro, F. Castelli, and M. G. Sarpietro, "Differential scanning calorimetry analyses of idebenone-loaded solid lipid nanoparticles interactions with a model of bio-membrane: A comparison with in vitro skin permeation data," *Pharmaceuticals (Basel)*, vol. 11, no. 4, 2018.

[144] M. S. Baig *et al.*, "Development and evaluation of cationic nanostructured lipid carriers for ophthalmic drug delivery of besifloxacin," *Journal of Drug Delivery Science and Technology*, vol. 55, p. 101496, 2020.

[145] S. Yu *et al.*, "Nanostructured lipid carrier (nlc)-based novel hydrogels as potential carriers for nepafenac applied after cataract surgery for the treatment of inflammation: Design, characterization, and in vitro cellular inhibition and uptake studies," *RSC Advances*, vol. 7, no. 27, pp. 16 668–16 677, 2017.

[146] L. Gómez-Lázaro *et al.*, "Assessment of in vitro release testing methods for colloidal drug carriers: The lack of standardized protocols," *Pharmaceutics*, vol. 16, no. 1, p. 103, 2024.

[147] A. C. Ortiz *et al.*, "Development of a nanostructured lipid carrier (nlc) by a low-energy method, comparison of release kinetics and molecular dynamics simulation," *Pharmaceutics*, vol. 13, no. 4, 2021.

[148] S. Hussain *et al.*, "Itraconazole-loaded polycaprolactone nanoparticle gel for enhanced transdermal delivery: Development, characterization, and ex

vivo evaluation," *International Journal of Nanomedicine*, pp. 15 655–15 681, 2025.

[149] A. Czajkowska-Kośnik, E. Szymańska, and K. Winnicka, "Nanostructured lipid carriers (nlc)-based gel formulations as etodolac delivery: From gel preparation to permeation study," *Molecules*, vol. 28, no. 1, 2022.

[150] Y. Zheng *et al.*, "Effects of carbopol(®) 934 proportion on nanoemulsion gel for topical and transdermal drug delivery: A skin permeation study," *International Journal of Nanomedicine*, vol. 11, pp. 5971–5987, 2016.

[151] M. Aslam *et al.*, "Application of box–behnken design for preparation of glibenclamide loaded lipid based nanoparticles: Optimization, in vitro skin permeation, drug release and in vivo pharmacokinetic study," *Journal of Molecular Liquids*, vol. 219, pp. 897–908, 2016.

[152] B. Das, A. K. Nayak, and U. Nanda, "Topical gels of lidocaine hcl using cashew gum and carbopol 940: Preparation and in vitro skin permeation," *International Journal of Biological Macromolecules*, vol. 62, pp. 514–517, 2013.

[153] M. Rosmiati, M. Abdassah, and A. Y. Chaerunisaa, "Effect of carrageenan as gelling agent on tocopherol acetate emulgels," *Indonesian Journal of Pharmaceutical Science and Technology*, vol. 5, no. 1, pp. 1–7, 2018.

[154] F. Sun *et al.*, "Preparation, characterization and pharmacological evaluation of tolterodine hydrogels for the treatment of overactive bladder," *International Journal of Pharmaceutics*, vol. 454, no. 1, pp. 532–538, 2013.

[155] K.-P. Wilhelm and H. I. Maibach, *OECD Guidelines for Testing of Chemicals*. CRC Press, 2012, pp. 509–511.

[156] M. Hemmati *et al.*, "Investigation of acute dermal irritation/corrosion, acute inhalation toxicity and cytotoxicity tests for nanobiocide®," *Nanomedicine Research Journal*, vol. 1, no. 1, pp. 23–29, 2016.

[157] C. Charmeau-Genevois *et al.*, "A simplified index to quantify the irritation/corrosion potential of chemicals–part i: Skin," *Regulatory Toxicology and Pharmacology*, vol. 123, p. 104922, 2021.

[158] "Oecd guideline for the testing of chemicals," Tech. Rep., 2016.

[159] V. M. Pierce, T. Bhowmick, and P. J. Simner, "Guiding antimicrobial stewardship through thoughtful antimicrobial susceptibility testing and reporting strategies: An updated approach in 2023," *Journal of Clinical Microbiology*, vol. 61, no. 11, pp. e00 074–22, 2023.

[160] C. Upadhyay *et al.*, "Preparation and evaluation of different herbal gels synthesized from chinese medicinal plants as an antimicrobial agents," *Pharmacological Research - Modern Chinese Medicine*, vol. 9, p. 100313, 2023.

[161] F. Zothanpuii, R. Rajesh, and K. Selvakumar, "A review on stability testing guidelines of pharmaceutical products," *Asian Journal of Pharmaceutical and Clinical Research*, vol. 13, no. 10, pp. 3–9, 2020.

[162] T. M. Almeleebia *et al.*, "Co-delivery of naringin and ciprofloxacin by oleic acid lipid core encapsulated in carboxymethyl chitosan/alginate nanoparticle composite for enhanced antimicrobial activity," *ACS Omega*, vol. 9, no. 6, pp. 6845–6860, 2024.

[163] N. C. Nogueira, L. L. F. de Sá, and A. L. M. de Carvalho, "Nanostructured lipid carriers as a novel strategy for topical antifungal therapy," *AAPS PharmSciTech*, vol. 23, no. 1, p. 32, 2021.

[164] J. Pardeike, A. Hommoss, and R. H. Müller, "Lipid nanoparticles (sln, nlc) in cosmetic and pharmaceutical dermal products," *International Journal of Pharmaceutics*, vol. 366, no. 1-2, pp. 170–184, 2009.

[165] A. Beloqui *et al.*, "Nanostructured lipid carriers: Promising drug delivery systems for future clinics," *Nanomedicine: Nanotechnology, Biology and Medicine*, vol. 12, no. 1, pp. 143–161, 2016.

[166] S. Ahalwat and D. C. Bhatt, "Development of novel lipid matrix for improved sustained release effect of a hydrophilic drug via response surface methodology," *Journal of Drug Delivery Science and Technology*, vol. 67, p. 102993, 2022.

[167] M.-H. Kim *et al.*, "Formulation and evaluation of nanostructured lipid carriers (nlcs) of 20 (s)-protopanaxadiol (ppd) by box-behnken design," *International Journal of Nanomedicine*, pp. 8509–8520, 2019.

[168] M. F. Aldawsari *et al.*, "Optimized ribociclib nanostructured lipid carrier for the amelioration of skin cancer: Inferences from ex-vivo skin permeation and dermatokinetic studies," *Saudi Pharmaceutical Journal*, vol. 32, no. 3, p. 101984, 2024.

[169] F. Tamjidi *et al.*, "Stability of astaxanthin-loaded nanostructured lipid carriers as affected by ph, ionic strength, heat treatment, simulated gastric juice and freeze–thawing," *Journal of Food Science and Technology*, vol. 54, no. 10, pp. 3132–3140, 2017.

[170] R. Jnaidi, "Development of nanostructured lipid carriers loaded with atorvastatin for the effective delivery and treatment against glioblastoma cells," Ph.D. dissertation, Universidade de Lisboa (Portugal), 2020.

[171] S. Das *et al.*, "Formulation design, preparation and physicochemical characterizations of solid lipid nanoparticles containing a hydrophobic drug: Effects of process variables," *Colloids and Surfaces B: Biointerfaces*, vol. 88, no. 1, pp. 483–489, 2011.

[172] E. Souto and R. Müller, "Investigation of the factors influencing the incorporation of clotrimazole in sln and nlc prepared by hot high-pressure homogenization," *Journal of Microencapsulation*, vol. 23, no. 4, pp. 377–388, 2006.

[173] S. Rawal, B. Patel, and M. M. Patel, "Fabrication, optimisation and in vitro evaluation of docetaxel and curcumin co-loaded nanostructured lipid carriers for improved antitumor activity against non-small cell lung carcinoma," *Journal of Microencapsulation*, vol. 37, no. 8, pp. 543–556, 2020.

[174] R. H. Müller, M. Radtke, and S. A. Wissing, "Nanostructured lipid matrices for improved microencapsulation of drugs," *International Journal of Pharmaceutics*, vol. 242, no. 1, pp. 121–128, 2002.

[175] P. O. Nnamani *et al.*, "Development of artemether-loaded nanostructured lipid carrier (nlc) formulation for topical application," *International Journal of Pharmaceutics*, vol. 477, no. 1, pp. 208–217, 2014.

[176] S. H. Hussein-Al-Ali *et al.*, "Preparation and characterisation of ciprofloxacin-loaded silver nanoparticles for drug delivery," *IET Nanobiotechnology*, vol. 16, no. 3, pp. 92–101, 2022.

[177] M. Y. Al-darwesh *et al.*, "Nanocapsule formation of ciprofloxacin-loaded zirconia nanoparticles coated with chitosan for antibacterial, antibiofilm, anti-inflammatory, and catalytic applications," *Journal of Cluster Science*, vol. 36, no. 4, p. 121, 2025.

[178] H. Ali, S. K. Singh, and P. R. P. Verma, "Preformulation and physicochemical interaction study of furosemide with different solid lipids," *Journal of Pharmaceutical Investigation*, vol. 45, no. 4, pp. 385–398, 2015.

[179] L. Kiss *et al.*, "Design and optimization of nanostructured lipid carrier containing dexamethasone for ophthalmic use," *Pharmaceutics*, vol. 11, no. 12, p. 679, 2019.

[180] A. Kudtarkar *et al.*, "Solid lipid nanoparticles of albendazole for treatment of toxocara canis infection: In-vivo efficacy studies," *Nanoscience & Nanotechnology-Asia*, vol. 7, no. 1, pp. 80–91, 2017.

[181] A. Sharma *et al.*, "Formulation and physicochemical evaluation of nanostructured lipid carrier for codelivery of clotrimazole and ciprofloxacin," *Asian*

Journal of Pharmaceutical and Clinical Research, vol. 9, no. 3, pp. 356–360, 2016.

[182] G. A. Shazly, "Ciprofloxacin controlled-solid lipid nanoparticles: Characterization, in vitro release, and antibacterial activity assessment," *BioMed Research International*, vol. 2017, no. 1, p. 2120734, 2017.

[183] V. Jenning, A. F. Thünemann, and S. H. Gohla, "Characterisation of a novel solid lipid nanoparticle carrier system based on binary mixtures of liquid and solid lipids," *International Journal of Pharmaceutics*, vol. 199, no. 2, pp. 167–188, 2000.

[184] W. Potong, T. Sookkumnerd, and P. Rattanaphanee, "Analysis of phase transformation of pure fatty acids and its mixtures by differential scanning calorimetry," in *TIChE International Conference*, Hatyai, Songkhla Thailand, 2011.

[185] J. Whiteley *et al.*, "A thermodynamic investigation into protein–excipient interactions involving different grades of polysorbate 20 and 80," *Journal of Thermal Analysis and Calorimetry*, vol. 149, no. 23, pp. 13 941–13 951, 2024.

[186] S. Hussein Ali, S. S. M. Al-Obaidy, and F. H. Mohammed, "Enhancing the antibacterial and anticancer activity of ciprofloxacin by encapsulating into shellac-chitosan nano particles (cnps)," *Journal of Nanostructures*, vol. 12, no. 3, pp. 546–556, 2022.

[187] P. Nnamani *et al.*, "Preparation, characterisation and in vitro antibacterial property of ciprofloxacin-loaded nanostructured lipid carrier for treatment of bacillus subtilis infection," *Journal of Microencapsulation*, vol. 36, no. 1, pp. 32–42, 2019.

[188] S. Sahoo *et al.*, "Structural analysis of ciprofloxacin-carbopol polymeric composites by x-ray diffraction and fourier transform infra-red spectroscopy," *Tropical Journal of Pharmaceutical Research*, vol. 10, no. 3, 2011.

[189] Y. J. Qi, N. Perveen, and N. H. Khan, "Comparative purity study of uv spectrophotometric and fourier-transform infrared spectroscopic (ftir) techniques for the determination of ciprofloxacin hydrochloride tablets," *Biomedical Journal of Scientific and Technical Research*, vol. 32, pp. 24 973–24 987, 2020.

[190] T. C. Mendonça *et al.*, "Development of nanostructured lipid carriers containing the antimicrobial ciprofloxacin for topical application," *Revista dos Trabalhos de Iniciação Científica da UNICAMP*, vol. 26, 2018.

[191] A. Zafar *et al.*, "Formulation and evaluation of topical nano-lipid-based delivery of butenafine: In vitro characterization and antifungal activity," *Gels*, vol. 8, no. 2, p. 133, 2022.

[192] F. Pi *et al.*, "Temperature dependence of structure and dynamic properties of oleic acid γ and α phases studied by ftir spectroscopy," *Bulletin of the Chemical Society of Japan*, vol. 84, no. 4, pp. 403–412, 2011.

[193] M. Bekhit *et al.*, "Radiation-induced synthesis of tween 80 stabilized silver nanoparticles for antibacterial applications," *Journal of Environmental Science and Health, Part A*, vol. 55, no. 10, pp. 1210–1218, 2020.

[194] S. P. Balguri *et al.*, "Development of nano structured lipid carriers of ciprofloxacin for ocular delivery: Characterization, in vivo distribution and effect of pegylation," *Investigative Ophthalmology & Visual Science*, vol. 56, no. 7, pp. 2269–2269, 2015.

[195] E. Fernandes *et al.*, "Spectroscopic studies as a toolbox for biophysical and chemical characterization of lipid-based nanotherapeutics," *Frontiers in Chemistry*, vol. 6, p. 323, 2018.

[196] S. Anantachaisilp *et al.*, "Chemical and structural investigation of lipid nanoparticles: Drug–lipid interaction and molecular distribution," *Nanotechnology*, vol. 21, no. 12, p. 125102, 2010.

[197] V. Andonova and P. Peneva, "Characterization methods for solid lipid nanoparticles (sln) and nanostructured lipid carriers (nlc)," *Current Pharmaceutical Design*, vol. 23, no. 43, pp. 6630–6642, 2017.

[198] L. Uhljar *et al.*, "In vitro drug release, permeability, and structural test of ciprofloxacin-loaded nanofibers," *Pharmaceutics*, vol. 13, no. 4, p. 556, 2021.

[199] A. A. A. Youssef, N. Dudhipala, and S. Majumdar, "Dual drug loaded lipid nanocarrier formulations for topical ocular applications," *International Journal of Nanomedicine*, pp. 2283–2299, 2022.

[200] T. M. Almeleebia *et al.*, "Co-delivery of naringin and ciprofloxacin by oleic acid lipid core encapsulated in carboxymethyl chitosan/alginate nanoparticle composite for enhanced antimicrobial activity," *ACS Omega*, vol. 9, no. 6, pp. 6845–6860, 2024.

[201] V. Chawla and S. A. Saraf, "Rheological studies on solid lipid nanoparticle based carbopol gels of aceclofenac," *Colloids Surf B Biointerfaces*, vol. 92, pp. 293–298, 2012.

[202] P. Kakade *et al.*, "Formulation development of nanostructured lipid carrier-based nanogels encapsulating tacrolimus for sustained therapy of psoriasis," *International Journal of Pharmaceutics*, vol. 660, p. 124172, 2024.

[203] G. Y. Noh, J. Y. Suh, and S. N. Park, "Ceramide-based nanostructured lipid carriers for transdermal delivery of isoliquiritigenin: Development, physicochemical characterization, and in vitro skin permeation studies," *Korean Journal of Chemical Engineering*, vol. 34, no. 2, pp. 400–406, 2017.

[204] A. Czajkowska-Kośnik, E. Szymańska, and K. Winnicka, "Nanostructured lipid carriers (nlc)-based gel formulations as etodolac delivery: From gel preparation to permeation study," *Molecules*, vol. 28, no. 1, p. 235, 2023.

[205] A. Kovács *et al.*, "Development of nanostructured lipid carriers containing salicyclic acid for dermal use based on the quality by design method," *European Journal of Pharmaceutical Sciences*, vol. 99, pp. 246–257, 2017.

[206] M. Rincón *et al.*, "Development of pranoprofen loaded nanostructured lipid carriers to improve its release and therapeutic efficacy in skin inflammatory disorders," *Nanomaterials (Basel)*, vol. 8, no. 12, 2018.

[207] F. Han *et al.*, "Nanostructured lipid carriers (nlc) based topical gel of flurbiprofen: Design, characterization and in vivo evaluation," *International Journal of Pharmaceutics*, vol. 439, no. 1-2, pp. 349–357, 2012.

[208] C.-C. Liao *et al.*, "Multifunctional lipid-based nanocarriers with antibacterial and anti-inflammatory activities for treating mrsa bacteremia in mice," *Journal of Nanobiotechnology*, vol. 19, no. 1, p. 48, 2021.

[209] A. Tariq *et al.*, "Reshaping antibiotic delivery: Chitosan-based polymeric hydrogel for transdermal treatment of drug resistant bacteria," *Polymers for Advanced Technologies*, vol. 35, no. 3, p. e6331, 2024.

[210] E. A. Ozon *et al.*, "Formulation and characterization of carbopol-based porphyrin gels for targeted dermato-oncological therapy: Physicochemical and pharmacotechnical insights," *Internation Journal of Molecular Science*, vol. 26, no. 8, 2025.